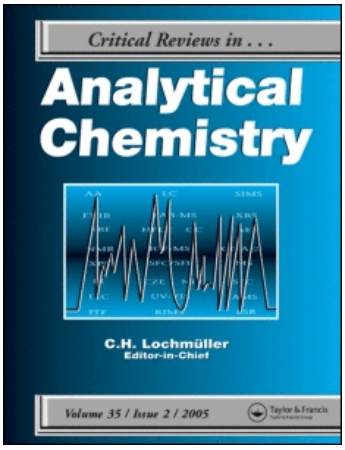

Critical Reviews in Analytical Chemistry
Publication details, including instructions for authors and subscription information:
http://www.informaworld.com/smpp/title~content=t713400837

Recent Advances in Emission Spectroscopy: Inductively Coupled Plasma Discharges for Spectrochemical Analysis

Ramon M. Barnes; P. W. J. M. Boumans

To cite this Article Barnes, Ramon M. and Boumans, P. W. J. M.(1978) 'Recent Advances in Emission Spectroscopy: Inductively Coupled Plasma Discharges for Spectrochemical Analysis', Critical Reviews in Analytical Chemistry, 7: 3, 203 — 296
To link to this Article: DOI: 10.1080/10408347808542702
URL: http://dx.doi.org/10.1080/10408347808542702

RECENT ADVANCES IN EMISSION SPECTROSCOPY: INDUCTIVELY COUPLED PLASMA DISCHARGES FOR SPECTROCHEMICAL ANALYSIS

Author: **Ramon M. Barnes**
Department of Chemistry
University of Massachusetts
Amherst, Massachusetts

Referee: P. W. J. M. Boumans
Analytical Atomic Spectroscopy Group
Philips Research Laboratories
Eindhoven, Netherlands

TABLE OF CONTENTS

I. INTRODUCTION

A. Scope

The inductively coupled plasma (ICP) spectroscopic source is a new and popular tool for spectrochemical analysis; its development since the early 1960s, especially during the past 5 years, has established that the ICP will play a major role in elemental analysis for the near future of analytical spectrochemistry. A critical evaluation of the ICP discharge is undertaken here only to establish a benchmark in the analytical progress, since, in the next half decade, applications and fundamental information are expected to surpass the accomplishments already achieved by a wide margin.

Of course, the ICP is not the sole new source presently under extensive study for emission spectroscopy. However, packaged commercially by numerous manufacturers and in the hands of researchers and analysts alike, the ICP is successfully solving practical analytical problems and providing a new tack for scrutinizing spectrophysical phenomena in discharges. Microwave, spark, DC plasma, and low-pressure emission spectroscopic sources will not be considered here, although many of their features demand equal attention.

The intent is to survey critically the basic instrumentation and performance of the ICP discharge in emission spectroscopy, to probe recent instrumentation developments and plasma operation, and to examine models of the discharge and processes therein occurring. Naturally, this intent will not be totally fulfilled since much of the current work is either proprietary or insufficiently advanced to discuss in detail.

B. Historical

Until recently, the induction heating of gases at reduced or atmospheric pressure as a spectroscopic source did not play as critical a role in spectrochemical analysis as arc and spark discharges or flames.[1] Although dedicated research continues on arc and spark discharges,[2] conventional arc and spark sources serve as workhorses of the industrial spectrochemical laboratory, and atomic absorption with flame and electrothermal atomizers have led to the growth of global applications of spectrochemical analysis since the mid-1960s. High-frequency (HF) electrodeless discharges, particularly those operated at atmospheric pressure, appear as the latest promising spectrochemical source type. Most advanced among the alternative HF spectrochemical sources, as measured by commercial production and industrial applications, is the ICP when applied in atomic emission spectroscopy (ICP-AES). Numerous authors have treated the development and spectrochemical application of HF electrodeless plasmas. Notable among these are the recent reviews by Sharp,[5] Fuller,[281] Greenfield et al.,[3] Butler et al.,[4] Fassel,[9] Fassel and Kniseley,[6] Kleinmann and Polej,[7] and Boumans.[8,116,256,279]

The development of induction plasma grew from research on low-pressure electrodeless ring discharges, first observed in 1884 by Hittorf[1] and studied subsequently by Thomson between 1891 and 1927.[11,12] Thomson made qualitative and quantitative observations under varying experimental conditions on the electrical properties and spatial intensity distribution of total discharge luminosity and spectra. He developed an induction theory for the electrodeless ring discharge and its theoretical conditions for ignition, and his expression for the magnetic and electrical field distributions as Bessel functions has been applied to induction plasmas even in recent years.[13] Disputing Thomson's model, Townsend and Donaldson[14] assumed that the discharge was produced by the electric field of the inductor rather than by the magnetic field. MacKinnon[15] showed that the contrasting views were caused by the different conditions under which the experiments were conducted.

Mavrodineanu and Hughes[16] traced the experiments using radio frequency (RF) excitation of low-pressure gases for spectrochemical analysis from the work of Tesla in 1891 through the early 1960s. Bochkova and Shreyder[282] and Boumans[8] also examined the experimental development of sealed, low-pressure, HF-excited discharges. The advantages resulting from the replacement of internal electrodes of DC glow discharges with external HF electrodes or an induction coil were recognized in the early spectrochemical applications of low-pressure HF discharge, for example, by Fenner[284], Gatterer[286], and Gatterer and Frodl[285]. As recently as 1977, Eckert[17] worked to develop a technique for trace elemental analysis with small sample sizes sealed into RF induction-

heated cylindrical and spherical lamps for which he developed a two-dimensional mathematical model. This and similar alternatives, such as those described by Agterdenbos and coworkers,[287-292] to emission spectrometry with open, flowing plasma sources provide extended periods of emission, because no major loss of sample exists, and the need for continuous replacement is minimal. As a consequence of the lengthy emission stability, multielement spectroscopic measurements with a sequentially scanning monochromator detector are practical for very small sample sizes.

Some other reduced pressure emission light sources using RF heating include capacitively coupled discharges and sealed electrodeless discharge lamps (EDL). The latter are described by Barnett et al.[18], Haarsma et al.,[19] and Keliher and Browner.[20] Although microwave EDLs are used primarily as light sources in atomic absorption and atomic fluorescence spectroscopy (AFS), Agterdenbos and co-workers[287-292] have explored applications of EDLs in AES for the determination of pico- and nanogram levels of Cd, In, Tl, Se, Zn, Pb, and Hg in water, acids, and blood. The capacitively coupled RF discharge,[21] like its close relative the inductively coupled discharge, is used industrially for plasma chemistry, plasma ashing, and plasma etching,[22] and has only recently been studied in detail spectroscopically and utilized for spectrochemical analysis.[23,24]

The major impact of RF discharges as excitation sources in spectrochemistry did not result from the applications of reduced pressure discharges, although they are simply generated. The important advance for spectrochemical adoption of induction-heated plasmas was the transition from low-pressure, closed systems to atmospheric-pressure, flowing systems. This two-step process took more than 20 years to complete. As a consequence, the ICP has had an analytical lifetime of slightly more than a dozen years.

The change from low-pressure, induction-heated plasmas to spectroscopic sources occurred during the fall and winter of 1941 to 1942 in Leningrad as the result of Babat's discovery that a ring discharge, once established, could be maintained while the pressure was raised to atmospheric pressure. Babat's systematic work was published first in 1942 in Russian[25] and after World War II in English.[26] Babat constructed a HF (2 to 77 MHz) push-pull vacuum tube oscillator with an output reaching 100 kW. This enabled him to obtain powerful electrodeless discharges with air inside quartz cylinders 15 cm in diameter and 150 cm long at pressures ranging from 0.1 to 760 torr. Typical induction coils consisted of several turns (i.e., five) of circular, square, or rectangular copper tubing (1 × 1 cm) with internal diameters greater than 10 cm and height of 5 cm. At 2.7 MHz, a coil current of 175 A was measured. Hollow resonator cavities for HF circuits at power levels exceeding 100 kW were described, and for large volume (e.g., 40 cm in diameter) discharges above 30 MHz, special polygonal inductors were constructed. The power levels were exceptional for the time; even today, they are not utilized for spectrochemical applications. As Dresvin[36] has emphasized, experiments were conducted under severe wartime conditions until the entire power system in Leningrad failed.

When the pressure in evacuated chambers was raised to atmospheric pressure, Babat could still maintain the induction discharge. He did not report experimenting with flowing systems at any pressure. To initiate the discharge at atmospheric pressure, he unsuccessfully tried NaCl-seeded flames and DC and 50-Hz arcs. Generally, the discharge was ignited at low pressure and maintained as the pressure was gradually elevated. In addition to these experimental studies, he derived the mathematical relations between frequency, power, and voltage gradient for induction discharges; he predicted that the current distribution in the discharge was like a metal conductor, and he thought that the discharge temperature should be highest on the tube axis and lowest at the walls. At atmospheric pressure, the induction discharge existed only if the power input was greater than 30 to 50 kW, which required a generator with 100- to 200-kW output. Babat found that the higher the frequency of the generator, the lower the current and power consumption required to form a stable discharge became. In describing this exceptional research, Babat had in mind the industrial applications of RF discharges for electrochemistry of gases, heating and fusion of fireproof materials, and creating high-intensity, economic light sources.

Induction heating technology for solids also

developed during this decade, and numerous texts document the extent to which this field advanced.[28-32,174] Unfortunately, the mathematical expressions and empirical relationships for the induction heating of metals are not accurately transferred to the much more complex situation found with gas discharges, although some concepts may be useful qualitatively.[13,33,34]

Stabilization of an inductively heated plasma discharge operated at atmospheric pressure and in gases flowing through an open-ended tube was achieved in the early 1960s; this discovery launched two major branches of induction-heated gas discharge technology: spectrochemical analysis and induction-arc engineering. Features of engineering and technological developments and applications of induction-heated plasmas were reviewed critically by Eckert,[35] Raizer,[13] Dresvin,[36] Czernichowski and Jurewicz,[37] Rykalin,[38] and Reed.[44]

The requirements and considerations of thermal plasma engineering differ significantly in many respects from the needs of spectrochemical analysis. Plasma engineering employs enormous power generators (as high as 1 MW), high material throughput, diverse discharge pressures, chemically reactive atmospheres, and large particle sizes, whereas in emission spectroscopy, the trend is to low-power supplies (0.5 to 2 kW), small generators, and microsample sizes. Because thermal plasma engineering and spectral analysis share common interests in plasma generation, discharge diagnostics, sample introduction, and sample vaporization, divergence between the fields comes in the difference in emphasis when the particle vaporizes. Thermal plasma engineering concentrates on reactions, condensations, and subsequent stages. Emission spectroscopy emphasizes atomization, excitation, and emission or radiation. Up to this point, the spectroanalyst has much to learn from the plasma engineer. As Rykalin[38] emphasized, an urgent need exists to develop engineering methods for calculating processes in HF plasmas, taking into account the dynamics of plasma gas flow, especially in turbulent conditions. Also, there is an urgent need to investigate the complex mechanisms of physicochemical transformations in turbulent nonisothermal plasmas, especially in nonequilibrium plasmas, and to collect data on thermodynamic and transport properties in a dissociated and partially ionized plasma state. These same needs exist in part for theoretical developments in spectrochemical analysis and are discussed in Section III.

ICP discharges in flowing, atmospheric pressure gases were first generated in 1961 by Reed.[39,40] In brief papers and in a later patent, he described the essentials of configuring the induction plasma and starting, stabilizing, and confining it. He varied gas compositions, measured temperatures, and established an energy balance. The ICP arrangement configured for crystal growing, as Reed described and applied it, is illustrated in Figure 1. In flowing gas ICP discharges, Reed found that the discharge was stabilized against the gas flow when it exceeded approximately 6 m/sec by introducing the gas

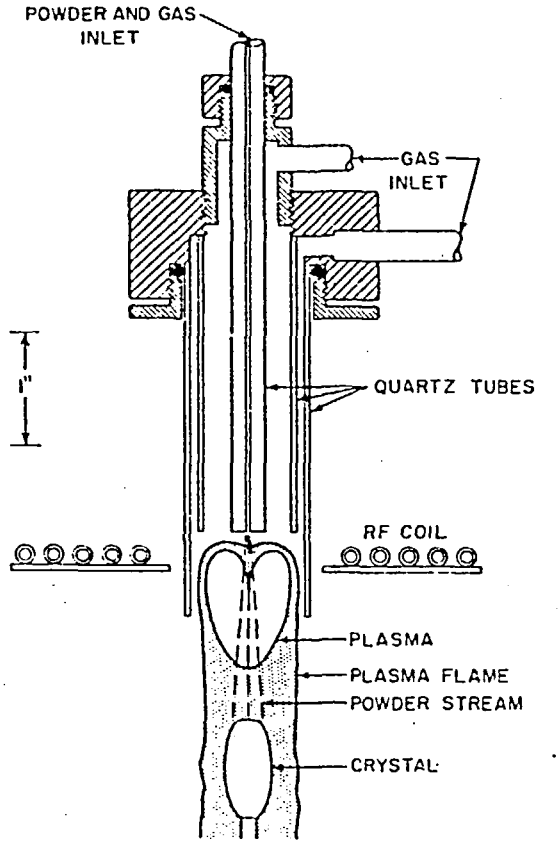

FIGURE 1. The original version of the ICP torch arranged for crystal growth. Gas flowing at high velocity through the center tube carries powder through the high temperature discharge to the molten cap of the crystal. A concentrator or pancake coil is used. (From Reed, T.B., *J. Appl. Phys.*, 32, 2534 (1961).) With permission.

into the quartz confinement tube tangentially, so as to create turbulence in the plasma region. Reed suggested that this tangential gas flow, called vortex stabilization, recirculated some of the plasma by forming a low-pressure region in the center of the tube so that the plasma could propagate against the gas flow in the coil. Otherwise, the discharge would be swept downstream and extinguished. Preferential flow along the walls centered the discharge and cooled the walls as well. Operating the ICP at 4 MHz with a 25-mm diameter quartz tube and power transferred to the plasma ranging from 1.6 to 3.1 kW, Reed found argon the simplest gas in which to start and operate the discharge. In addition, the ICP was operated at higher power levels with pure oxygen and argon mixtures containing as much as 20% hydrogen or 60% helium or air. The initial temperature values for the argon discharges which reached 19,000 K maximum were later found to be too high.[41,227]

The plasma tube geometry used for crystal growing, shown in Figure 1, was Reed's major application, and details of a water-cooled copper injection tip which was inserted into the discharge to insure powder introduction into the plasma can be located in Reference[45]. These clear examples of powder sample introduction into the high-temperature discharge[40] appeared to stimulate the beginning of ICP spectrochemical analysis. The same properties specified for growing crystals (electrodeless generation, controlled atmosphere, high temperature, large cross section, and low particle velocity) serve as the basis for spectral analysis.[43] In a subsequent article, Reed[42] emphasized that powders injected through the discharge would sometimes vaporize completely, which suggested that the ICP discharge could be useful as a spectroscopic light source. He illustrated this with colored photographs of the ICP with introduction of BaF_2 and Al_2O_3; however, he observed that a single powder feeding device would not suffice when a variety of powders needed to be fed. Reliable injection of powders into the ICP remains a major spectrochemical problem today.

The synthetic aspects of high-temperature plasma chemistry, achieved particularly with induction heating, and the apparatus, plasma characteristics, and applications were described by Reed,[44] Beguin et al.,[46] and Hamblyn and Reuben.[47] Plasma chemistry in induction plasmas represents one major alternative to spectrochemical analysis. However, except for plasma geometry and some decomposition studies, little interaction between the disciplines of synthesis and analysis has occurred, presumably since the majority of spectrochemical applications utilize solution rather than solid samples, and gas phase chemical reactions are neither encouraged nor documented in the ICP operating in argon at atmospheric pressure. As research continues into the desolvation, vaporization, and atomization phenomena occurring for analytical samples in the ICP, some solid-gas and gas phase chemical reactions might be discovered; however, reactions in the ICP employed under conditions for spectral analysis appear to be generally free of major chemical effects.[296]

Part of the delay in developing a stable ICP discharge after Babat's publication rested upon designing reliable methods for heat protection of the discharge. Intensive work began about 1958,[35-37] and water jackets, sectioned, metallic, water-cooled walls, and porous dielectric walls were designed. Reed's approach to gas stabilization has proven effective and nearly universal for spectrochemical applications.

Two groups were stimulated by Reed's publication to begin work independently toward establishing the spectrochemical practicality of an ICP discharge. Recently, Greenfield[48] and Fassel[49] recounted events leading to their initial papers demonstrating the analytical potentials of the ICP appearing, respectively, in 1964[50] and 1965.[51] Mainly through the efforts of Greenfield and co-workers[3] and Fassel and colleagues[6] in the 1960s and early 1970s, the ICP has become a commercially successful product and a viable analytical tool. The comprehensive review prepared by Greenfield et al.[3] documents major activities occurring during the first decade of the analytical utilization of the ICP. In the 5 years following these initial analytical demonstrations, diverse systems and arrangements were explored to determine the full potential of the ICP with solution and powder samples in absorption as well as emission spectroscopy. Some of the ICP operating conditions used for both analytical and engineering studies undertaken between 1964 and 1974 are summarized in Table 1. A few recent operating conditions have been added as well. Since the

TABLE 1

Some ICP Operating Parameters 1964—1977

Gas Flow Rates (l/hr)					
Aerosol[a] carrier (sample)	Auxiliary (plasma)	Plasma (coolant)	Frequency (MHz)	Discharge shape	Ref.
300	300	1020	36	Toroidal	50,52
30	24	1320	3.8	Ellipsoidal	51,55
30	180	1080	36	Ellipsoidal	58
1155	1155	468	4	Ellipsoidal	183
1080—1200	1080—1200	0	5	Ellipsoidal	65-69
25	40	800	36	Ellipsoidal	60,63
4—20	16—80	500—800	40	Ellipsoidal	195
12.6	45	1180	31	Ellipsoidal	70,71
102	102	1800	4.8	Ellipsoidal	61
120	36	1200	30	Ellipsoidal	118
84	125	1528	3	Toroidal	223
102	45	1020	30	Toroidal	62
2.4—4.8	2.4—3.0	1000—1080	8	Ellipsoidal	163
2.4—4.8	26.4—28.8	300—480	8	Ellipsoidal	163
30	450	450(N_2)[b]	36	Toroidal	171
120—210	900	3840(N_2)[b]	7	Toroidal	201
60—120	0	900	52.3	Toroidal	78
120	420	1200	5.4	Toroidal	77
180	0	900	36	Ellipsoidal	108,109
290	420	1320	5.4	Toroidal	131
66	0	600	30	Toroidal	119
84	0	600	27	Toroidal	33
72	0	882	27	Toroidal	210
276—780(324)	0	1020	51.5	Toroidal	82
90—150	300—420	1200 (420)[c]	5.4	Toroidal	127
120—130	600—2100	1200—4200(N_2)[b]	7	Toroidal	73
60	0	570	27	Toroidal	92
60—150	0	540—600	40	Toroidal	72
48	0	300	26.5	Toroidal	173
50.4	0	540	27	Toroidal	145

[a] Fassel et al.[194] suggested a clarification in naming various gas flows according to their function as follows: (1) coolant gas to plasma gas, (2) plasma gas to auxiliary gas, and (3) aerosol gas to aerosol carrier gas.

[b] (N_2)indicates flow of nitrogen.

[c] 1200 starting flow; 420 operating flow.

as flow rate and the discharge shape are critical to achieving superior analytical results, ese parameters and the generator frequency re given. In the review by Greenfield et al.,[3] a milar table also identified the generator type nd manufacturer, nominal power level, and ebulization technique. Butler et al.[4] also stipated ICP tube configuration and discharge mperature in their review. As Fassel has comented,[49] this period was evolutionary. One iterion of the progress between 1964 and 1969 the improvement made in powers of detection r the determination of metallic elements in solution. Table 2 summarizes the limits of detection reported in both emission and absorption spectroscopy during that time. Fassel[283] recently presented a similar table with values obtained through 1976.

Greenfield et al.[50] had initially recognized the necessity to form a discharge with an axial pathway through its center into which sample aerosol could pass. Figure 2, taken from a patent issued to Greenfield et al.,[52,53] shows the combined nebulizer-plasma tube arrangement which guaranteed formation of this tunnel or hole in the discharge. The similarity to Reed's

TABLE 2

Limits of Detection 1964—1969 (μg/ml)

Element Wavelength (nm)	1964[50]	1965[54]		1965[58]		1965[56]	1966[60]	1966[57]	1967[56]	1967[59]		1967[63]	1968[61]		1969[62]
	Emission	Emission	Emission	Emission	Emission	Emission	Emission	Absorption	Emission	Emission	Absorption	Emission	Emission	Absorption	Emission
Al															
396.15	50	0.5	2	3	3	—	—	0.6	0.02	0.5	0.1	—	—	—	0.002
394.4	—	—	—	—	—	—	—	1	—	—	—	—	—	—	—
309.2	—	—	—	—	—	—	—	1	—	—	—	—	1	30	—
Sb															
287.7	—	—	—	—	—	—	—	—	5	—	—	—	—	—	—
259.8	—	—	—	—	—	—	—	—	—	—	—	—	—	—	0.2
As															
278.0	—	—	—	25	—	—	—	—	—	—	—	—	—	—	—
228.81	—	—	—	—	—	—	—	—	—	—	—	—	—	—	0.1
Ba															
455.40	—	10	1	—	—	—	1.4	—	0.002	—	—	—	—	—	0.0001
Bi															
472.25	—	20	—	—	—	—	—	—	—	—	—	—	—	—	—
B															
249.67	—	—	—	—	—	—	—	—	—	—	—	—	—	—	0.03
249.8	—	—	—	—	—	—	—	—	—	—	—	—	0.5	—	—
Cd															
326.1	—	—	—	—	20	—	—	—	—	—	—	—	—	—	—
228.8	—	—	—	—	—	—	1.1	—	—	—	—	—	—	—	0.03
Ca															
422.67	—	0.005	0.5	0.5	0.2	0.003	—	0.2	—	—	—	—	0.5	1	—
393.4	1	—	—	0.5	0.8	0.002	—	0.7	0.002	—	—	—	1	—	—
Ce															
418.66	—	—	—	—	—	—	—	—	—	—	—	—	—	—	0.007
Cr															
425.44	20	—	—	—	—	—	—	—	—	—	—	—	—	—	—
357.8	—	—	—	—	0.3	—	—	—	—	—	—	—	—	—	0.001
359.3	—	—	—	—	—	—	—	—	0.03	—	—	—	—	—	—
Co															
345.35	100	0.2	5	—	—	—	—	—	0.1	—	—	—	—	—	0.003
352.9	—	—	—	—	—	—	—	—	—	0.1	—	—	—	—	—
Cu															
324.8	10	0.01	1	1.2	0.2	—	—	—	—	—	—	—	1.7	1.5	—
327.4	—	—	—	—	—	—	—	—	0.01	—	—	—	—	—	—
Hf															
339.98	—	—	—	—	—	—	—	—	—	—	—	—	—	—	0.01
Fe															
										—	—	—	—	—	—
															0.005

TABLE 2 (continued)

Limits of Detection 1964—1969 (μg/ml)

Element Wavelength (nm)	1964[50]	1965[54]		1965[55]		1965[56]	1966[60]	1966[57]	1967[58]	1967[59]		1967[63]	1968[61]		1969[62]
	Emission	Emission	Emission	Emission	Emission	Emission	Emission	Absorption	Emission	Emission	Absorption	Emission	Emission	Absorption	Emission
238.2	—	—	—	—	—	0.1	—	—	—	—	—	—	—	—	—
373.4	—	—	—	—	—	—	—	—	0.1	—	—	—	—	—	—
259.9	—	—	—	—	—	—	—	—	—	—	—	0.2	—	—	—
La															
408.6	—	—	—	50	50	—	—	—	—	—	—	—	—	—	0.003
b															
405.78	—	0.8	—	—	—	—	1.6	—	0.3	0.1	—	2.0	—	—	0.008
283.31	—	—	5	—	—	—	—	—	—	—	—	2.0	—	—	—
Mg															
285.21	—	0.03	2	2	2	—	0.2	0.06	—	—	—	—	—	—	—
279.55	5	—	—	—	—	—	—	—	0.005	—	—	—	—	—	—
518.36	—	—	—	—	—	—	—	—	0.1	—	—	—	—	—	—
Mn															
403.07	10	0.05	1	2	1	—	0.3	—	—	0.01	—	—	—	—	—
257.6	—	—	—	—	—	—	—	—	0.05	—	—	—	—	—	—
Hg															
253.65	—	0.5	—	—	—	—	—	—	—	—	—	—	—	—	—
Mo															
379.8	—	—	—	—	—	—	—	—	0.05	0.5	0.1	—	—	—	—
313.3	—	—	—	—	—	—	—	—	—	—	—	—	0.8	20	—
Ni															
341.48	5	—	—	—	—	—	—	—	0.05	—	—	0.5	—	—	—
352.4	—	—	—	—	1	—	0.5	—	—	—	—	0.5	—	—	0.006
Nb															
353.53	—	—	—	—	—	—	—	100	—	—	—	—	—	—	—
405.89	—	—	—	—	—	—	—	40	—	—	—	—	—	—	0.01
407.97	—	—	—	—	—	—	—	40	—	—	—	—	—	—	—
410.09	—	—	—	—	—	—	—	30	—	—	—	—	—	—	—
P															
253.5	—	—	—	—	10	—	—	—	—	—	—	—	—	—	—
213.6	—	—	—	—	—	—	4	—	—	—	—	—	—	—	0.1
Re															
346.05	—	—	—	—	—	—	—	30	—	—	—	—	—	—	—
Rb															
7800	—	—	—	—	—	—	—	10	—	—	—	—	—	—	—
Si															
251.6	—	—	—	3	—	—	—	—	—	—	—	—	—	—	—
Ag															
338.3	—	—	—	—	—	—	—	—	—	0.5	0.1	—	—	—	—
328.1	—	—	—	—	—	—	—	—	—	—	—	—	1	0.5	—

TABLE 2 (continued)

Limits of Detection 1964—1969 (μg/ml)

Element	Wave (nm)	1964[50]	1965[54]		1965[55]		1965[56]	1966[60]	1966[57]	1967[58]	1967[59]		1967[63]	1968[61]		1969[62]
		Emission	Emission	Emission	Emission	Emission	Emission	Emission	Absorption	Emission	Emission	Absorption	Emission	Emission	Absorption	Emission
Sr																
40		—	—	1	—	—	—	—	—	0.002	—	—	—	—	—	0.00002
46		—	—	—	0.09	0.09	—	—	—	—	—	—	—	—	—	—
Ta																
26		—	—	—	—	—	—	—	—	—	—	—	—	2	>100	—
26		—	—	—	16	—	—	—	—	—	—	—	—	—	—	—
30		—	—	—	—	—	—	—	—	—	—	—	—	—	—	0.07
Th																
40		—	—	—	40	40	—	—	—	—	—	—	—	—	—	0.003
Sn																
28		—	—	—	—	—	—	—	—	1	—	—	—	—	—	—
34		—	4	—	—	—	—	—	—	—	—	—	—	—	—	—
Ti																
36		—	—	—	—	15	—	—	—	—	—	—	—	—	—	—
36		—	—	—	—	7	—	—	—	—	—	—	—	—	—	—
Ti																
36	3.19	—	—	—	—	9	—	—	—	—	—	—	—	—	—	—
46	7.48	—	—	—	—	5	—	—	—	—	—	—	—	—	—	—
Ti																
33		—	—	—	—	—	—	—	—	0.03	—	—	—	0.4	—	0.003
W																
40		—	—	—	3	3	3	—	—	—	—	—	—	—	—	0.002
46		—	—	—	—	—	3	—	—	—	—	—	—	—	—	—
U																
40		—	—	—	—	—	—	—	—	—	—	—	—	—	—	0.03
V																
31		—	0.1	10	—	—	—	—	—	—	—	—	—	1.3	40	—
31		—	—	—	—	—	2	—	—	0.5	—	—	—	—	—	0.006
43		—	—	—	—	—	—	—	—	—	—	—	—	—	—	—
Y																
33	1.03,407.74	—	—	—	—	—	20	—	—	—	—	—	—	—	—	0.0002
36	1.24,464.37	—	—	—	—	—	10									
Zn																
33		—	4	—	—	—	—	—	—	1	—	—	0.7	—	—	—
48		—	—	—	30	—	—	—	—	—	0.1	—	—	—	—	—
21		—	—	—	—	—	—	—	—	—	0.01	3.3	—	—	—	0.009
Zr																
34		—	—	—	15	15	—	—	—	—	—	—	—	—	—	0.005

Note: rption denotes atomic absorption measurement, and emission denotes emission measurement.

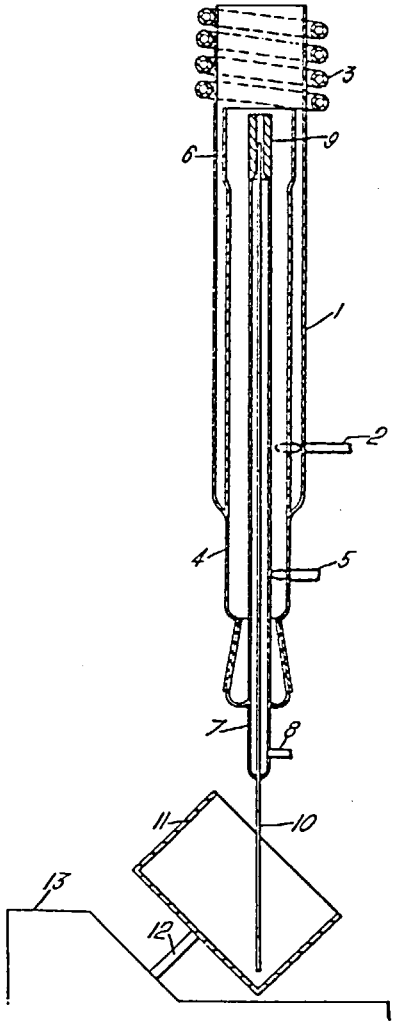

FIGURE 2. Patented ICP torch for spectrochemical analysis with three coaxial gas flows; (1) quartz confinement tube with 25-mm outer diameter, (2) tangential plasma (coolant) gas inlet, (3) 30-mm induction coil comprised of 3.5 turns of 6-mm diameter copper tubing, (4) quartz tube for auxiliary (plasma) gas, (5) tangential auxiliary (plasma) gas inlet, (6) open end of auxiliary gas tube with 20.5-mm diameter and 22-mm length located 20 to 40 mm from open end of outer confinement tube, (7) aerosol carrier gas tube with (8) aerosol carrier gas inlet which terminates at (9) a capillary nozzle, (10) an optional capillary tube which acts as an integral nebulizer — not commonly used with external nebulizer and spray chambers, (11) an inclined drum holding sample and rotating around (12) the shaft driven by (13) a motor. (From Greenfield, S., Jones, I. L. W., and Berry, C. T., U.S. Patent 3, 467, 471, September 16, 1969.)

configuration in Figure 1 is apparent, but the sample need not be introduced solely by means of the integral nebulizer. Generally, sample aerosol is generated pneumatically or ultrasonically in an external spray chamber, and solvent is sometimes removed by means of an optional desolvation arrangement. As indicated in Table 1, the arrangements used by Fassel et al.[51,57] and Veillon and Margoshes[61] during this time did not permit formation of a center channel under their operating conditions until 1968, when Dickinson[218] duplicated Reed and Greenfield's concept to force sample aerosol along the discharge centerline. When combined with a desolvation apparatus and a coupling and tuning unit in 1969, Dickinson and Fassel[62] achieved powers of detection superior to any ICP values published previously. This report stands as a major landmark in ICP progress.[1] Dickinson and Fassel not only defined an experimental arrangement that would work on a practical basis, but they also demonstrated that elements diverse in nature could be determined both in a way superior to previous ICP efforts and on a basis competitive with atomic absorption spectrophotometry (AAS) using flame atom cells. Equally important in convincing possible manufacturers and industrial users was the clear documentation of reduced or negligible interelement interference effects, notably solute vaporization, compared to other spectroscopic sources with solution samples. The report by Veillon and Margoshes[61] completely disregarded the importance of sample introduction into the discharge by removing the central injection tube completely. They reported serious solute vaporization interferences resulting, presumably, from the inefficient heating of analyte as it passed around instead of through the discharge.

The introduction of the ICP spectroscopic source came at a time of exponential activity in AAS and the capabilities of the ICP for single element analysis had to match those of AAS.[49] Not until 1969 could this claim be made for the ICP. The interest in AAS channeled some of the early ICP studies toward testing the ICP discharge as an atom reservoir for AAS. Wendt and Fassel,[57] Greenfield et al.,[64] Britske et al.,[59] Bordonali et al.[65-69] Barnett et al.,[70,71] and Veillon and Margoshes[61] made exploratory measurements with ICP-AAS. Bordonali and Biancifiori[69] also received a patent in 1972 covering

the analysis of trace elements by ICP-AAS. Application of the ICP in emission rather than absorption has proven to be more widely accepted even in light of the recent evaluation by Abdallah et al.,[72] who suggested reasons for the limited capabilities in early measurements.

Although the original ICP arrangement was patented[52,53] by Greenfield et al. and marketed by Radyne,[56] relatively few instruments were set up.[3,101,108,109] After Dickinson and Fassel's improvements in 1969, another 4 years were needed for development and engineering to produce a marketable instrument system. Meanwhile, early ICP systems in the hands of Greenfield and co-workers were unobtrusively solving analytical problems on a routine basis.[73] The first modern commercial ICP emission spectrometric instrument was introduced in 1974 by the Applied Research Laboratories, Sunland, Calif.,[74,75] and this was followed in 1975 by an instrument produced by the Jarrell Ash Division of Fisher Corporation, Waltham, Mass. Since that time, other manufacturers have offered instruments and components[76,281] (Tabel 9), but engineering developments are still underway at a number of other companies.

Further momentum was added to the ICP drive when the results given by Dickinson and Fassel were verified independently, using totally different ICP instruments and conditions in 1972, by Souilliart and Robin[77] and Boumans and de Boer.[78] To indicate the status of ICP detection capabilities in 1974,[6] these values are compared in Table 3, along with those obtained by Fassel and colleagues, to those reported for flame absorption, emission, and fluorescence techniques. As commercial instrumentation has become available during the past 5 years, emphasis in ICP research has shifted from demonstrating powers of detection to demonstrating other performance characteristics such as reliability, stability, precision, and accuracy needed for daily routine analysis. Examples of these are given in Section I.C.

Since the early 1970s, ICP pioneers have been joined by equally enthusiastic spectroscopists in investigating the properties and applications of the ICP source. Their combined publications account for the majority of papers dealing with the ICP to the present. Robin, Mermet, and colleagues,[72,77,79,126-135,159,160,250,252,275] Boumans and de Boer,[78,87,103-106,116,122,124,149,150,237-239,256,278-280] Kirkbright et al.,[80,96,108-110,125,136] Scott et al.,[33,84-86] Kornblum and de Galan,[82,83] Ohls et al.,[81] and Barnes et al.[34,88,117,161,173,180,181,190,191] have made public research contributions to the development of the ICP during the past five years. In the main body of this report, details of these efforts will be described.

Recent advances in both research and applications have also encouraged the publication of a monthly newsletter beginning in 1975. The ICP Information Newsletter, edited by Barnes,[89] provides reports on current ICP publications, conferences and lectures, applications, and original research.

Evaluating the first 13 years of spectrochemical analysis with the ICP source, Boumans and de Boer,[78,116] Fassel,[283] Fassel and Kniseley,[6] Greenfield et al.,[3] Sharp,[5] and Winefordner et al.[91] agreed that the ICP is an exceptional source. Barnes[90] emphasized that the ICP has evolved in the history of spectrochemical analysis at a time when its growth both commercially and in fundamental research is encouraged; he predicted that the ICP may well become one of the best characterized and most effectively applied spectrochemical sources yet discovered.

Arguments for these points of view will surface in each of the following sections, which treat details of instrumentation, plasma properties and interactions with samples, and spectral excitation.

C. ICP Characteristics

1. Introduction

A brief survey of analytical, chemical, and physical properties of the ICP discharge for spectrochemical analysis is presented in this section. The quality of analytical results obtained with the ICP in emission spectroscopy is represented by its accuracy, dynamic range, limits of detection, precision, and sensitivity. Instrument stability and reliability and interelement interference effects directly affect these characteristics. Physical properties measured in the ICP include spatial distributions of time-averaged values of temperature, electron and analyte number densities, pressure and velocity, and electrical and magnetic fields. These influence the location and magnitude of the emission sig-

TABLE 3

Comparison of Experimentally Determined Detection Limits (μg/ml)

	ICP			Flame		
Element	AL[a]	B and deB[b]	S&R[c]	AAS	AFS	AE
Ag	0.004	—	0.03	0.005	0.0001	0.008
Al	0.002	0.002	—	0.03	0.005	0.005
As	0.04	0.4	—	0.1	0.1	50
Au	0.04	—	0.04	0.02	0.05	4
B	0.005	0.08	0.03	6	—	30
Ba	0.0001	0.00002	—	0.05	—	0.002
Be	0.0005	0.0004	—	0.002	0.01	0.1
Bi	0.05	—	—	0.05	0.05	2
Ca	0.00007	0.00002	—	0.001	0.000001	0.0001
Cd	0.002	0.003	—	0.001	0.00001	0.8
Ce	0.007	0.002	0.03	—	0.5	10
Co	0.003	—	—	0.005	0.005	0.03
Cr	0.001	0.0003	—	0.003	0.004	0.004
Cu	0.001	0.0001	—	0.002	0.001	0.01
Dy	0.004	—	0.009	0.2	0.3	0.05
Er	0.001	—	0.01	0.1	0.5	0.04
Eu	0.001	—	0.003	0.04	0.02	0.0005
Fe	0.005	0.0003	—	0.005	0.008	0.03
Ga	0.014	0.0006	—	0.07	0.01	0.01
Gd	0.007	—	0.01	4	0.08	2
Ge	0.15	0.004	—	1	20	0.5
Hf	0.01	—	0.04	8	100	20
Hg	0.2	0.001	—	0.5	0.02	40
Ho	0.01	—	0.01	0.1	0.1	0.02
In	0.03	—	—	0.05	0.002	0.003
La	0.003	0.0004	0.006	2	—	2
Lu	0.008	—	0.01	3	3	0.2
Mg	0.0007	0.00005	0.00005	0.0001	0.001	0.005
Mn	0.0007	0.00006	—	0.002	0.002	0.005
Mo	0.005	0.0002	—	0.03	0.06	0.1
Na	0.0002	0.0003	—	0.002	—	0.0001
Nb	0.01	—	0.002	1	1	0.06
Nd	0.05	—	0.01	2	2	0.2
Ni	0.006	0.0004	—	0.005	0.003	0.02
P	0.04	0.07	—	—	—	—
Pb	0.008	0.002	—	0.01	0.01	0.1
Pd	0.007	0.002	—	0.03	—	0.05
Pr	0.06	—	0.03	10	1	0.07
Pt	0.08	—	—	0.1	—	2
Rh	0.003	—	—	0.03	0.1	0.02
Sb	0.2	—	—	0.1	0.05	0.6
Sc	0.003	—	—	0.1	0.01	0.01
Se	0.03	—	—	0.1	0.04	100
Sm	0.02	—	—	2	0.1	0.1
Si	0.01	—	—	0.1	—	5
Sn	0.3	0.03	—	0.02	0.05	0.3
Sr	0.00002	—	—	0.01	0.01	0.0002
Ta	0.07	—	0.03	5	—	20
Tb	0.2	—	0.02	2	0.5	0.03
Te	0.08	—	—	0.1	0.05	200
Th	0.003	—	—	—	—	200
Ti	0.003	0.0002	0.001	0.09	0.1	0.2
Tl	0.2	—	—	0.03	0.008	0.02
Tm	0.007	—	0.01	0.2	0.1	0.02
U	0.03	—	—	—	—	10

TABLE 3 (continued)

Comparison of Experimentally Determined Detection Limits (μg/ml)

	ICP			Flame		
Element	AL[a]	B and deB[b]	S&R[c]	AAS	AFS	AE
V	0.006	0.0002	0.001	0.02	0.07	0.01
W	0.002	0.001	0.1	3	—	0.5
Y	0.0002	0.00006	0.0005	0.1	—	0.04
Yb	0.0009	0.00004	0.005	0.04	0.01	0.002
Zn	0.002	0.016	0.05	0.002	0.0002	50
Zr	0.005	0.0004	0.005	5	—	10

[a] Ames Laboratory, U.S. Department of Energy, Iowa State University, Ames. Detection limits represent concentrations required to produce a line signal twice as great as the SD of the background scatter (noise).
[b] Reference 78. Detection limits reported on the same basis as Ames Laboratory data.
[c] Reference 77. Dectection limits represent concentrations required to produce a line signal six times as great as the SD of the background scatter (noise).

nals and noise from analyte and discharge gas. In turn, the physical properties of the discharge are controlled by the operating characteristics of the equipment arrangement and depend on the chemical and physical properties and quantities of the discharge gas, analyte, and solvent. Practical accommodation of these parameters to reach a high quality of analytical results requires appropriate calibration procedures.

Many of the physical properties of the induction plasma reported prior to 1970 were considered by Eckert,[35] Greenfield et al.,[3] and Raizer.[13] Most of these measurements describe physical or engineering induction discharges rather than spectroanalytical ICP discharges. Only within the past few years have ICP discharges for spectrochemical analysis come under close scrutiny, so that many values obtained recently are related to the analysis process. In much the same way, the analytical characteristics of the ICP have become best documented as commercial instruments are applied to the daily job of routine sample analysis. Therefore, typical values are summarized to represent current practices. Commercial ICP instruments incorporate computer programs to calculate analytical properties on a sample-to-sample basis, so that the variations of analytical properties are readily available to the instrument operator.

Boumans[116,124] evaluated emission spectroscopy for the routine simultaneous multielement analysis of solutions with various excitation sources, including the ICP, high-temperature flames, current-free and current-carrying DC plasmas, and microwave plasmas. He concluded that even though precise data on instrument and operating costs, ease in operation, and overall reliability of the equipment were lacking at the time, the analytical performance of the ICP was superior to that of alternative excitation sources.

More recently, Boumans[239] made a tentative comparison of the glow discharge lamp, ICP, and DC carbon arc for universal analysis. He concluded that the ICP will be the preferred source if a system for universal analysis should cover both samples presented as solids and solutions. However, if the system should be limited only to solid samples, then a more detailed assessment of the three sources must be made on the basis of the following factors: time and cost of sample preparation, required accuracy and detection limits, cost of expendable materials, and the general arrangement of the laboratory, particularly the availability of chemical analysts who can deal reliably with the dissolution of solids and handling of solutions.

2. Accuracy and Stability

Winge et al.[93] have observed that a significant bias in analytical results may be produced during the first 30 min of operation, because of

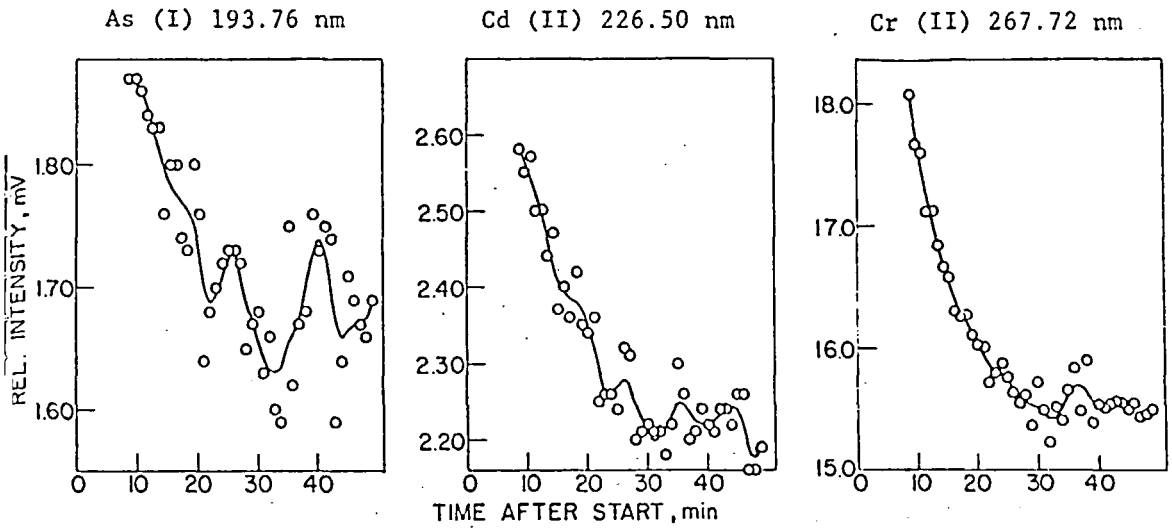

FIGURE 3. Time-intensity stabilization curves for the background of a 1.1-kW ICP source with a deionized water sample measured at 3 or 31 channels of a commercial ICP spectrometer system. (From Winge, R. K., Katzenberger, J. M., Kniseley, R. N., and Fassel, V. A., Annual Progress Report for Interagency Agreement EPA-IAG-D6-0417, Iowa State University, Ames, 1977. With permission.)

insufficient warm-up time given the ICP instrument, especially the power supply and components in the discharge source chamber. Time-intensity curves for three element channels in a multichannel spectrometer are shown in Figure 3 during the warm-up period. Individual differences for each element begin to appear during later periods. Once the system has stabilized, long-term (i.e., 8 hr to 0.5 year) stability may be only slightly poorer (±2 to 5%) than short-term (i.e., 0.5 to 8 hr) values (less than ±1%). Some short-term stability values obtained from a reference sample that was determined three times at approximately equal time intervals during a normal analysis sequence are listed in Table 4.

Measurement of accuracy depends upon analysis of reference samples and/or comparison with alternative methods. The values obtained by Dahlquist et al.[94] are represented in Figure 4 for the simultaneous determination of trace elements in complex biological matrices. Similar comparisons were reported by Scott et al.[84,86,92] for rocks, soils, and plant materials. The accuracy of analysis of two ICP systems for five elements in diverse standard reference steel samples with comparison to certified values is illustrated in Table 5 for three different ICP-AES systems.[95] The changes in matrix appear not to influence the accuracy significantly if straightforward precautions are followed. Elaborate precautions for matching sample and standard solution compositions are not required with ICP-AES. For example, Dahlquist et al.[94] established analytical calibration functions with multielement synthetic reference solutions containing a constant amount of acid and matrix elements (Na, K, P, Ca, and Mg) as analytes prepared by using simple gravimetric and volumetric procedures. Similarly, Butler et al.[95] based their analysis of ferrous alloys upon fixed acid content synthetic reference solutions comprised of only Fe and the analyte. They made no attempt to match the overall composition of the samples and synthetic reference solutions, since the pure Fe solution served completely as the blank for background corrections and the matrix for reference solutions. As Dahlquist et al.[94] demonstrated, the precision and accuracy of the ICP with a commercial multichannel spectrometer system are sufficient to distinguish subtle differences in sample preparation and procedures within certified ranges of standard reference materials. The variation in the ratios of matrix elements and their concentration has, in general, little or no effect on the accuracy with which analyses are made.

3. Calibration and Dynamic Range

Statistical data on analytical curves for 13

TABLE 4

Reproducibility of Analytical Data From a Reference Sample Run at Regular Intervals During a Normal Analytical Sequence

Element	Wavelength (nm)	Reference standard (μg/l)	Measured average (μg/l)	SD (μg/l)	Relative SD (%)
Al	308.22	1000	984	17	1.7
Al	396.15	1000	1000	66	6.6
As	193.76	200	193	44	23
B	249.68	200	199	6.8	3.4
Ba	455.40	200	201	1.4	0.70
Be	313.04	2	2.1	0.09	4.3
Co	238.89	100	101	2.9	2.9
Cr	267.72	20	19	2.5	13
Cu	324.75	20	20	0.6	3
Fe	259.94	4000	3950	58	1.5
Hg	253.65	200	197	13	6.6
Mn	257.61	200	196	2.5	1.3
Mn	403.08	200	196	6.2	3.2
Ni	231.60	100	105	5.4	5.1
Pb	220.35	200	283	31	11
Pb	405.78	200	232	10	4.5
Sb	206.84	200	241	22	9.1
Sn	303.41	200	229	73	32
Sr	407.77	2000	2030	11	0.54
V	292.40	20	23	1.2	5.2
Y	371.03	20	21	0.4	1.9
Zn	213.86	1000	1020	16	1.6

From Winge, R. K., Fassel, V. A., Kniseley, R. N., DeKalb, E., and Haas, W. J., *Spectrochim. Acta*, B32, 327 (1977). With permission.

elements in steel collected over a period of a year are given in Table 6. Not only are the curves essentially linear over a range of up to 4 orders of magnitude, but the change in slope is generally less than ±4% during the period. Reproducibility of independent calibrations reveals drift which typically ranges from 0.4 to 4% for commercial instrument systems.

Kirkbright and Ward[80,96] predicted and demonstrated that a longer linear calibration range could be achieved with the ICP source than with a flame. Human and Scott[85] measured the self-reversal of resonance lines for high analyte concentrations in the ICP and compared experimental profiles of spectral lines to theoretical profiles. Analytical curves for three Ca II lines, shown in Figure 5, exhibit different degrees of self-absorption at high concentration levels.[97] Since the 315.89-nm line is some three orders of magnitude less intense than the other two lines, its calibration remains linear to 500 mg/l, whereas the others bend. The upper extent of linearity depends upon the operating parameters of the ICP, the spectral line selected, and the spectrometer readout system.[85]

4. Precision

The precision, expressed as relative standard deviation (SD), of total measured intensities from the ICP is generally less than 1% when the analyte signal is a large part of the total signal, because of the stability of the discharge. Generalized relations between the relative SD and concentration multiples of the detection limit and/or background equivalent concentration (BEC) were given by Boumans[238] and Ajhar et al.[98] The BEC of an analyte is the concentration that will give a signal equal to the background emission. A graphical representation is shown in Figure 6.[98] The curve was calculated on the basis of 0.4% relative SD for both line and background intensities. Different matrices have little effect on the basic relationships. Spectral background intensities are re-

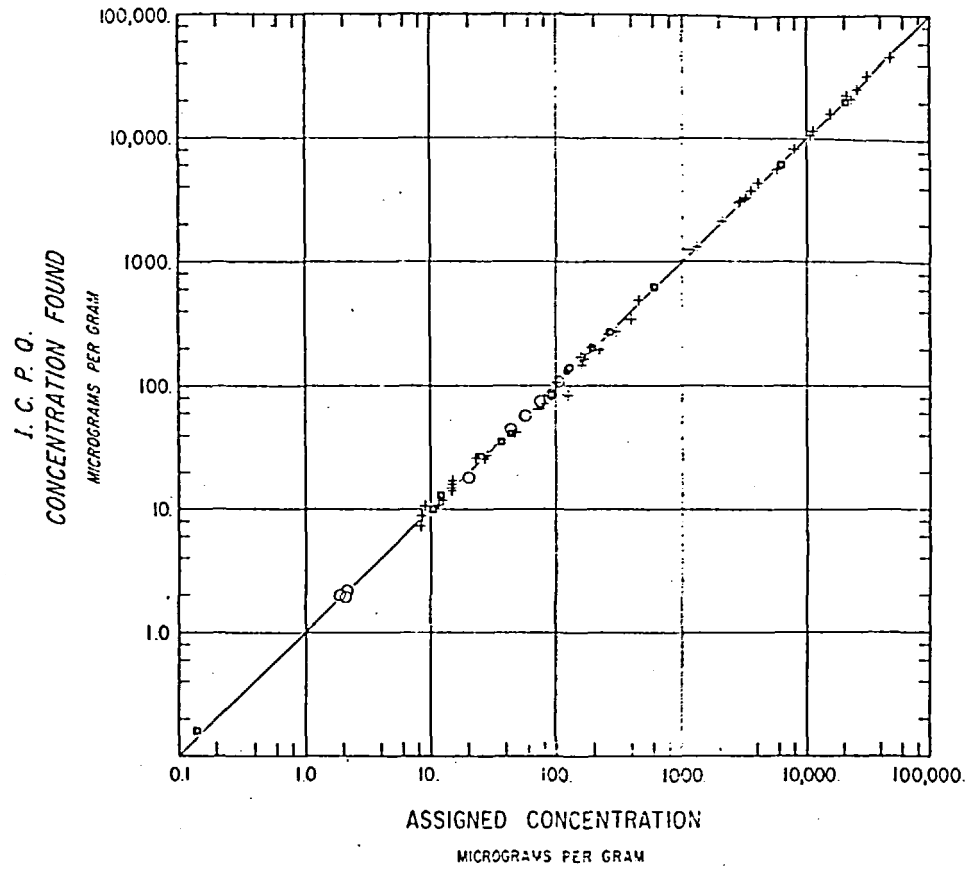

FIGURE 4. Comparison of results obtained by ICP-AES for reference materials plotted against the certified values. NBS standard reference material — orchard leaves and bovine liver; □ for Ca, Mg, Sr, Ba, Fe, Cu, Zn, Mn, and Pb; diverse plant digests from Le Comite Inter-Institutes d'Etude des Techniques Analytiques de Diagnostic Foliare (CII); + for Ca, Mg, Fe, Cu, Zn, and Mn; and independently certified commercial control blood sera; O for Ca, Mg, Fe, Cu, and Zn. (From Dahlquist, R. L., Knoll, J. W., and Irons, R. D., 3rd Annual Meeting FACSS and XIX CSI and VI ICAS, Abstr., Paper No. 80, Philadelphia, 1976. With permission.)

ported to be 100 times smaller and 3 times more stable with the ICP than with most other spectrochemical emission sources.[99]

The relative SD of the background signal of the ICP is approximately constant at less than 1% (e.g., 0.3 to 0.6%) over a wide range of operating conditions, and only at very low power levels does the standard deviation increase.[87,100,122] Thus, the evaluation of signal-to-background ratio with ICP operating conditions is sufficient to define detection limits[78,122] and optimize ICP conditions. Even with photographic detection, precision values on the order of 2% are obtained for the analysis of nickel alloy solutions,[101] and these values are extremely good for a photographic method.

5. Detection Limits

The stability and precision of ICP generators, spectrometers, and readout systems are sufficiently reliable so that limits of detection now depend more upon the type of nebulizer and nebulization arrangements than upon the remainder of the measurement.[102] As Boumans and de Boer[87,122,256,280] and Olson et al.[102] have emphasized, the detection limits depend directly upon the rate of solvent-free aerosol reaching the discharge in low power argon plasmas. Because ultrasonic nebulizers produce aerosols of greater number density and of more uniform particle size than pneumatic nebulizers,[102] ultimate detection limits using ultrasonic nebulizers have been reported. In contrast, rou-

TABLE 5

Accuracy Studies

Element	NBS sample no.	Matrix	System I (wt %)	System II (wt %)	System III (wt %)	NBS value (wt %) Average	NBS value (wt %) Range
Al	19g	Open hearth (0.2% C)	0.032 ± 0.001	0.033 ± 0.0007	0.030	0.031	0.027—0.033
	33c	3 Ni	0.033 ± 0.001	0.037 ± 0.001	0.031	0.032	0.030—0.034
	169	77 Ni-20 Cr	0.095	0.10	0.130	0.095	0.095—0.105
Cr	19g	Open hearth (0.2% C)	0.370 ± 0.016	0.375 ± 0.015	0.360	0.374	0.369—0.380
	33c	3 Ni	0.055 ± 0.004	0.052 ± 0.002	0.051	0.052	0.049—0.056
	129b	Bessemer (0.1% C)	0.018	0.020	0.021	0.018	0.014—0.019
Cu	160	19 Cr-9 Ni-3 Mo	0.051	0.05	0.048	0.053	0.047—0.06
	169	77 Ni-20 Cr	0.014	0.014*	0.015	0.015	0.013—0.02
	341	20 Ni-2 Cr	0.150 ± 0.002	0.130 ± 0.006	0.150	0.152	0.145—0.159
Mn	19g	Open hearth (0.2% C)	0.56 ± 0.007	0.59	0.57	0.55	0.55 —0.559
	33c	3 Ni	0.73 ± 0.01	0.73	0.78	0.73	0.73 —0.735
	73c	Stainless steel	0.33 ± 0.005	0.31 ± 0.004	0.28	0.33	0.325—0.34
Ni	73c	Stainless steel 13 Cr	0.240 ± 0.007	0.230 ± 0.006	0.220	0.246	0.241—0.255
	111b	1 Mn-2 Ni	1.80	1.78	1.82	1.81	1.80 —1.83

* This sample was run on a time integration of 20 sec without the internal reference channel. Use of the internal reference channel to control the integration caused low results, probably as a result of a spectral interference within the bandpass of the internal reference channel. This sample has very high concentration of Ni and Cr.

TABLE 6

Statistical Data on Analytical Curves Obtained by Linear Least Squares Fit to a Log-Log Plot

Element	Conc. range (wt %) in steel	Slope	Relative SD of slope (%)	Relative SD of intensities (%)
Al	0.002—1.0	1.03	1.60	4.61
Cr	0.002—20	1.00	1.31	3.57
Cu	0.002—2.00	0.990	1.22	3.13
Mn	0.002—2.0	1.04	1.07	3.23
Ni	0.01 —10	1.04	2.03	4.37
Nb	0.005—0.2	0.986	2.31	3.15
W	0.005—0.2	0.991	2.86	2.43
Zr	0.005—0.2	0.971	3.70	5.05
Ce	0.005—0.1	1.01	3.88	2.34
La	0.005—0.1	0.970	0.903	0.943
Pr	0.005—0.1	0.980	1.47	1.53
As	0.002—0.1	0.985	2.73	7.10
Pb	0.001—0.02	0.971	1.86	1.79

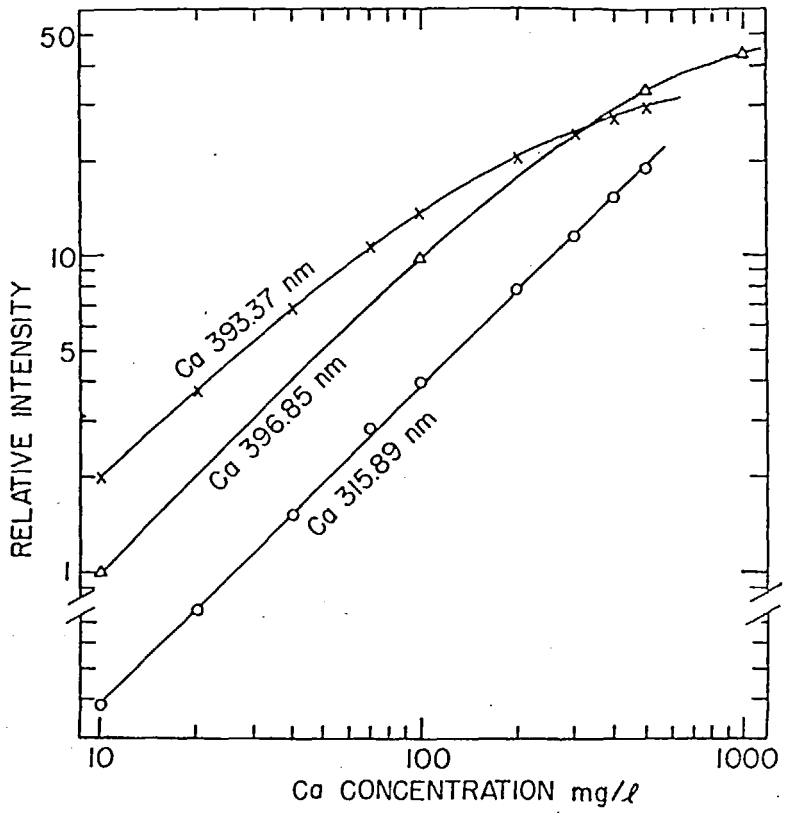

FIGURE 5. Analytical curves for calcium that illustrate the different degrees of self-absorption associated with the three calcium ion lines. (From Winge, R. K., Katzenberger, J. M., Kniseley, R. N., and Fassel, V. A., Annual Progress Report for Interagency Agreement EPA-IAG-D6-0417, Iowa State University, Ames, 1977. With permission.)

tine commercial ICP systems use one of a variety of pneumatic nebulizers, which restrict practical detection limits currently reported. A list of the best current limits of detection is given in Table 7 for both ultrasonic and pneumatic nebulizers. Olson et al.[102] directly compared the differences in detection limits for pneumatic and ultrasonic nebulizers with and without solvent removal. For the conditions investigated, desolvation was required with ultrasonic nebulization. However, approximately an order of magnitude improvement was achieved with the ultrasonic compared to the pneumatic system. Detection limit values vary in routine analysis from day-to-day and even hour-to-hour, although variation is usually within a factor of 1.5 to 2. In general, the detection limits in ICP-AES are not appreciably affected by the presence of a matrix in the solution, unless spectral interference occurs either as a coincidence of a spectral line or band emitted by the matrix with the most sensitive line of the analyte or as a substantial enhancement of the background as a result of stray light originating from strong emission by certain matrix elements (e.g., Ca, Mg, Al, Na).[3,6,104,165,211,238]

6. Multielement Capability and Choice of Optimum Conditions for Simultaneous Multielement Analysis

Because ICP-AES is an emission method, its capabilities for simultaneous multielement analysis (SMEA) are fundamentally excellent[116,124] In an emission method, the signals of all analytes are generated simultaneously in the excitation source; these signals can be detected simultaneously after dispersion by a suitable spectroscopic instrument. However, in an emission method, the widely different chemical and physical properties of the chemical elements and their compounds cannot be circumvented; thus, the generation of signals

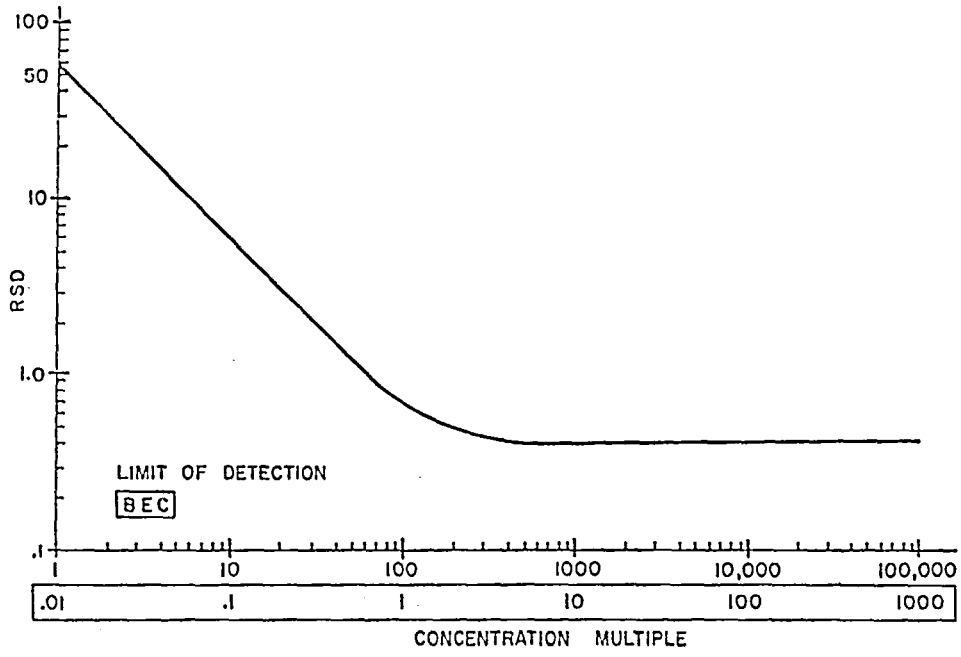

RELATIVE STANDARD DEVIATION VS CONCENTRATION MULTIPLE

FIGURE 6. Relative standard deviation (RSD) in % as a function of multiples of limit of detection (upper scale) and background equivalent concentration (BEC) in lower scale. (From Ajhar, R. M., Dalager, P. D., and Davison, A. L., *Am. Lab.*, 8 (3), 71 (1976). With permission.)

from a given sample can never be entirely optimized for all constituents simultaneously. Therefore, the task of achieving some acceptable compromise arises. In addition, optimization may be specified differently depending upon the analytical problem. Various questions can be raised in this context,[303] for example:

1. How easy or difficult is it to find compromise conditions for SMEA with ICP-AES?
2. Which experimental parameters should be considered to play a major role in selecting these conditions?
3. What sacrifices have to be made eventually?
4. Is the result of the compromise closer to the ideal than that which can be reached with other sources?

Various investigators[33,62,73,78,104] have documented that for a given ICP generator, coupling configuration, and plasma tube arrangement, the critical parameters for analysis are power input to the discharge, flow rates of the gases and sample aerosol, and observation region in the plasma. Dickinson and Fassel[62] and Boumans and de Boer[78] explicitly demonstrated that single-element optimization of detection limits is feasible by varying one or more of these critical parameters. In turn, the results of these investigations indicated that the selection of experimental conditions to achieve a compromise for SMEA would not be difficult. Actually, in defining compromise conditions, Boumans and de Boer[104] and Larson et al.[115] considered additional analytical characteristics as well as detection limits and the balance of detection limits among various elements. It was found that, in addition to detection limits, interferences depend critically on the principal parameters of the ICP for a given arrangement (carrier gas flow rate, power input, observation height).[104,115] This dependence is illustrated (Figure 7) for the interference effect of KCl on three spectral lines and their detection limits as functions of principal parameters in the argon ICP explored by Boumans and de Boer.[104] Assuming that the three spectral lines were representative, Boumans and de Boer tentatively derived from the data in Figure 7 compromise experimental conditions under which, on one hand, a good balance would be achieved in the

TABLE 7

State-of-the-art detection limits (cl) in 1977 reported for argon ICP discharges operated with either an ultrasonic nebulizer (USN) with desolvation or a pneumatic nebulizer (PN) without desolvation.[a]

Element	Wavelength (nm)	cl (ng/ml) (USN)	Ref.	cl (ng/ml) (PN)	Ref.
Ag I	328.07	—	—	2	97
Al I	396.15	0.2	104, 116, 124	1	256, 279, 303
Al I	308.22	0.4	102	7	102
As I	193.76	2	102	30	102
As I	228.81	6	104, 116, 124	30	256, 279, 303
Au I	267.59	—	—	0.9	256, 279, 303
B I	249.77	0.1	104, 116, 124	0.2	256, 279, 303
Ba II	455.40	0.01	104, 116, 124	0.06	256, 279, 303
Be I	234.86	0.003	104, 116, 124	0.03	256, 279, 303
Bi I	289.80	10	106	50	256, 279, 303
C II	193.04	—	—	100	111
Ca II	393.37	0.0001	104,116, 124	0.0005	256, 279, 303
Cd I	228.80	0.2	104, 116, 124	0.3	256, 279, 303
Cd II	226.50	0.07	102	0.4	303
Ce II	418.66	0.4	104, 116, 124	2	256, 279, 303
Co II	238.89	0.1	102	0.4	256, 278, 279, 303
Cr II	267.72	0.08	102	0.5	256, 278,279, 303
Cr I	357.87	0.1	104, 116, 124	1	256, 278, 279, 303
Cu I	327.40	0.06	104, 116, 124	0.3	256, 279, 303
Dy II	353.1	—	—	4	6
Er I	400.8	—	—	1	6
Eu II	381.97	—	—	0.06	256, 278, 279, 303
Fe II	259.94	0.09	104, 116, 124	0.2	256, 279, 303
Fe II	261.19	0.5	102	7	102
Ga I	417.21	0.6	104, 116, 124	3	256, 279, 303
Gd II	342.25	0.4	106	2	256, 279, 303
Ge I	265.12	0.5	104, 116, 124	2	256, 279, 303
Hf II	339.98	—	—	10	6
Hg I	184.96, 253.71	—	398	1	108
Ho II	345.6	—	—	3	334
I I	206.16	—	—	10	94
Ir I	322.1	—	—	90	107
K I	766.5	—	—	30	112
La II	408.67	0.1	104, 116, 124	0.4	256, 279, 303
Li I	670.78	0.02	116, 124	0.3	256, 279, 303
Lu I	451.9	—	—	8	6
Mg II	279.55	0.003	104, 116, 124	0.01	256, 279, 303
Mn II	257.61	0.01	102	0.06	256, 279, 303
Mo I	286.41	0.3	102	0.5	102
N (NH)	336.0	—	—	100[b]	110
Na I	588.99	0.2	104, 116, 124	0.1	256, 279, 303
Nb II	309.42	0.2	104, 116, 124	1	256, 279, 303
Nd II	401.22	0.3	106	1.5	256, 279, 303
Ni I	352.45	0.2	104, 116, 124	2	303
Ni I	341.48	—	—	1	256, 279, 303
Os I	290.9	—	—	6	337
P I	253.56	15	104, 116, 124	30	256, 279, 303
Pb II	220.35	1	102	15	107
Pb I	283.31	2	104, 116, 124	10	256, 279, 303
Pd I	360.95	2	104, 116, 124	6	256, 279, 303
Pd II	248.89	2	104, 116, 124	6	256, 279, 303
Pr II	422.5	—	—	10	334
Pt I	265.95	0.9	106	2	256, 279, 303
Rh	—	—	—	6	6
Ru I	349.9	—	—	90	337

TABLE 7 (continued)

State-of-the-art detection limits (cl) in 1977 reported for argon ICP discharges operated with either an ultrasonic nebulizer (USN) with desolvation or a pneumatic nebulizer (PN) without desolvation [a]

Element	Wavelength (nm)	cl (ng/ml) (USN)	Ref.	cl (ng/ml) (PN)	Ref.
S I	182.03	—	—	30	94
Sb I	217.5	—	—	15	107
Sc II	361.3	—	—	0.4	334
Se I	196.03	1	102	15	107
Si I	251.6	—	—	2	303, 113
Sm II	359.26	—	—	0.5	256, 278, 279, 303
Sn I	284.00	—	—	10	256, 278, 279, 303
Sn I	303.41	3	104, 116, 124	20	256, 279, 303
Sr II	407.77	0.003	104, 116, 124	0.02	256, 279, 303
Ta II	296.51	5	72	70	6
Tb II	350.92	0.1	106	0.5	256, 279, 303
Te I	238.58	—	—	15	256, 279, 303
Th II	401.91	—	—	3	6
Ti II	334.94	0.03	104, 116, 124	0.2	256, 279, 303
Tm II	346.22	—	—	0.15	256, 279, 303
U I	385.96	1.5	106	8	256, 279, 303
V II	309.31	0.06	104, 116, 124	0.2	256, 279, 303
V II	311.07	0.09	102	2	102
W II	276.43	0.8	104, 116, 124	5	256, 279, 303
Y II	371.03	0.04	104, 116, 124	0.08	256, 278, 279, 303
Yb II	369.42	0.02	104, 116, 124	0.1	256, 279, 303
Zn I	213.86	0.1	102, 104, 116, 124	0.3	256, 279, 303
Zr II	343.82	0.06	104, 116, 124	0.3	256, 279, 303

Note: The detection limits taken from 104, 106, 116, 124, 256, 278, 279, and 303 represent concentrations required to produce a net line signal twice as great as the SD of the background signal, and the results are for a 15-sec integration time and a medium spectral resolution (i.e., 1-m monochromator, 1200 rulings/mm grating, 25-μm slits). Spectral lines below 360 nm were measured in the second order and lines above 360 nm in the first order.

[a] The table lists the lowest values reported in the literature.
[b] Gas evolution technique.

detection limits of various analytes, and on the other hand, the overall powers of detection and the interference level would be well equilibrated. Their choice turned out to be a fortunate one, because excellent detection limits for many elements proved to be compatible with a low overall interference level.[87,104,150] Boumans and de Boer used these originally selected compromise conditions for various years[303] and showed recently[122,280] that again adequate compromise conditions, though with different numerical values of principal parameters, could be found even when they changed their experimental facilities.

If the approach taken by Boumans and de Boer was primarily empirically analytical, Fassel et al.[114,115] incorporated significant fundamental work into their analytical studies of the ICP and made detailed analyses of spatial distributions of emission from the argon plasma and from analyte elements introduced into the ICP. Studies of spatial distributions provide diagnostic signals from which temperatures and electron and analyte number densities can be derived with the objective of characterization of the analytical ICP discharge, as will be discussed in detail in Section III. Spatial distributions depend upon the equipment used and the operating parameters of the ICP configuration as listed below:

Analytical
- Gas flow rates and number
- Spectral observation zone
- Power level
- Nebulization and desolvation

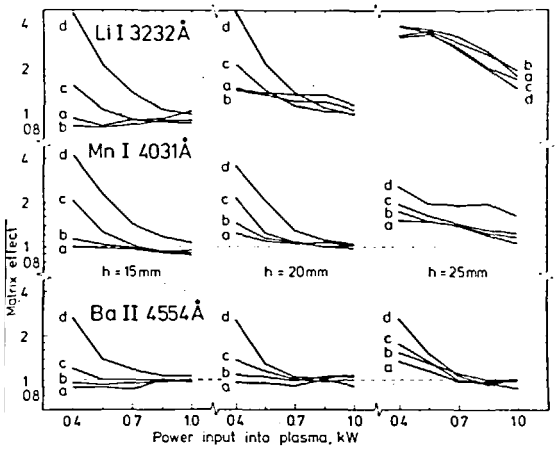

A

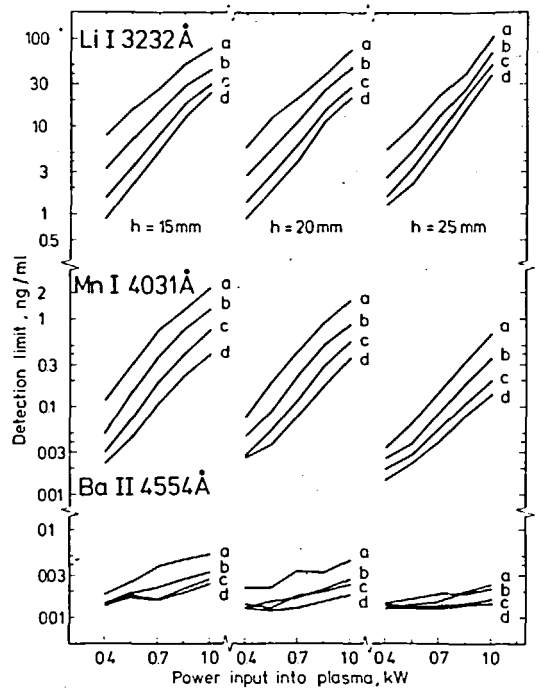

B

FIGURE 7. Matrix effect of KCl and detection limits in an argon ICP operated with an ultrasonic nebulizer as functions of the power input (P), the observation height (h), and the carrier gas flow rate (F_c). (A) Matrix effect of 2 mg/ml KCl for Li I, 323.2 nm; Mn I, 403.1 nm; and Ba II, 455.4 nm. (a) $F_c = 1.1$ l/min; (c) $F_c = 1.5$ l/min; (d) $F_c = 1.7$ l/min. (B) Detection limits attained with the three spectral lines under similar conditions. The following conditions were chosen as compromise conditions for simultaneous multielement analysis: P = 0.7 kW, h = 15 mm, and $F_c = 1.3$ l/min. (From Boumans, P. W. J. M. and de Boer, F. J., *Spectrochim. Acta*, B30, 309 (1975). With permission.)

- Spectral line selection
- Equipment
  - Operating frequency
  - Generator type
  - Power level
  - Magnetic flux density
  - Coil geometry
    - Diameter
    - Length
    - Pitch
    - Number of turns
    - Tubing diameter shape
    - Plating
  - Torch geometry
    - Number of tubes
    - Diameters and shapes
    - Length
    - Flow configuration
    - Material
    - Construction quality
  - Sample
    - Form
    - Nebulization
    - Desolvation
  - Transfer Optics
  - Spectrometer
  - Detectors
  - Readout
  - Data analysis, presentation

As an example of changes in spatial emission, in Figure 8 the intensity of the Ca, 422.7-nm line on the centerline of the ICP as a function of observation zone for four different power input values and aerosol flow rates is illustrated.[113] The simultaneous recording of each profile utilized a unique linear photodiode array arrangement, which will be described in Section II.B.3. These results and the radial excitation temperatures derived from Fe I-line emission at three observation heights and two aerosol flow rates in the presence and absence of sodium in the analyte (see Figure 9) demonstrate that excitation temperature as well as the analyte emission drops as aerosol flow rate increases.[114] However, excitation temperature and electron number density distributions (shown in Figure 10) do not change significantly with the addition of sodium at each aerosol flow rate and observation height.

These results support the conclusion drawn from empirical analytical approaches[6,87,115,122]

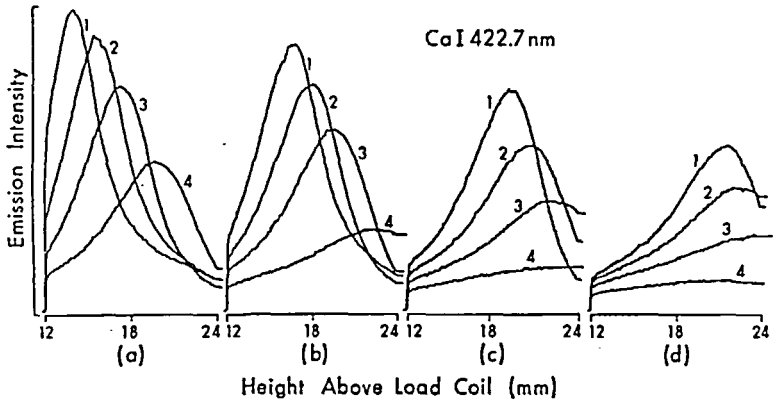

FIGURE 8. Spatial profiles of Ca I, 422.7-nm emission corrected for background as a function of aerosol carrier flow rate ((a), 0.9 l/min; (b), 1.0 l/min; (c), 1.1 l/min; (d), 1.2 l/min) and discharge power (curve 1, 2 kW; curve 2, 1.75 kW; curve 3, 1.5 kW; curve 4, 1.25 kW) obtained with a silicon linear photodiode array system. (From Edmonds, T. E. and Horlick, G., *Appl. Spectrosc.*, 31, 536 (1977). With permission.)

that appropriate selection of experimental conditions (such as observation zone, power input, and carrier gas flow rate) can provide simultaneously excellent limits of detection for multielement analysis and a high degree of freedom from interelement effects. They also provide a solid basis for using relatively low carrier gas flow rates (on the order of 0.8 to 1.5 l/min) in argon ICP discharges to achieve optimum analytical performance.[6,87,115,122] Results of recent fundamental studies by Kornblum and de Galan[83,189] further justify the empiricists' use of relatively low carrier gas flow rates. They also showed[160] that not only the volume flow rate but the linear cold gas velocity can be an important factor. Since the linear velocity of the aerosol gas flow depends upon the injection-tube orifice diameter (among other parameters),[336] optimum conditions found by different investigators using different orifice diameters for the aerosol injection tube (see Table 8) provide approximately the same cold gas velocity.[278] For example, Kalnicky et al.[114] recommended a 1 l/min carrier gas flow rate for their ICP with a 1.5-mm aerosol tube orifice diameter, whereas Boumans and de Boer[122,280] favored 1.45 l/min for a 1.80-mm aerosol-tube orifice diameter. Genna and Barnes[336] recently observed that the actual linear velocity, as well as the entire velocity distribution of the argon gas flow, leaving the aerosol injection tube orifice depends upon the presence and configuration of the pneumatic nebulizer and aerosol spray chamber.

Experience indicates that high carrier gas flow rates should be avoided in analytical applications.[83,189] Ohls et al.,[81,297] who initially used high flow rates because their nebulizers could not operate well at low flow rates, confirmed the findings of earlier workers when a low-flow nebulizer better suited for their purpose became available to them. Boumans and de Boer[122,278,280] consider the carrier gas flow rate as the most critical parameter as well as the most convenient and effective variable of their ICP when optimizing conditions for either SMEA or single-element analysis. Along with others,[97] they use rigorous means (i.e., precision pressure gauge and mass flow meter) to regulate this flow when operating their ICP with a cross-flow pneumatic nebulizer. An illustrative example is given in Figure 11, which shows the dependence of the matrix effect (defined as the ratio of the net line signals measured with solutions with and without matrix, respectively, and containing the same concentration of analyte) of 10 mg/ml KCl on the carrier gas flow rate for various spectral lines at fixed power (1.15 kW) and observation height (15 mm above the top of the coil) as measured in an argon ICP operated with a pneumatic nebulizer.[122,278,280] Three features are illustrated in Figure 10:(a) the very pronounced matrix effect at high carrier gas flow rate, (b) justification for choosing 1.45 l/min carrier gas flow rate as compromise for SMEA (after power and observation height were fixed), and (c) the possibility

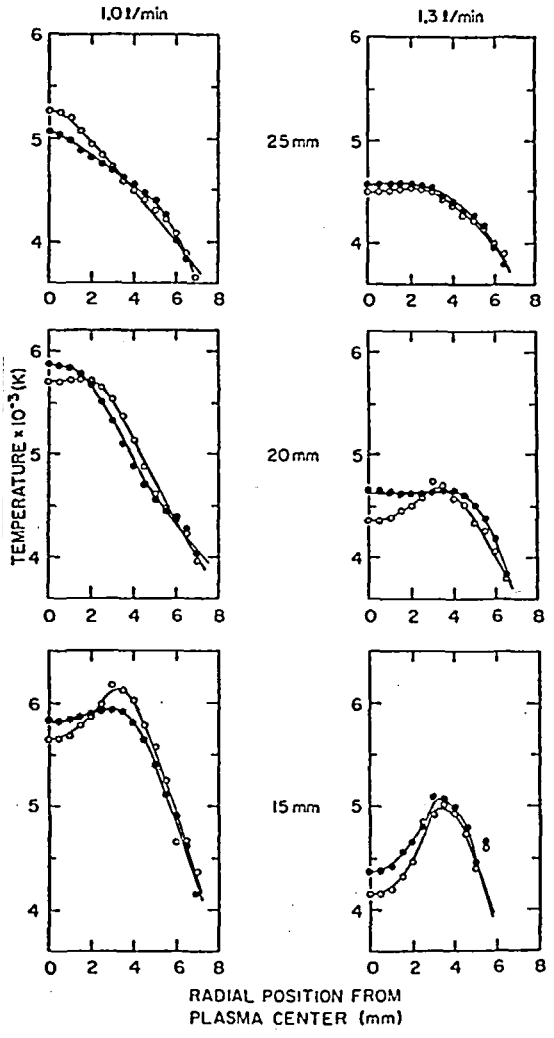

FIGURE 9. Radial Fe I excitation temperatures at 1.0 kW for three observation heights above the induction coil and two aerosol carrier flow rates for 150 μg of Fe per milliliter (open circles) and 150 μg of Fe per milliliter with 6.9 mg of Na per milliliter (closed circles). (From Kalnicky, D. J., Fassel, V. A., and Kniseley, R. N., *Appl. Spectrosc.*, 31, 137 (1977). With permission.)

for using the carrier gas flow rate as a convenient and effective variable for single-element optimization of the matrix effect. Furthermore, as indicated in Figure 11, the matrix effect of KCl under compromise conditions is always between ±20% and often between ±10%. Boumans et al.[278,280] also demonstrated that the compromise conditions selected on the basis of KCl interference are applicable to other matrices including phosphate.

Analyte emission and excitation follow atomization and vaporization of sample aerosols. These processes depend upon the operating properties, especially the sample flow into the discharge. Spatial distributions of pressure as an indicator of the particle trajectory within the ICP at two aerosol flow rates are presented in Figure 12. The absence of solute vaporization interferences for phosphate and aluminum on calcium in the ICP[94,115] indicates that formation of refractory compounds, as observed in flames, is negligible in the ICP under appropriate operating conditions. Common pictures of ionization interference and incomplete vaporization or dissociation of solute developed for flames and arc plasmas do not appear applicable in the argon ICP as the result of the combined high temperature, high electron density, and the possibility of specific excitation processes. The existence of departures from local thermal equilibrium (LTE) in argon ICP discharges is becoming well documented,[83,114,132,189,318] and it appears that some of the favorable analytical properties of argon ICP discharges, particularly the low detection limits reached with ionic lines and the relative freedom from interferences from alkali metals, are due to the non-LTE conditions of the plasma, which, in turn, may be connected with the ionization-excitation mechanisms involving metastable argon species.[122,327] This topic is discussed in Section III.B.5.

II. INSTRUMENTATION

A. The ICP-AES System

1. Introduction

The ICP discharge is generated by inducing a magnetic field in a flowing, conducting gas, usually argon or argon and nitrogen, by means of a water-cooled copper coil which surrounds quartz or boron nitride confinement tubes through which the gas flows (Figure 13). Typically two or three separate flows are employed, as indicated in Table 1, to sustain the high temperature discharge, to prevent the confinement tube walls from melting, to position the discharge, and to form the discharge into an annular shape through which a sample aerosol can be transported by the aerosol carrier gas. Commonly, RF generators at frequencies in a range between 7 and 50 MHz and, in the U.S., especially at FCC-allowed Industrial-Scientific-Medical (ISM) frequency bands at 27.12 or

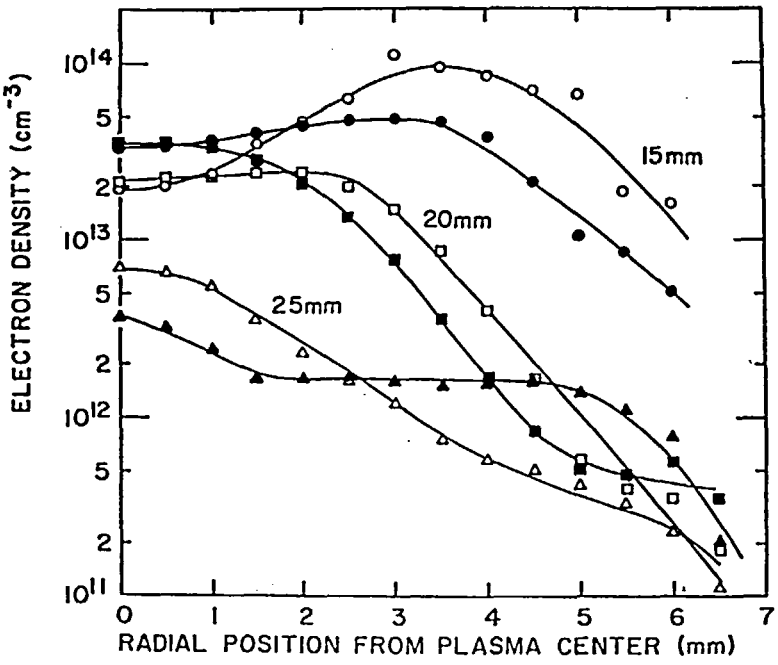

FIGURE 10. Radial electron number density distribution calculated with the Saha-Eggert's equation at 15, 20, and 25 mm above the induction coil for Mg atom/ion combinations; 10 μg of Mg per milliliter (open symbols) and 10 μg of Mg per milliliter with 6.9 mg of Na per milliliter (closed symbols). (From Kalnicky, D. J., Fassel, V. A., and Kniseley, R. N., *Appl. Spectrosc.*, 31, 137 (1977). With permission.)

40.68 MHz produce power levels transferred to the discharge in the range of 0.4 to 3 kW with argon and up to 10 kW with argon aerosol carrier and nitrogen plasma (coolant) gases. A typical ICP system for AES includes the RF generator, a transmission line, a tuning and coupling unit, the induction coil, a plasma tube arrangement, a sample introduction system, imaging optics, a monochromator or multichannel spectrometer, and analog or digital readout and control.[33,62,117] Alternative arrangements were described by Greenfield et al.,[73] Boumans et al.,[78,103,116,122] Kornblum and de Galan,[82] and Robin et al.[72,77]

Although values for gas flows, power level, and spectral observation zone in the discharge differ for each spectrochemical arrangement, usually one set of operating conditions is found experimentally which provides analysis of multiple elements simultaneously with a minimum influence from concomitant elements in the sample.[104] A typical range of conditions for an argon ICP is a plasma (coolant) flow of 10 to 20 l/min, auxiliary (plasma flow) of 0 to 0.5 l/min, aerosol carrier (sample) flow of 0.8 to 1.5 l/min, power in the discharge of 0.4 to 1.8 kW, and observation zone measured from the top of the induction coil of 15 to 20 mm. Solutions are taken up by the nebulizer at a rate between 1.5 and 3.0 ml/min (Table 8).

HF generators and sample introduction components of ICP-AES instrument systems were reviewed by Greenfield et al.[3] They discussed oscillator types, power levels, and frequency as well as the plasma cell, nebulizers, solids introduction, vaporization techniques and physical properties of the discharge. Butler et al.[4] summarized operating parameters and performance of various ICP systems for the analysis of solutions and powders with illustrations of plasma torch design for each system. Boumans[116] discussed problems related to the design and construction of a complete instrument for routine multielement analysis of solutions. Since one ICP-AES arrangement has not been proven best, commercial and research systems differ somewhat in approach and equipment.

Dickinson and Fassel[62] described an arrangement which incorporated all of the essential components of a modern research ICP system.

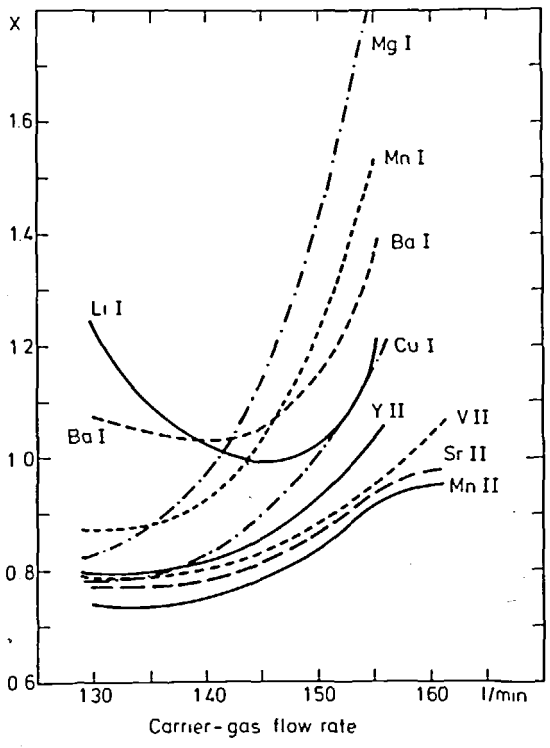

FIGURE 11. Matrix effect (X) of 10 mg/ml KCl on various spectral lines as a function of the carrier gas flow rate at constant power (1.15 kW) and observation height (15 mm) in an argon ICP operated with a pneumatic nebulizer. Spectral lines: Ba I, 553.55 nm; Li I, 670.78 nm; Mn I, 403.08 nm; Mg I, 285.21 nm; Cu I, 327.40 nm; Mn II, 257.61 nm; Sr II, 407.77 nm; V II, 309.31 nm; Y II, 371.03 nm. Orifice diameter in carrier gas tube is 1.80 mm. (From Boumans, P. W. J. M. and de Boer, F. J., Paper No. 19 presented at 20th C.S.I. and 7th I.C.A.S., Prague, September 1977. With permission.)

A commercial induction heating, free-running generator set to operate at 30 MHz was coupled to a remotely located induction coil by an air transformer, coaxial cable transmission lines, and a commercial tuning and coupling circuit.[71] These circuits and their parameters were later calculated by Schleicher and Barnes[117] in adapting the same system approach to another generator. The remote coupling unit provided the flexibility of conveniently and accurately positioning the entire discharge relative to the entrance optics of a scanning monochromator, as illustrated in a figure * given by Barnett et al.,[71] who applied the system for ICP-AAS. Sample aerosol was produced ultrasonically and desolvated in a furnace. Addition of the tuning unit to match impedances of the discharge with the generator freed Fassel and co-workers[62,71,118] from the difficulty in producing and maintaining the ICP discharge that restricted Wendt and Fassel,[51,55] when the working coil was attached directly to the generator without impedance matching.

The same arrangement was applied by Kniseley et al.[119] with an improved pneumatic nebulizer[120] for the determination of trace metals in blood, and later by Butler et al.,[95] along with a similar but higher power generator, for the analysis of steels. In the latter study, three different spectrometer and readout systems were employed, including two scanning spectrometers and a multichannel direct reading spectrometer. The multichannel and scanning spectrometers were positioned to read simultaneously emission from a single discharge to expand the wavelength coverage and element range of the direct reading instrument.

Scott et al.[33] substituted a table-top sized, fixed frequency generator operating at 27.12 MHz with 50-Ω output impedance, transmission lines, and adjustable impedance matching circuit in another research arrangement. Scott et al.[86] later used a similar table-top generator along with a 0.5-m monochromator for the determination of uranium in rocks,[86] and analysis of soil[92] and plant materials[84] on a sequential element basis. Kirkbright et al. combined a similar generator and a 1.0-m monochromator for analysis of ammonia in solutions,[110] for determination of phosphorus in milk powders,[125] and for the spectrum study of sulfur.[136]

These relatively small, crystal-controlled, constant frequency generators with constant output impedance and matching arrangements are popular in commercial ICP-AES instruments produced in the U.S.,[76] where three of the four leading manufacturers employ the same HF generators in their ICP instruments (see Table 9).

The ICP-AES instruments devised by Greenfield et al.,[3,52,73] Kirkbright et al.,[108,109] Ward,[111] Newland and Mostyn,[101] Watson et al.,[121] Boumans and de Boer,[78,103,122,278,280] Kornblum and de Galan,[82,83] Ohls et al.,[81] and Robin et al.[72,77,79,126-135] differ in some major respects from those produced commercially in the U.S.

* Figure 1 in Reference 71.

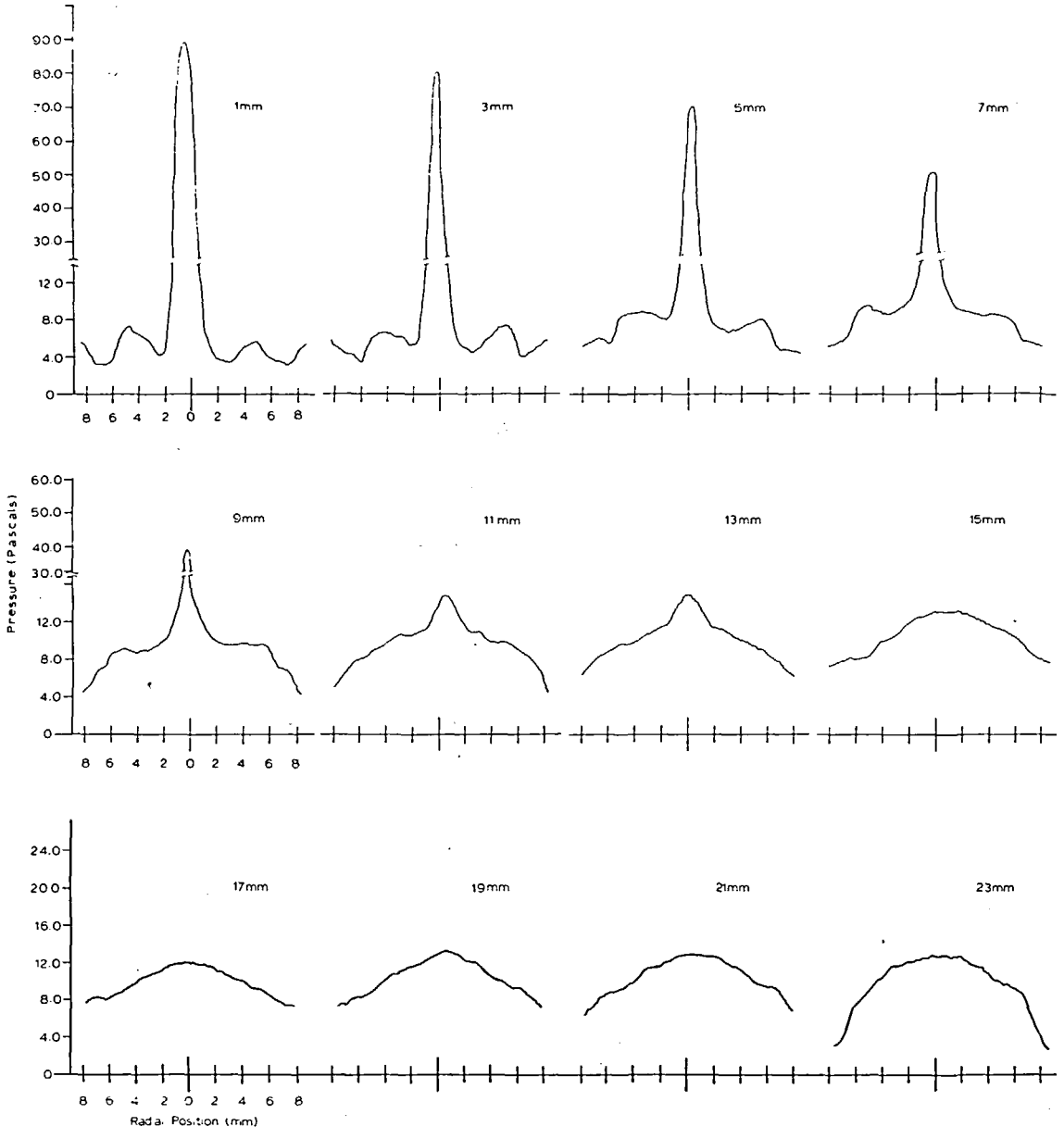

FIGURE 12. Radial pressure distributions recorded in a 0.95-kW argon ICP discharge operated at 26.5 MHz for aerosol carrier flow rates of 0.85 l Ar per minute (A) and 1.20 l Ar per minute (B) as a function of axial position from the top of the intermediate quartz tube. The torch terminated at 18 mm, and the induction coil extended from 0 to 15 mm. The torch inner diameter was 18 mm centered at 0 mm, and the 1.5-mm diameter injection orifice was located 3 mm below the bottom of the induction coil. Plasma (coolant) and auxiliary argon flows were 10.4 l/min and 0 l/min, respectively. Maximum pressures correspond to velocities of 43 m/sec (A) and 65 m/sec (B).

Commercial European ICP-AES systems incorporate many of the major features and some of the same system components (Table 9).

Greenfield et al.[50,54,73] conducted their work with systems based upon Radyne Ltd. (Workingham, England) free-running generators, first with a flame spectrometer and a large quartz spectrograph, and since the early 1970s, with a 30-channel polychromator. They developed an automated sample handling device for

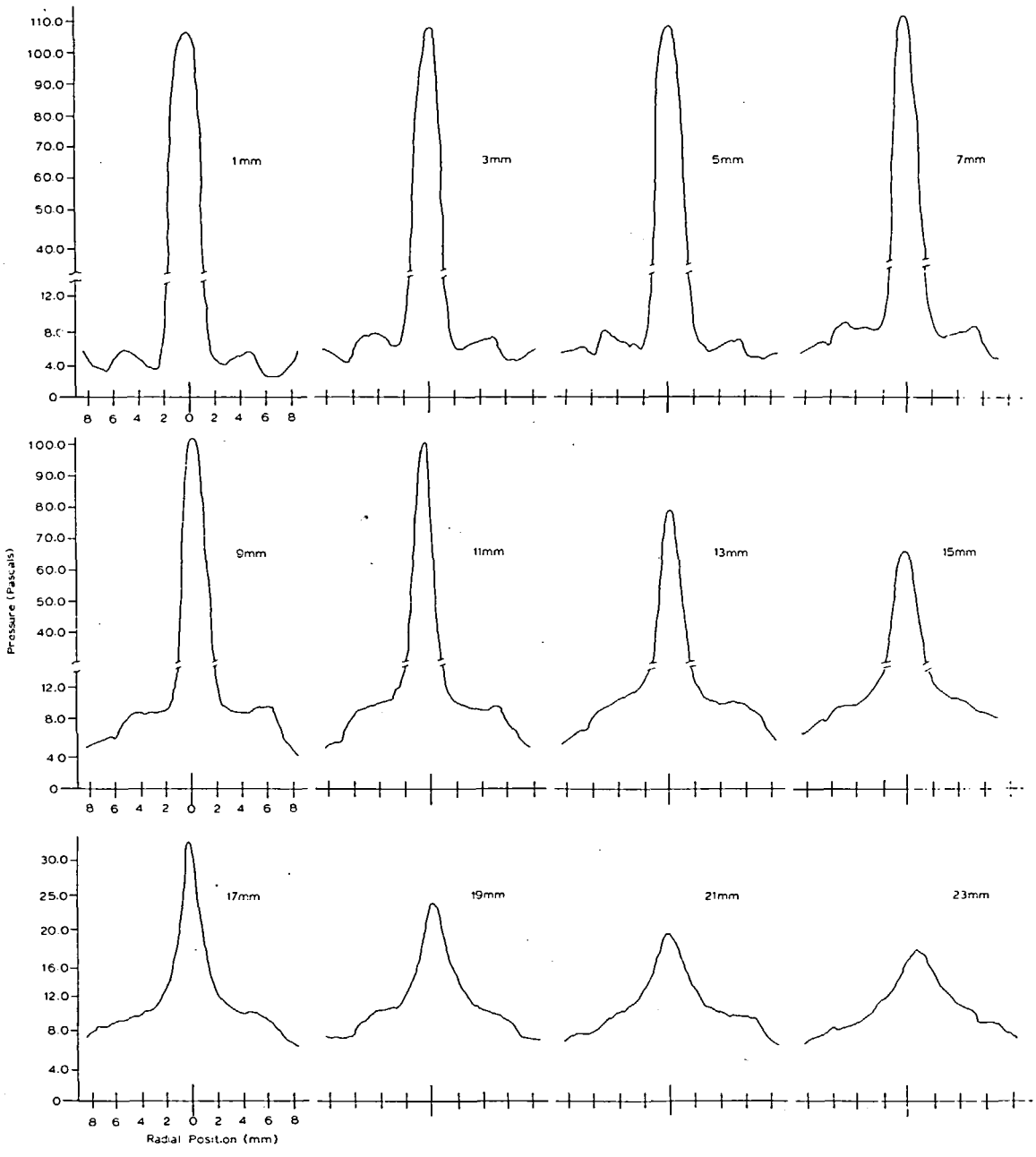

Figure 12B

multiple routine analysis. Similar arrangements were applied by Kirkbright et al.,[109] except with a monochromator, by Mostyn et al.[58,101] with grating and prism spectrographs, and by Watson et al.[121] with a 3.4-m Ebert spectrograph and 24-channel spectrometer. Common to these instruments is the ability of the large RF generator to operate with sufficient output power to sustain discharges in diatomic gases or mixed argon-diatomic gases.[3] Typically, nitrogen is circulated as plasma (coolant) gas with flow rates of 20 to 70 l/min and nominal generator output power of 2 to 15 kW. Greenfield et al.[73] estimated the efficiency of power transfer to the plasma to be approximately 50%.

The research ICP-AES instruments used by Boumans and de Boer[78,87,103,104,105] and Kornblum and de Galan[82,83,189] couple Philips pro-

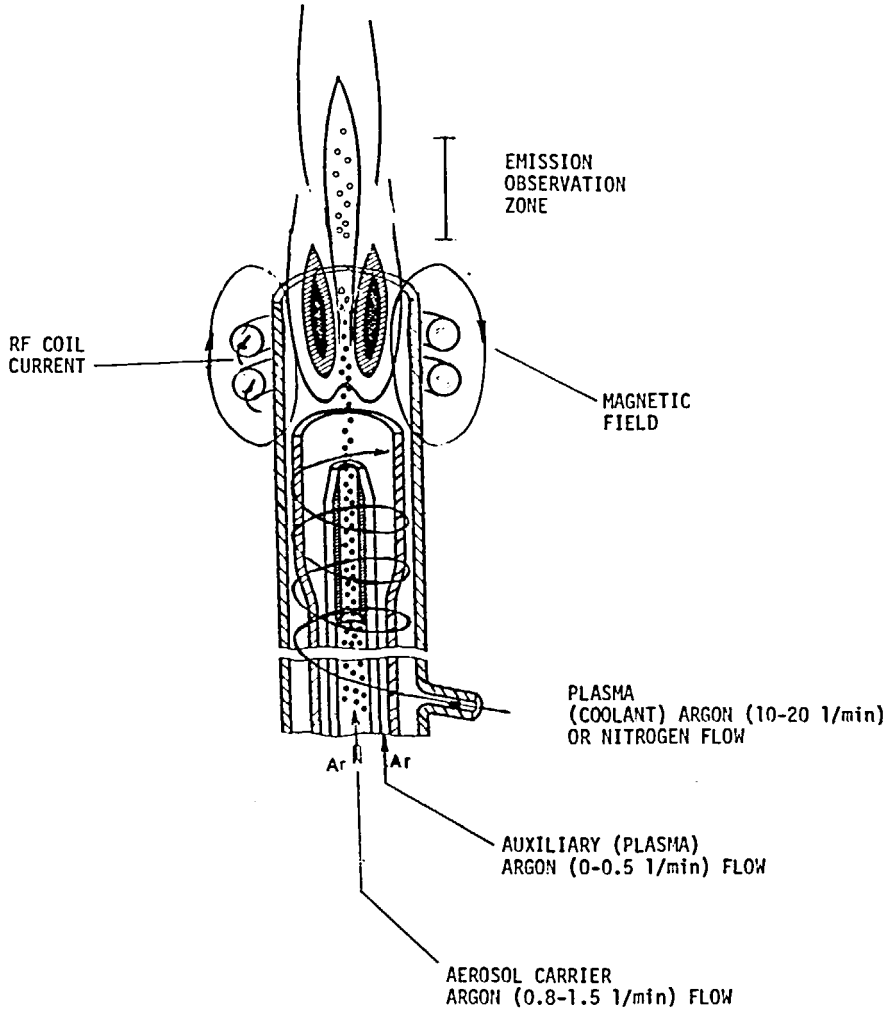

FIGURE 13. A schematic representation of the ICP discharge and induction coil surrounding the confinement tubes. Typically, the emission observation zone is located 15 to 20 mm above the top of the coil if the outer confinement tube is terminated a few millimeters above the coil. The sample is introduced through a nozzle into the central channel of the discharge.

totype RF generators operating at approximately 50 MHz with monochromators using movable plasma stands, ultrasonic or pneumatic nebulization, and desolvation. The RF generator is a Colpitts oscillator consisting of a power supply and a separate generator to which the coil is rigidly attached. Power stabilization of the RF generator and a dual-channel dual-monochromator were described by Boumans et al.[78,103] The system devised by Kornblum and de Galan for the examination of spatial distributions of temperature and other properties in the ICP exhibited optical resolution elements in the discharge of 140 by 140 μm^2 to 880 by 880 μm^2 at the edge with stepping motor control over the position of the discharge relative to the entrance aperture of the monochromator.[83] The entire plasma assembly and generator was mounted so that it rolled over sliding bars up to 20 mm with 0.1 mm resolution.

In the most recent arrangement described by Boumans and de Boer,[122] a new prototype free-running RF generator with automatic power transfer stabilization and pneumatic nebulization was combined with the dual-channel, dual-monochromator arrangement previously employed. Recently introduced by M.B.L.E. (Manufacture Belge de Lampes et de Materiel Electronique S.A.), Brussels (Belgium), subsidiary of Philips Analytical, Einhoven (The Neth-

TABLE 8

ICP Operating Parameters for Interelement Interference Studies

Frequency (MHz)	Power (kW)	Work coil		Cold linear gas velocity (m/s)		Volume flow carrier gas (l/min)	Coolant to carrier volume flow ratio	Observation height (mm)	Observation window		Ref.
		No. of turns	I.D. (mm)	Coolant	Carrier				Axial (mm)	Lateral (μm)	
3.4	5[a]	5[b]	24	2.92	0.42	0.5	44	90	21	50	55
4.8	5[a]	2[b]	ca.28	4.5	0.16	1.7	18	100	5	60	61
5.4	6.6[a]	3	30	1.73	10.6	2	10	20	10	50	77
5.4	6.6[a]	3	30	6.4	8.25	1.5	13	20	10	50	127
7	6	3	40	8.5—30	13.3	2—3	35—36	5	2	ca.80	170
27	1[c]	2	22	3.1	9.4	1	10	15—20	ca.5[d]	50	257
27	1[c]	2	22	4	10.8	1	9.5	20	5	25	84
27	1[c]	2	22	4	10.8	1	9.5	20	5	25	92
27	4[a]	1.5	22	4.2	10.8	1	10	20	5	25	86
27	1.7—2	2	27	3.1	10.8	1.1	9.1	18	4	25	95
27	1.03—1.25	2	22	3.7	9.4/12.2	1/1.3	12/9.2	15—25	4	15	151
27	1.03	2	22	3.7	9.4	1	9.2	20	4	15	115
27	1.2	2	22	5.1/6	13.1/15.3	1	15/12.5	15	4/6	15	165
30	2.5[a]	2	24	2.3	16	1.7	10	5—40	4	20	62,147
36	2.5[a]	3	44.5	ca.2.4	16.6	0.5	36	Footnote d	2—4[d]	50	58
36	2.5[a]	2.5	32	3.2	2.7	0.5	15	17.5	2	ca.80	109,171
36	2.5[a]	3.5	44.5	ca.1.3	Footnote d	Footnote d	—	>20[d]	3	10	50
40	1.3[c]	5	32	4	7.9—12	0.75—1.15	16—10	5—25	4[d]	25[d]	128
50	0.4[c]	2.5	28	5.7	2.9	5.4	3.15	2—6	2	2000	82
50	0.4—1[c]	2	30	6.7	6.6—47	0.7—5	27—3.8	15—25	5	2000	104
50	0.7[c]	2	30	6.7	12.3	1.3	14.6	15	5	25	150
50	0.7[c]	2	30	6.7	8.5	1.3	14.6	15	5	2000	87
50	0.53[c]	2.5	28	5.7	15	1.36/4.5	12.5/3.8	7.5/30	0.25	250	189
50	1.15[c]	2	21.5	5.7	9.5	1.45	13.1	15	5	2000	122,278

[a] Maximum.
[b] Pancake type.
[c] Effective.
[d] Not given.
[e] Estimated from a drawing.

From Kornblum, G. R. and de Galan, L., *Spectrochim. Acta*, B32, 455 (1977). With permission.

TABLE 9

Commercial ICP-AES Instruments

ICP system manufacturer	Spectrometer model	Number of channels	Reciprocal dispersion (nm/mm)	Wavelength range (nm)	Focal length (m)	ICP model	Power output (kW)	Frequency (MHz)	ICP generator manufacturer
Applied Research Laboratories, Sunland, Calif.	Quantometer QA137	48	0.52 or 0.92	190—461.5 170—820	1.0	ICPQ	2 or 3	27.12 Crystal-controlled	Henry Radio, Los Angeles, Calif.
	3500 ICP	Sequential[a]	—	175—880	1.0	—	2	27.12	Henry Radio, Los Angeles, Calif.
En Vallaire, Switzerland	33 000LA	64	0.695 or 0.35	190—610	1.0	Quanto-plasma	—	27.12	—
Baird Atomic, Bedford, Mass.	FAS-2PL	30	0.60 or 0.30	210—590	1.0	—	—	27.12 Crystal-controlled	Plasma Therm, Kresson, N.J.
Jarrell Ash, Waltham, Mass.	Mark III Plasma Atom Comp 96-975	50[b]	0.54 or 0.86	168—500	0.75	ICAP	—	27.12 Crystal-controlled	Plasma Therm, Kresson, N.J.
Instruments SA, Inc.	JY38P	Sequential[a] HR1000	0.4	180—450	1.0	—	1.5/ 2.5/ 5.0	27.12 Crystal-controlled	Plasma Therm, Kresson, N.J.
J-Y Optical Systems Division, Metuchen, N.J. and Longjumeau, France	JY 48P	48	0.45 or 0.58	175—450 or 210—590	1.0	—	1.5/ 2.5/ 5.0		
Labtest Equipment Co., Los Angeles, Calif.	ICP 2100	42	0.81, 0.68, 0.59, 0.46, or 0.23	187.5—407.5, 337.5—815.0 to 187.5—455.0, 187.5—227.5	1.0	—	2	27.12 Crystal-controlled	Plasma Therm, Kresson, N.J.
	Plasmaspan 700	Sequential	2.0	190—800	0.35	—	2	27.12 Crystal-	Labtest, Australia

TABLE 9 (continued)

TABLE 9 (continued)

Commercial ICP-AES Instruments

ICP system manufacturer	Spectrometer model	Number of channels	Reciprocal dispersion (nm/mm)	Wavelength range (nm)	Focal length (m)	ICP model	Power output (kW)	Frequency (MHz)	ICP generator manufacturer
Kontron GmbH, Eching/ Munich, Germany	Labtester 2100	42	0.46 (1st order) 0.23 (2nd order)	187.5—455.0	1.0	Plasma-spec	2.5, 4.0, 7.0, 10.0	27.12 Huth-Kuehn cavity	Linn Elektronik, Hersbruck, Germany
	J-Y HRS 2	Sequential[a]	0.6	180—550	0.6		2.5, 4.0, 7.0, 10.0	27.12 Huth-Kuehn cavity	Linn Elektronik, Hersbruck, Germany
M.B.L.E.,[c] Brussels, Belgium	PV 8490	50[d]	0.5	190—700	1.5		2	50 ± 1 Colpitts	Philips

[a] High-resolution monochromator.

[b] An additional flexible channel is available as a 50-cm monochromator, which is attached with appropriate entrance optics to the spectrometer and the readout of which is incorporated in the measuring console. This device makes it possible to add externally any spectral window within the wavelength range of the monochromator.

[c] Subsidiary of Philips Analytical, Einhoven, The Netherlands.

[d] An additional flexible channel is available as a "roving" slit-detector assembly within the spectrometer, and the readout is incorporated in the measuring console. The device has provisions for rough and fine tuning of the wavelength setting, and this makes it possible to add internally any spectral window within the wavelength range of the spectrometer.

erlands),[123] a commercial ICP-AES system based upon the experience of Boumans and de Boer combined a free-running RF generator at 50 MHz and a 1.5-m concave grating spectrometer. The spectrometer can be constructed with a unique "roving" slit-detector assembly that enables the measurement of any spectral line within the wavelength range of the instrument and effectively adds a variable wavelength channel to the conventional arrangement established by the fixed exit slits and detectors. This moving slit arrangement provides flexibility similar to that achieved with a separate monochromator added to the spectrometer. The performance of the latter arrangement in ICP applications was recently evaluated by Ward.[294]

Robin, Mermet, and co-workers operated a number of ICP arrangements since their initial studies in the mid 1960s (summarized by Mermet).[79] A commercial, 5.4-MHz, 6 kW-generator and 2-m Fastie-Ebert monochromator with holographic grating were combined with a three-exit slit arrangement, so that one to three spectral lines could be observed simultaneously.[131] The configuration was applied in the diagnostics of the ICP discharge, identification of new spectral lines, and study of excitation mechanisms and chemical and ionization interferences,[126,127,130,131] as well as for spectrochemical analyses.[77] A recent system employing a commercial 40-MHz generator[72] was applied in atomic emission and absorption,[128,129] spectroscopy for analysis, study of interferences, excitation processes and plasma diagnostics,[133,134,295] and determination of oscillator strengths.[295]

Ohls et al.[81,137,297] applied prototype free-running and crystal-controlled generators, a 1-m multichannel spectrometer with 17 elements, and a microcomputer readout and display system in the analysis of steel solutions and wastewaters. Two pneumatic nebulizers produced substantially different sample flows, which resulted in major changes in the emission distribution in the ICP.

Danielsson and Soderman[138] measured line-to-background ratios and detection limits in an ICP by means of an image dissector echelle spectrometer,[141] whereas, others have compared conventional spectrometers with commercial echelle grating spectrometers for ICP analysis.[139] Although investigations with various ICP-AES arrangements have provided excellent research and routine results, other configurations are being tested as the pace of commercial competition in the ICP-AES field intensifies.

Although research ICP instruments are designed to provide optimum performance, commercial ICP-AES instruments give the best cost-to-performance ratio. Different compromises are involved in the final arrangement for each category of instrument.[154,239,256] For commercial instruments these compromises involve modifying existing spectrometers to accommodate the ICP source rather than designing an integrated ICP-spectrometer:

1. Approximating background and interference contributions rather than making true background and interference measurements and corrections
2. Selecting analytical wavelengths to minimize most but, necessarily, not all spectral overlaps, and to maximize sensitivity but only when an exit slit and/or photomultiplier tube can be fitted along a possibly crowded focal curve
3. Reducing stray light to satisfactory levels but not adding expensive hardware components
4. Using compromise ICP operating conditions and measurement times for a balance between sensitivity and interference effects in simultaneous multichannel detection rather than optimum conditions for sequential single element determinations.

Cost-to-performance ratio also depends upon the time available for analysis, number of elements to be determined, required detection limits, accuracy and precision, and capital, personnel, and operating budgets.

2. Commercial Instruments

The number of ICP-AES commercial instruments has increased during the 4 years following the first instrument introduction in 1974. In 1976, Fuller[140] listed commercially available emission spectrometers with conventional and ICP sources. Since then, new ICP-AES instruments have been announced.[281] Table 9 compiles key properties of commercial ICP discharges for atomic emission spectroscopy that

have been advertised, demonstrated, or delivered. In most cases, the ICP generator and discharge stand are customized to attach to standard spectrometers, which may have been upgraded to receive the ICP source. Among changes in spectrometers required for ICP analysis are attempts to reduce optically unwanted light at the detectors, to introduce background correction hardware and software, to extend readout dynamic range to 6 decades, and to provide selection of spectral lines best suited for the ICP source. Current ICP-AES systems generally come equipped with dedicated minicomputers to perform control, data collecting, and processing functions.

In general, spectroscopy instrument manufacturers have chosen not to produce their own RF generators, although many of them specify unique requirements for those ordered from generator suppliers. Generator manufacturers produce RF sources alone or equipped with ICP apparatus so that a customer may attach the arrangement directly to a conventional spectrometer or spectrograph. Among manufacturers of generators which have been successfully used for ICP spectroanalysis are the following: Electronique Scientifique et Industrielle-R.C. Durr (Albertville, France), Henry Radio (Los Angeles), International Plasma Corp. (Hayward, California), Lepel High Frequency Laboratory (Maspeth, N.Y.), Linn Electronik (Hersbruck, Germany), Plasma Therm (Kresson, N.J.), and Radyne Ltd. (Workingham, England).[76] Other custom units have been adapted for ICP applications.[3] The ICP source presently available from M.B.L.E., Brussels (Belgium)[123] uses a generator specifically designed for the ICP. This generator evolved from a first prototype employed by Boumans and de Boer[78,87,103,104] through a second prototype,[122,280] the specifications of which were derived from the ICP-AES experience of this group into the commercial version.

The introduction and steady improvement in performance and capabilities of commercial ICP-AES systems are well documented only at trade shows, conferences, and in marketing literature. Abstracts of many of the conference presentations have been reprinted in the *ICP Information Newsletter* and papers by Davison et al.,[74] Jones et al.,[75] Ward,[144,230,294] Dahlquist et al.,[94] Ajhar et al.,[98] and Dalager et al.[99] review the progress in these developments.

Little work has been done on comparative evaluations of commercial ICP-AES instruments, although Winge et al.[97] reported results of an extensive evaluation of one commercial ICP-AES instrument. This study revealed the need to reduce stray light levels reaching the photodetectors and develop empirical methods for correction of matrix-related background shifts. Both of these topics are discussed in Section B.4. Many aspects of ICP instrumentation were discussed during informal conferences at Noordwijk, The Netherlands in 1976[142] and 1978.

3. Special Instruments

The majority of ICP installations are either composite arrangements assembled by researchers using local or commercial components or commercial ICP-AES systems complete with generator, nebulizer, spectrometer, computer, and readout. However, special instruments which might be constructed on demand or under contract may be tailored to solve specific problems. One such ICP-AES instrument designed for residual fuel analysis for marine applications was described by Allemand.[143] A unique requirement for this instrument design was that of an unattended, on-line, cyclically programmed analyzer that would be applied as a loop-monitor component in a semiautomatic or completely automatic fuel treatment system. This unique instrument featured an improved ICP discharge tube arrangement, a fuel atomization system with no solvent dilution requirement, an impedance matching network with no change between ignition and operating modes, and a dynamic background correction device. The dynamic background correction design has since been incorporated into a commercial ICP-AES instrument,[144] and the discharge tube configuration has been further studied.[145] Impedance matching network design has progressed as well.[146] Details of these developments are given in Sections B.1 and B.2.

4. Performance Comparison with Other Emission Sources or Competitive Analysis Methods

Selecting an ICP source for the solution of specific problems or as a general spectroanalytical tool is best made when potential users have a clear idea of their individual needs and/or can travel to user or manufacturer's laboratories to test each instrument type first hand.

Unfortunately, not many have the resources to make extensive comparisons with all emission sources, so that the few available detailed literature comparisons among instruments and techniques weigh heavily in selection of new instruments.

An important point to stress in comparing ICP-AES with other approaches is that a number of established methods, such as flame- and electrothermal-AAS, spark-AES, and X-ray fluorescence spectrometry (XRF), exist, and in particular fields of application, these methods are often completely adequate. Since development of these methods proceeds continuously and instrumentation is always improving (enhancing the cost-to-performance ratio), comparisons must be timely. An attempt to replace these approaches with ICP-AES may be unrealistic. The judgment of the position of a relatively new technique, such as ICP-AES, among established analysis methods depends primarily upon assessing the extent to which the new technique can fill existing gaps, in other words, defining the areas in which the new method yields results where the established methods fail or in which the new method provides similar results but at lower cost and/or greater convenience. An entirely satisfactory assessment of ICP-AES compared to established analysis methods is not easy and perhaps premature presently, because standard commercial ICP-AES instruments are only now becoming widely available.

In contrast, an assessment of ICP-AES among related, nonestablished techniques is far easier, because the literature provides many results of detailed experimental comparisons and critical reviews that show the ICP usually provides performance superior to those of nonestablished techniques. In fact, this superiority led instrument manufacturers to select ICP instead of alternative sources for AES analysis of solutions. A few years ago various sources for solution analysis, e.g., high-temperature flames, DC plasma jets, microwave-induced plasmas, capacitively coupled microwave plasmas, and ICPs, still had to be considered as possible alternatives.[4,8,9,78] It soon became clear[3,6,116,149,256,279] that the ICP had many properties that would make it the preferred source.

Greenfield et al.[3] concluded after an extensive literature review of most DC plasma jets, microwave and capacitively coupled sources, and ICP discharge that the ICP was superior to both plasma jets and microwave discharges if detection limits were the criterion. The sensitivity of the ICP, with several exceptions, was found to be greater than either of the other two types of sources. Freedom from matrix effects and electrode contamination, as well as a linear calibration range, favored the ICP. However, the ICP was more expensive than either of the other source types. Pforr[63] compared the spectrochemical results obtained with a 40-MHz ICP, a 40-MHz quarter-wave coaxial discharge, and a Kranz plasma jet and found that the best sensitivity was obtained with the ICP.

Flame techniques, especially atomic absorption spectrophotometry, establish major analytical performance criteria by which the ICP must be judged for single element analysis. Fassel and Kniseley[6] compiled a comparative list of limits of detection (reproduced in Table 3) to demonstrate the merits of the ICP. Recently, Fassel[147] compared the ICP to AAS with electrothermal atomizers for the analysis of ultra trace concentration levels in limited volume liquid samples. The combination of analysis capability and an unusual degree of freedom from interelement effects were cited as a major ICP advantage, since for 1-ml sample volumes, the relative levels of detection of the ICP and electrothermal atomizers in AAS appeared comparable. On an absolute basis, however, the electrothermal atomizers were superior to the ICP.

Winefordner et al[91] reviewed multielement atomic spectroscopic methods as well. They considered atomic absorption flame and nonflame spectrometry, atomic fluorescence flame and nonflame spectrometry, and atomic emission spectrometry with flame, ICP, and microwave sources. Signal-to-noise ratio, experimental limits of detection, and other analytical parameters served as criteria. The authors concluded that, if a large number of elements needed to be determined, the present choice had to be ICP-AES with multichannel or programmed, rapid-scan, good-resolution spectrometers. For a limited number of elements, either an AES or AFS system was recommended.

Kirkbright and Ward[80,96] predicted and then verified experimentally that ICP-AES has a longer linear working range for analytical curves than an inert gas shielded nitrous oxide-

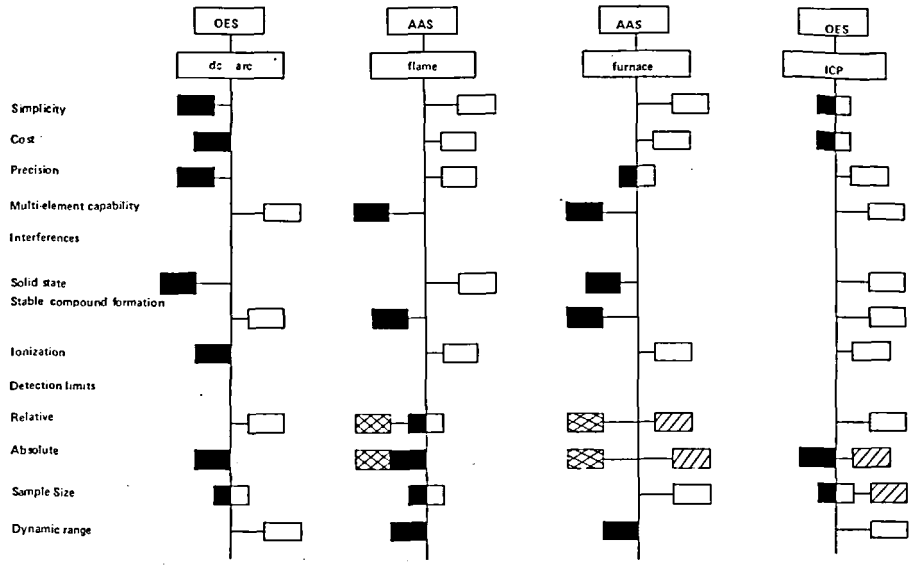

FIGURE 14. Comparative assessment of DC arc optical emission spectroscopy (DC arc OES), flame atomic absorption spectrophotometry (flame AAS), electrothermal atomic absorption spectrophotometry (furnace AAS), and inductively coupled plasma optical emission spectroscopy (ICP-OES). Positive qualities are represented by open boxes displaced to the right (From Boumans, P. W. J. M. and de Boer, F. J., *Proc. Anal. Div. Chem. Soc.* (London), 12, 140 (1975). With permission.)

acetylene flame. Since the absolute value of emitted intensity at any line was found to be much higher in the ICP than in the flame, lower concentrations and reduced sample uptake rates were possible with the ICP. Boumans and de Boer[78] also compared a premixed nitrous oxide-acetylene flame with the ICP to determine the feasibility of simultaneous multielement analysis. Although an argon-shielded premixed flame offered promise for simultaneous flame emission analysis, Boumans and de Boer[104] discontinued their efforts on flame AES in favor of ICP-AES.

Other evaluations of the ICP and electrical discharges were made by Fassel,[9] Boumans and de Boer[116,149,239,256,279] Kleinman and Polej,[7] and Sharp.[5] Boumans and de Boer[149] considered simplicity, cost, precision, multielement capability, interferences, detection limits, sample size, and dynamic range in their evaluation of flame and furnace AAS, DC arc emission spectroscopy, and ICP discharge. Each property is represented by the position and shading of a block in Figure 14 for each method. The farther a block is displaced to the right from the vertical line, the better the characteristics were judged to be. A white block indicates positive and a black block negative judgment. The need to improve both the cost and precision of the ICP was emphasized, along with the importance of developing attitudes to achieve a balance between costs and profits. The advantages of a multielement technique must be weighed against the implementation costs. Boumans[239] also evaluated the ICP discharge, the glow discharge, and the DC arc source for universal analysis.

Definitive experimental comparisons were conducted with commercially available microwave plasma discharge sources called capacitively coupled microwave plasma (CMP) or single electrode plasma (SEP). Both Boumans et al.[150] and Larson et al.[151] examined the ICP and the CMP under carefully controlled laboratory conditions. In the study of Boumans et al.,[150] detection limits, sensitivities, precision, background levels, and matrix effects were contrasted for 14 spectral lines of 12 elements in pure aqueous solutions as well as three matrix solutions. In all respects, the ICP discharge was found superior to the CMP as an excitation source for simultaneous multielement analysis of solutions. The ICP displayed better overall powers of detection, far smaller matrix effects (especially ionization interference effects), higher sensitivity, better reproducibility,

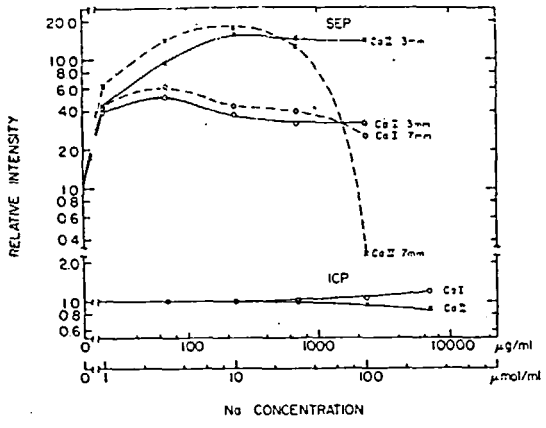

A

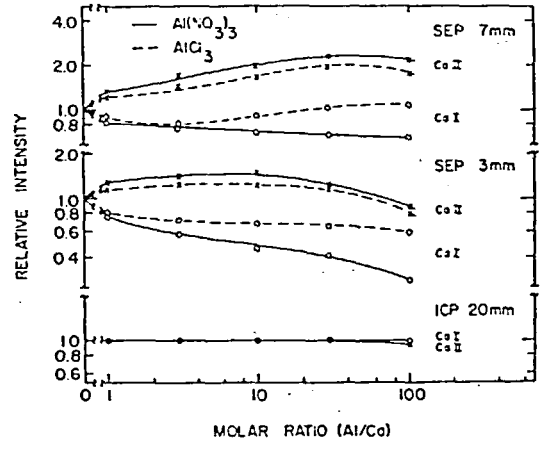

B

FIGURE 15. Comparison of the effect of Na (A) and Al (B) on Ca emission in a capacitively coupled single-electrode microwave plasma (SEP) and ICP. Calcium concentration of 0.5 μmol/ml; lines, Ca I 422.7 nm and Ca II 393.4 nm; height of observation for SEP, 3 or 7 mm above electrode, and ICP 20 mm above the load coil. Reprinted with permission from Larson, G. F. and Fassel, V. A., *Anal. Chem.*, 48, 1161, (1976). Copyright by the American Chemical Society.

smaller background variations, and the possibility for defining fixed compromise operating conditions for analyses of a large variety of analytes and matrices.

The investigation conducted by Larson et al.[151] focused on the comparison of interelement effects in the two discharges. Atom and ion emission from Ca, Cr, Mo, and Zn in the presence of various concentrations of Na, and from Ca in the presence of Al and phosophate were considered. The results obtained in the Na (Figure 15A) and Al (Figure 15B) addition tests are reproduced in Figure 15. For these conditions, negligible changes were observed in the ICP discharge, whereas severe changes were found in the microwave discharge.

For complex biological matrices, Irons et al.[152] evaluated energy-dispersive X-ray fluorescence spectroscopy (XRF) and ICP-AES for sensitivity, precision, and accuracy in the analysis of up to 13 elements in standard reference materials, compound mixtures, and supplemental samples. The important criteria in this evaluation included tissue preparation requirements, sensitivity for detection and quantification of trace elements in biological samples, accuracy and reliability in complex matrices, data handling requirements, and capacity for analyzing large numbers of samples. They concluded that the ICP is slightly more sensitive for most elements. XRF required biological samples to be in a dried form, which could be cumbersome. Because the ICP requires solution samples, the relative sensitivity in tissue specimens was limited; however, for blood, urine, or aqueous solutions, the ICP held the advantage of detection limits. For both techniques, analytical precision was limited by the operator error in duplicating sample preparations. Accuracy and recovery tests for both compared favorably with AAS. With an integrated computer in the ICP instrument, data handling and analysis were more easily obtained. Operating costs for ICP or XRF were expected to be similar. The selection of the most suitable technique rested on the type of sample and particular element of interest.

A recent polemic between Plesch[298] and Boumans[299] concerning the relative merits of XRF and ICP-AES fixed on the question of cost and complexity. Considering that the cost of a complete ICP-AES instrument (including source and spectrometer) may cover a wide range depending on the scope of the envisaged analysis problem, Boumans admitted that the cost of even the cheapest commercial ICP-AES instruments with adequate performance would not be much less than the least expensive XRF instrument. He concluded that for the time being instrument costs do not constitute the decisive factor for choosing between the two instrument

types. However, Boumans argued that the detection limits of ICP-AES solution analysis, both with respect to the solution and the dissolved solid matrix, are generally three orders of magnitude better than wavelength-dispersed XRF; owing to the high cost and/or complexity of the work involved in preconcentration, XRF cannot be considered competitive with ICP-AES for trace analysis. For concentration ranges covered with both methods, definitive conclusions about the preferred method can be drawn only for concrete situations for which the analytical performance requirements are precisely specified and calculations of cost-to-performance ratios can be made. The outcome of this evaluation, according to Boumans, will depend in part on the infrastructure of the laboratory and on whether the samples are solutions or solids or both.

An evaluation of the relative merits of ICP-AES and XRF is still embryonic, which is understandable, since a "newcomer" is being compared with an established technique. A recent review by Jenkins[300] in which energy-dispersive and wavelength-dispersive XRF are juxtaposed might not only give an insight into the relative positions of the two X-ray techniques, but also provide some useful starting points for further comparisons of XRF and ICP-AES.

Scott and Kokot[92] demonstrated that differences in results from ICP and AAS analysis of soil samples resulted mainly from enrichment effects occurring in the AAS determination. In an evaluation of values obtained for plant material digests using ICP, AAS, XRF, and DC arc techniques, Scott and Strasheim[84] found a smaller SD with the ICP technique.

Boumans et al.[278] compared wet chemical analysis techniques (including AAS) and ICP-AES for single-element determinations in the daily practice of a service group in the research laboratory of a large electronics industry. In typical nonroutine analysis, ICP-AES could easily cope with problems that were beyond the normal scope of AAS and chemical analysis or could only be treated by other methods if a time-consuming preconcentration or separation were included. On the other hand, analysis problems that were normally managed by AAS or chemical analysis could be conveniently and satisfactorily solved by ICP-AES as well.

These publications and other evidence show that ICP-AES is a competitive analysis technique and the ICP discharge is a competitive source within the field of AES. Many of its performance characteristics make it the best source for multielement and single-element analysis of solutions. However, more careful, thorough comparisons are needed. For example, a commercial DC plasma arrangement designed by Elliott and marketed with an echelle spectrometer by Spectrametrics Inc., Andover, Mass. was not included in the evaluation made by Greenfield et al.[3] Until now, only preliminary comparisons have been made between it and the ICP,[153] and these suggest advantages for the ICP. Although some laboratories are equipped with both types of instruments, no detailed evaluation has yet been published — a situation which will undoubtedly change soon.

Finally, as Boumans[154] has emphasized, a single ICP does not exist — only various versions which display similarities and dissimilarities in their characteristics. On the whole, the similarities predominate and allow spectrochemists to obtain comparable results. The differences among ICP sources originate in generator design (related to frequency, power coupled to the discharge, and mode of oscillator operation), plasma tube arrangement (i.e., torch or burner), gas flow configurations and types of gases used, nebulizers, and whether solvent removal facilities are employed. The design of low-cost and/or high-performance components and systems is of high priority in a number of ICP research and development efforts. Each of these and other system components are treated in detail in the next section.

B. System Components

1. RF Generators

a. Types

The conversion of DC to HF power in oscillators or amplifiers requires large amounts of power. When HF generators inductively produce plasmas for spectrochemical analysis, these power levels must be produced with a minimum detrimental influence on the analytical results. At high power levels, vacuum tubes are the usual generating sources for all frequencies above 10kHz. While a wide variety of oscillator circuits exist, the fundamental requirement for oscillation is the presence of positive feedback from output to input; the difference

in circuits rests in the manner in which feedback from plate to grid is accomplished. The Lepel generator used by Fassel and coworkers[57,62,218,277] and Truitt and Robinson,[163] the STEL generator employed by Souilliart and Robin[77] and the Forrest Electronics device applied by Barnes et al.[88,117] are tuned-plate-tuned-grid oscillators. The Radyne generators applied by Greenfield et al.,[73] Ward,[111] and Kirkbright et al.[108,109] are Colpitts oscillators as are the Philips generators employed by Boumans et al.,[78,103,122,278,280] Kornblum and de Galan,[82] and Visser et al.[155] The frequency stability of the output of these generators depends upon the generator loading unless the load is decoupled by an intervening amplifier or buffer. In contrast, crystal-controlled generators provide constant frequency regardless of the load. Although rigorous stabilization of frequency has not been established experimentally as essential for the analytical performance of ICP-AES, the stability of power transfer is critical.[256]

Tank circuits (which govern the frequency of oscillation and from which the generated RF energy is ultimately drawn by the load coil and plasma) can consist of various combinations of inductive and capacitive components. For example, the shape of tank inductors can range from multiturn coils to cavities. Linn[157] discussed the advantages of a 27.12-MHz cavity used in a Huth-Kuehn oscillator supplied commercially by Linn and Kontron (Table 9). Power stability depends mainly upon the power supply and mechanical construction. Transmission lines, either open or coaxial, can be used as tank circuit resonators in the same way and for the same frequency ranges as cavity circuits. In the commercial generator built by Durr and applied by Abdallah et al.,[72] quarter-wavelength tuned lines are used in grid-cathodes as well as in the tank circuits in a push-pull triode oscillator. Tuned lines are ideally suited for the push-pull operation at very high frequencies and can easily be made self-decoupling by feeding supply lines through the line members; the load coil can be supplied through parallel coupling lines. Babat[25,26] also used a push-pull oscillator with lecher lines in the filament circuit along with lines in the plate and grid circuits.

Frequency stability in self-excited oscillators can be improved by replacing the frequency-determining circuit of the oscillator with a piezoelectric crystal, which can undergo stable vibrations with changing time and temperature. This results in a constant resonant frequency, and oscillator stabilities are generally better than 1 part in 100,000. Thick crystals are usually made with fundamental frequencies ranging from about 4 kHz to 10 MHz, with higher frequencies generated by overtone or harmonic vibrations of the crystal. Alternatively, the frequency can be multiplied in the secondary stages of a HF generator. A block diagram of a commercial Plasma Therm crystal-controlled generator popular for ICP discharges is given in Figure 16.[156] The generator consists of a conventional Colpitts oscillator, frequency doubler, buffer and drive control, and power amplifier sections. Typically, vacuum tubes operated under class C conditions for power efficiency are employed in power amplifiers and oscillators. Generally, the class C amplifier is operated with a resonant-circuit load, or tank circuit, in the plate circuit tuned to the frequency of the grid input. An effective load resistance is inductively coupled into the tank circuit to provide means of taking power out of the tank.

The International Plasma Corp. generator used by Fassel et al.,[33,165] Peterson,[277] Scott et al.,[86] and Kirkbright et al.[110,125,136] and the Henry Radio generator incorporated in the Applied Research Laboratories (ARL)-ICP instrument (Table 9) and applied by Montaser and Fassel[176] also employ Colpitts oscillators and a somewhat similar buffer-power amplifier arrangement. A Lepel crystal-controlled generator was employed by Allemand,[143] and Linn[157] described a crystal-controlled generator with a 27.12-MHz cavity-tuned power amplifier.

Recent developments in high-power, HF transistor technology have led to the design of solid state power amplifiers, and since all except the power amplifier stage can be readily designed with semiconductors, a solid state RF generator is feasible. However, in the past, solid state RF generators for ICP-AES have been prohibitively expensive in comparison to vacuum-tube arrangements. Further technological and production developments that reduce costs of solid state amplifiers which produce power output sufficient to operate ICP discharges may lead to smaller and more efficient solid state RF generators.

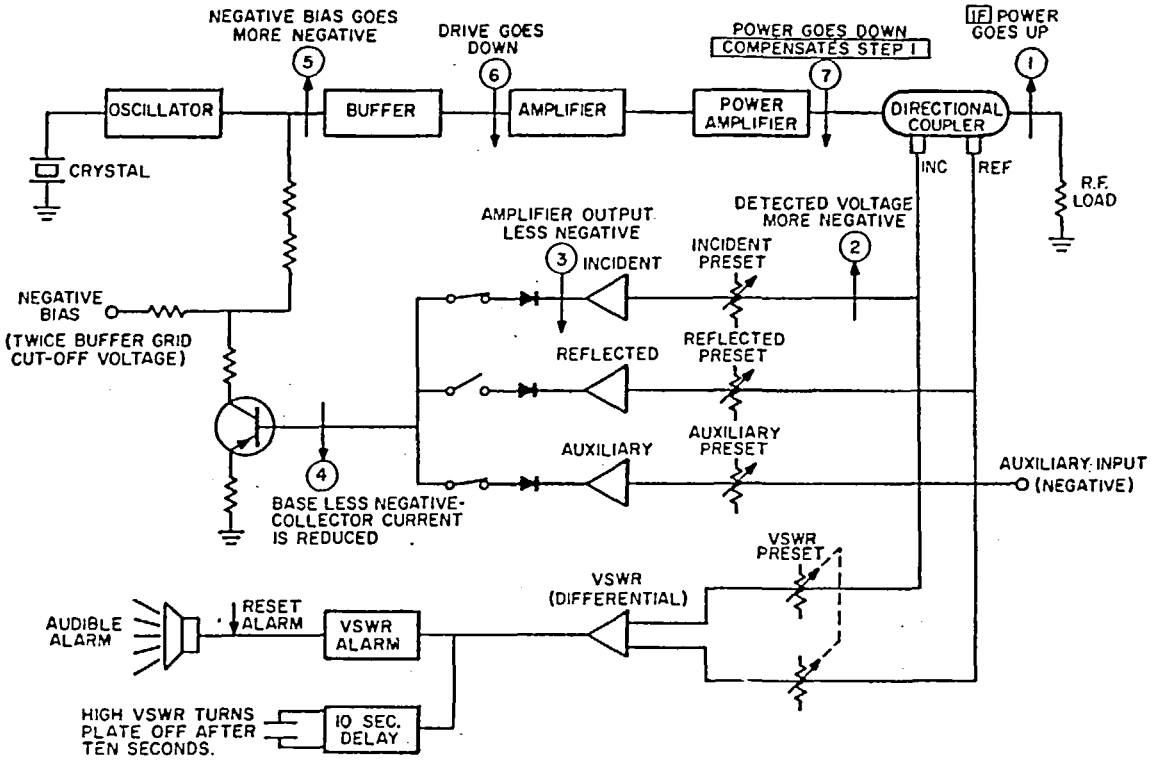

FIGURE 16. Schematic representation of crystal-controlled RF generator illustrating the action of the constant forward-power feedback circuit (steps 1 to 7). The ICP is represented by the RF load in the circuit, and the oscillator, buffer, and amplifiers comprise the basic components of the generator. (From Plasma Therm, Kresson, N.J. With permission.)

b. Performance

Linn[157] discussed the technical requirements for RF generators used for ICP-AES, and Greenfield et al.[3,73] outlined the various opinions on the merits of crystal-controlled vs. non-crystal-controlled generators for ICP-AES. Regardless of the stability of the generator frequency, the generator output power experienced by the discharge must be stable. High voltage and filament power supply ripple, for example, introduce undesirable modulation of the RF envelope at the ripple frequency. Kalnicky et al.[114] demonstrated that with the forward power envelope modulated at 60 Hz by the power tube filament supply, the relative intensities of analyte and Ar I emission lines observed in an ICP yielded erroneous time-averaged excitation temperature values. Only when the 60-Hz ripple was eliminated were actual time-independent temperature values obtained. Further filtering was needed by Kalnicky et al. to reduce a 120-Hz ripple. Butler et al.[95] suggested that a 50% peak-to-valley 120-Hz ripple on the RF power envelope was probably responsible for the loss in stability in one of two ICP-AES systems when the discharge was overloaded with water vapor from the nebulizer. Partial desolvation was necessary for that generator, whereas a second generator with three-phase supply and additional filtering in the DC power supply ran in a stable manner when aerosol was injected directly into the discharge. Peterson[277] investigated plasma modulations for three RF generators using high framing speed photography. Lepel,[95] Plasma Therm, and International Plasma Corp.[114] generators were characterized by their measured output voltage ripple magnitude and frequency and the predominant frequency of oscillation of the discharge. Ripple varied from less than 0.5% for a generator with low-ripple specifications to greater than 25%. The outer envelope and tail flame of the discharge oscillated regularly at frequencies between 60 and 360 Hz. As the ripple voltage was reduced by circuit modifications, the dominant discharge modulation was

decreased. Specifications on modern generators maintain the RF envelope ripple to a 1% maximum. Greenfield et al.[52,53] patented the concept of modulating the ICP at 100 to 360 Hz to obtain time varying radiation and stroboscopic temperature selection. Dagnall et al.[171] considered the consequence of emission modulation on sychronized detection. Gold[166] measured the local plasma velocity which resulted from power supply ripple modulation. A change of 20% in velocity was found for a small 300-Hz ripple. Linn[157] discussed how ripple problems could be corrected through proper component selection and generator design.

Ajhar et al.[98] demonstrated the importance of forward power regulation on emission lines which changed 40 to 160% when power supply line voltage changed by ±6% without regulation. With closed-loop power control, the intensity variations were reduced to about 1%. Standard power-line regulators could not achieve the same output power stability and regulation; Ajhar et al. suggested that application of an internal reference technique would also be unable to compensate for these changes since different spectral lines responded unequally. Larson et al.[115] added a feedback circuit to their ICP Corporation (Hayward, Calif.,) crystal-controlled generator to maintain constant forward power by controlling the screen grid voltage of the oscillator. Montaser and Fassel[176] altered the impedance matching network and described a forward power regulator and pulsing network for a Henry Radio generator. Automatic power control is offered as a standard option for some crystal-controlled generators,[156] and the action is illustrated in Figure 16. The controller accepts forward and reflected power signals and an auxiliary input independently or simultaneously to control the RF generator output power by changing the bias voltage on the buffer stage. Demers and Priede[302] recently demonstrated a two- to threefold decrease in background fluctuations when forward RF power was regulated. They and Boumans and de Boer[87] also monitored the stability of conditions in the ICP by measuring the Ar line emission. Although monitoring and controlling the power output to provide a constant spectral emission intensity instead of power level has been suggested, no published results are available. The manufacturer's literature claims that problems with power changes during the warm-up period (Figure 3) are totally eliminated with automatic power control; however, a practical warm-up time of about 10 to 15 min is still needed. Frequency stabilization as well as background noise stabilization during the initial warm-up with a tuned-plate tuned-grid generator[117] also requires 10 to 15 min.

Boumans et al.[103] discussed power stabilization for their Colpitts oscillator. Power consumption remained constant with small changes in the impedance of the discharge, even though the fundamental frequency changed. The extent of frequency shift with sample type was measured by Greenfield et al.,[73,158] and Allemand and Barnes[146] recently measured the change in plasma impedance with the introduction of sample aerosol. Unfortunately, direct power measurements with frequency-variable generators are not convenient, and therefore, precise verification of these concepts is not possible. With these generators, the power stability is judged by the stability of the anode current, which, in turn, corresponds to the stability of the spectral output, particularly the background intensity or the intensity of an Ar line.[303]

Even with a crystal-controlled generator and tuned circuit, Allemand and Barnes[146] demonstrated that, with a dummy load electrically identical to the plasma, power transfer efficiencies could be measured experimentally to within ±5%. However, they found that the measurement of voltages and currents in the matching network required corrections for the influence of the measurement probe. Because the matching circuit could be modeled precisely, they found computing the voltages and currents was more accurate than measuring them.

c. Frequency

Today, frequency selection depends more upon meeting government restrictions than upon fundamental considerations. During the development of the ICP for spectrochemical analysis, frequency was considered to be a very critical factor.[62] As indicated in Tables 1 and 8, operating frequencies ranged from 1 to more than 50 MHz. As Boumans[154,256] emphasized, the shielding techniques used in ICP-AES instruments should be sufficient to insure that the

spectrometric equipment is free from RF interference. Measures taken to achieve this goal are generally the same as those needed to make an RF generator that operates beyond a permitted ISM frequency band conform to international regulations. In other words, ICP instruments must be adequately shielded whether the frequency is permitted or not. Therefore, the choice of frequency for commercial ICP-AES equipment can be based on considerations other than government regulations. Greenfield et al.[73] illustrated their contention that little variation in the ICP discharge exists at different frequencies, because the injector gas flow can be made to form a toroidal discharge at both low (e.g., 7 MHz) and high (e.g., 36 MHz) frequencies.[3] Operation of crystal-controlled RF generators at 27.12 or 40.68 MHz has become an industrial standard. Consequently, the 27-MHz band is now very popular for ICP-AES instruments manufactured in the U.S. Central frequencies of generators without crystal control can be changed relatively easily, and values of 26,30,36,40, and 50 MHz (Table 8) have provided satisfactory analytical results, while both the RF shielding requirements in the laboratory and the government RF radiation standards can be easily met. For example, Abdallah et al.[72] operate their generator at 40 MHz, and Boumans et al.[78,122] operate at 50 MHz.

Abdallah et al.[72] compared temperatures, electron densities, and limits of detection for 13 elements produced by RF generators working at 5 and 40 MHz using essentially identical spectrometric measuring equipment. Besides lower excitation and ionization temperatures, lower electron number densities were also measured in the 40-MHz discharge.[159,160] An appreciable improvement in limits of detection, especially for P and W, resulted from a reduced continuum background, and improved background stability and signal-to-noise ratio. However, the lower temperature of the 40-MHz discharge led to weaker intensities than those recorded with the 5-MHz discharge.

By applying a computer model of the ICP discharge, Barnes and Schleicher[161] were able to calculate possible effects of frequency on the properties of the discharge. Temperature distributions, radial power input in the induction coil, energy balance, and total power levels were computed for frequencies ranging from 15 to 70 MHz for an ICP configuration with properties and dimensions given by Boumans and de Boer.[78,103] Two of these results are represented in Figure 17. The computed total power as a function of applied magnetic flux density at 15, 30, 50, and 70 MHz is plotted in Figure 17A, and the energy loss terms for gas enthalpy and radiation as a function of total input power at the same frequencies is represented in Figure 17B. The computations predict that at otherwise identical operating conditions, the discharge is easier to sustain at 70 MHz than it is at 15 MHz and that, as the frequency is increased, the axial and radial temperature gradients decreased. In the higher frequency discharge, the maximum temperature is lower than in the low frequency discharge, although the maximum power density is shifted toward the outer wall with increased frequency. In Figure 17B, radiation losses corresponding to a higher background become pronounced as the frequency is lowered at all power input values, although a considerably smaller portion of energy is lost as effective gas heating. Radiation loss increases faster than gas enthalpy which suggests that applying more power to the discharge will decrease the signal-to-background ratios. Unfortunately, these types of behavior have not been experimentally verified as functions of frequency, although fairly extensive experimental verification exists for the dependence of signal-to-background ratios on the power at constant frequency.[122]

Operation of induction discharges at low frequencies is attractive, as relatively inexpensive generating equipment can be used. Eckert[35,162] explored the possibilities of generating thermal electrodeless plasmas at frequencies below the RF range. He achieved an induction glow discharge operating at 9.6 kHz.

d. Coupling and Impedance Matching

Transferring the generator power to the discharge efficiently depends upon the configuration of the interconnection between the generator output tank, the ICP load coil, and their relative effective impedance. As the ICP discharge starts and whenever a sample is introduced into it, the effective impedance of the discharge changes,[146] which is reflected in the effective impedance of the induction coil apparent at the output of the generator. Each type of

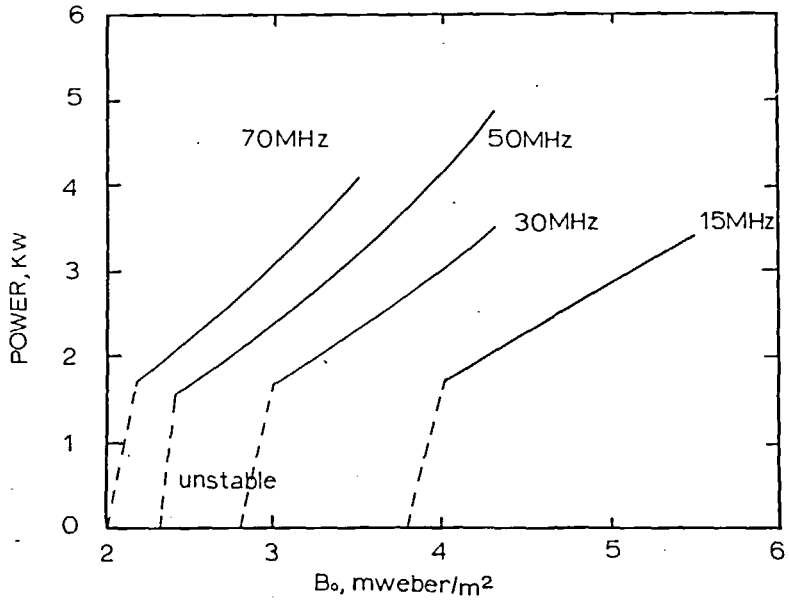

FIGURE 17A. Computed total power dissipated in an ICP as a function of magnetic flux density for frequencies of 15, 30, 50, and 70 MHz. The dashed lines represent regions of unstable operation. (From Barnes, R. M. and Schleicher, R. G., *Spectrochim. Acta*, B30, 109 (1975). With permission.)

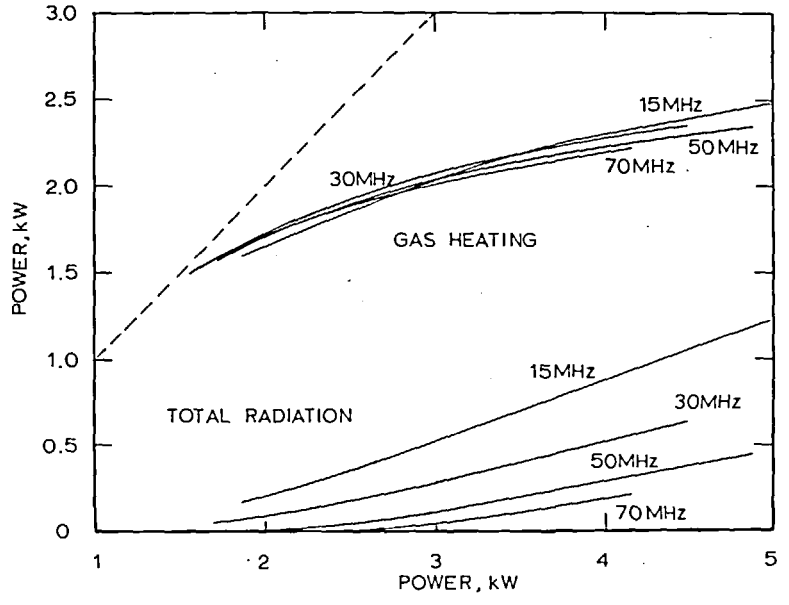

FIGURE 17B. Computer simulation values for energy loss terms (gas enthalpy and total radiation) as a function of the total power input into the discharge at 50 MHz. (From Barnes, R. M. and Schleicher, R. G., *Spectrochim. Acta*, B30, 109 (1975). With permission.)

generator can have a number of configurations to transfer the RF power to the discharge to accommodate these impedance changes.

Typically, crystal-controlled RF generators operate with a constant output impedance, e.g., 50 Ω; for efficient operation, the impedance matching of the discharge and induction coil must make the ICP appear to the generator as a load equal to the generator output impedance. When for convenience, the load is located some distance from the amplifier, the power can be fed to the load through a low-impedance (e.g., 50 Ω) cable, and the shielded cable can be installed without coupling to other circuits.

Oscillator circuits can be inductively coupled to the ICP induction coil. Dickinson and Fassel[62] used a commercial impedance matching circuit to couple the RF generator to the induction plasma. The generator was linked to the circuit through low-impedance coaxial cables which provided mobility to the matching circuit housing and the induction coil. This arrangement substantially increased the ease of operation compared to earlier arrangements. Schleicher and Barnes[117] analyzed this conjugate matching circuit and demonstrated the tuning characteristics of the arrangement with and without the ICP discharge ignited. One objective was to design a circuit which required minimum retuning when the plasma was ignited.

Allemand[143] treated the conditions for a crystal-controlled generator with 50-Ω output and he and Barnes[146] have since developed an exact model of the entire tuning and impedance matching circuit before, during, and after ignition. A constant impedance is maintained at both ends of the cable with a matching circuit. Since the effective impedance of the matching network changes when the discharge is started, one or more of the tuning circuit elements, usually variable vacuum capacitors, must be adjusted to provide a 50-Ω load to the generator. Scott et al.[33] described a manually tuned, three-variable capacitor matching network, and in another arrangement,[156] two servo motors dynamically retuned two vacuum capacitors. After Allemand's analysis, this latter circuit was redesigned with the elimination of one of the servo motors.[146]

When the ICP induction coil is incorporated as part of the generator oscillator tank circuit,[52,73,78,103,122] the frequency of the generator changes to accommodate to the new impedance values, no additional means for tuning are necessary; the output power remains constant.

e. *Power and Power Measurements*

Almost every publication related to the ICP discharge provides as part of the experimental description an indication of the power of the generator; however, few give the actual power input to the discharge, because its determination is inconvenient and its accuracy is relatively poor. Knowing the power in the discharge is not important in routine spectrochemical analysis, since other easily measured and indicated parameters serve as benchmarks for reproducible operation. Nevertheless, for experimental verification of theoretical studies and for interlaboratory comparison of spectroscopic measurements, accurate power input values are necessary.

Techniques for power measurement in the discharge depend upon the type of generator and experimental arrangement. Power measurements for crystal-controlled generators, as illustrated in Figure 16, directly provide forward and reflected power values which indicate the power transmitted to the impedance matching circuit. These instrument-mounted, in-line wattmeters are generally accurate to ±5% full scale, although standard calorimeters used for wattmeter calibration may have measurement uncertainties greater than ±0.5%. For self-exciting oscillator generators, the power must be measured by alternative methods such as calorimetry or pyrometry,[164] and during the operation of the ICP, the instantaneous power delivered to the discharge cannot be readily determined. Greenfield et al.[73,170] estimated by means of calorimetric measurements on a dummy load that the power transfer efficiency was about 50%, although the accuracy of the measurement was questioned. Boumans and de Boer[104,122] also used a dummy load to calibrate the output of their generators. These measurements were based on the assumption that the power input to the dummy load and the ICP discharge were the same if the diameter of the dummy load were chosen so that the settings of primary voltage, grid current, and anode current were the same as those obtained with an ICP discharge. The calorimetrically measured

power input to the dummy load must be corrected for the experimentally determined power input to the work coil, and an accuracy of 5% can be achieved. Kornblum and de Galan[82] related the RF power emitted by the induction coil to the anode current of the same type of generator by a pick-up coil measurement. The major limitation in these measurements is making the dummy load appear to the generator and/or tuning circuit as if it were the discharge. Allemand and Barnes[146] designed a dummy load consisting of a resistor compound baked on a boron nitride ring to match exactly the impedance of a 1.2-kW discharge during an experimental verification of computed efficiency of power transmission. Schleicher and Barnes[117] evaluated both pyrometric and calorimetric power measurements and reported that two independent plasma input power measurements gave a coupling efficiency of 65% and an overall efficiency of 35%. The power input to a dummy graphite load was measured as a function of impedance matching tuning values, but the graphite load did not give identical conditions as the discharge. Ohls et al.[167] have used a special sensitive wattmeter to measure discharge stability and effects of salt concentration in the analyte.

Bogdain et al.[168] reported a preliminary energy flow in an RF generator in which 43% of the energy was input to the induction coil, 10% was lost in the impedance matching box, 2.5% lost in the transmission cable, and most of the remaining energy (30%) was lost in the vacuum tube. Careful design with modern oscillator tubes can provide up to 80% efficiency in power output from the generator. Reviews of older measurements of the total energy flow in RF generators and induction plasmas can be found in the articles by Czernichowski and Jurewicz,[37] Dresvin,[36] and Reed.[42] The 10% loss in the impedance matching box is a typical value, and it must be considered when the power input for crystal-controlled generators is given; however, depending upon the design and construction of the impedance matching network, the loss can be as high as 100%. Barnes et al.[88,161] predicted the spatial distribution of power input to the ICP as well as the power input distribution for a number of different analytically useful ICP configurations. The direct measurement of spatial power distribution has not been attempted.

As more fundamental and practical studies are conducted with the ICP, accurate measurements of basic operating parameters must be made and reported to allow quantitative rather than qualititative comparisons among laboratories. The approach taken by Barnes et al.[88,161] indicates that magnetic flux density is the independent variable, while power input to the discharge is the dependent variable. Since spatial distributions of magnetic flux density measurements can be made, as demonstrated by Eckert,[172] the magnetic flux density might well serve as the standard for interlaboratory comparisons.

Setting aside the problem of accurately knowing the power delivered to the discharge, the question of ICP discharge power has focused on two approaches for spectrochemical analysis with the ICP. One approach employs low-power discharges, generally ranging from 0.4 to 2.5 kW, operated exclusively in argon. The majority of manufacturers sell ICP-AES instruments with these ranges in mind because of the documented performance and moderate cost for a 2- or 3-kW generator (Table 9). The other approach, promoted by Greenfield and colleagues[73,148,169,170] utilized large, moderate-power generators (5 to 25 kW) with argon and a diatomic gas, usually nitrogen. The spectrochemical effect of input power is to change the spatial location of analyte and background emission,[104] as illustrated in Figure 8 for analyte emission in an argon ICP for power levels from 1.25 to 2 kW. Similar shifts were reported by Boumans and de Boer[104] for powers between 0.4 and 1.0 kW in an argon ICP and by Watson et al.[121] for powers between 5 and 12 kW in an argon-nitrogen ICP discharge. Edmonds and Horlick[113] observed substantially different spatial emission responses to power changes for ion and atom lines; the ion line emission distribution was more dependent upon power than that of the atom line, in agreement with the observations of Boumans and de Boer.[104] However, the latter investigators report[104,122] an entirely different behavior for the detection limits achieved with either atom or ion lines (see Figure 7). Since the relative SD of the background signal was approximately constant under the conditions of their experiments, the behavior of the detection limits reflects that of the signal-to-background ratios. In Figure 7B, the signal-to-background ratio of the ion line varies much

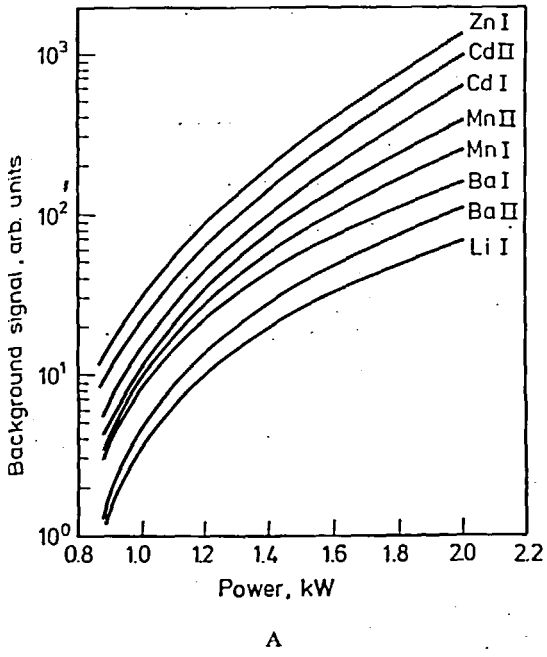

A

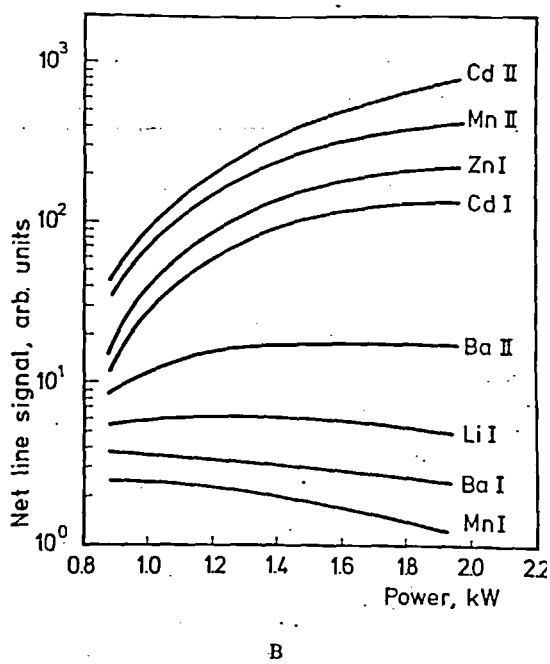

B

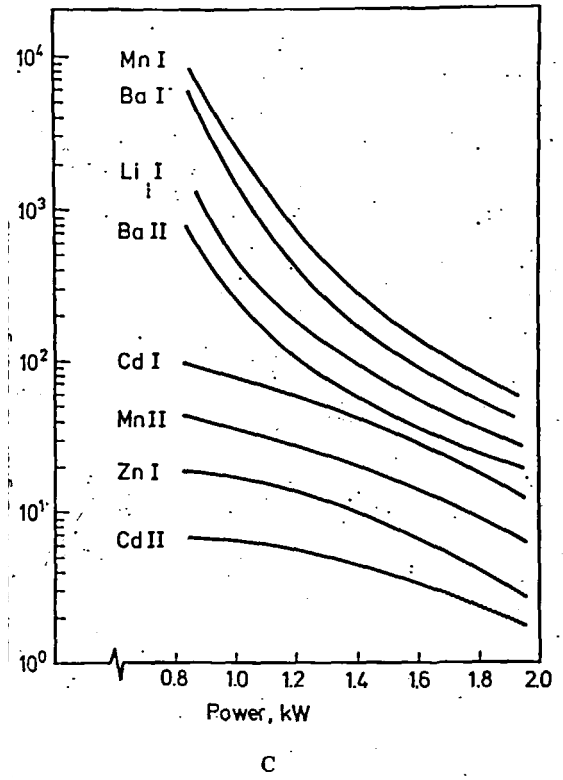

C

FIGURE 18. Background signal, net line signal, and signal-to-background ratio as functions of the power input to an argon ICP at fixed observation height (15 mm) and carrier gas flow rate (1.3 l/min). Spectral lines: Cd II, 226.5 nm; Cd I, 228.80 nm; Zn I, 213.86 nm; Mn II, 257.61 nm Mn I, 403.08 nm; Ba II, 455.40 nm; Ba I, 553.55 nm; Li I 670.78 nm. (A) The background was measured in the vicinity of the relevant spectral lines and the curves were arranged in order of increasing slope from bottom to top to reveal clearly how the background signal at the various wavelengths increases with power. A scaling factor that interrelates the background signal at various wavelengths can be derived from data in the original work. (B) The curves for the net line signals were arranged in order of shape and slope to reveal clearly the relationship between shape and slope and the type of line, whose "hardness," as indicated by the norm temperatures (T_{norm}) estimated for the argon ICP, increases approximately from bottom to top: Li I: T_{norm} = 2850 to 4900 K; Mn I: T_{norm} = 3700 to 6300 K; Ba I: T_{norm} = 2650 to 4500 K; Ba II: T_{norm} = 6600 to 8000 K; Cd I: T_{norm} = 11000 K; ZN I; T_{norm} = 11500 K; Mn II: T_{norm} = 14000 K; Cd II: T_{norm} = 156000 K. (C) The curves of signal-to-background ratio vs. power give the true signal-to-background ratios for the following concentrations (μg/ml) of the analytes: Li I, 3.5; Ba I, 800; Ba II, 4.0; Mn I, 150; Mn II 0.09; Zn I, 0.2; Cd I, 1.0; Cd II, 0.1. The measurements were actually performed at concentrations in a range between 0.01 and 4.0 μg/ml depending on the detection limits. (From Boumans, P. W. J. M. and de Boer, F. J., *Spectrochim. Acta*, B32, 365 (1977). With permission.)

ess with power, observation height, and carrier as flow rate than that of the two atom lines. ecently, Boumans and de Boer[122] made a more etailed analysis of the dependence of signal-to-background ratios on power in their argon ICP discharge produced with a new RF generator. Results for fixed observation height and carrier gas flow rate are shown in Figure 18, which

demonstrates that the background signal at various wavelengths sharply increases with power, whereas net line signals either increase at a much slower rate or decrease. Boumans and de Boer concluded that, with their new experimental facilities, the highest signal-to-background ratios (and consequently, lowest detection limits) are also reached at low power. Boumans and de Boer[122] further analyzed the behavior of the net line signals in terms of norm temperatures and concluded that the picture of Figure 18B can be qualitatively explained on this basis. They[293] distinguished for convenience between "hard" lines and "soft" lines. Atom lines of elements with a high first ionization potential (e.g., Cd I, Zn I) and ion lines of elements with a high second ionization potential (e.g., Cd II, Mn II) were denoted "hard," while atom lines of elements with a low to medium ionization potential (e.g., Li I, Ba I, Mn I) and ion lines of elements with a low second ionization potential (e.g., Ba II) were classified as "soft". The position of the Ba II line in the latter category was substantiated by studying the dependence on power of the net line signals of La I, La II, and La III.[122]

In developing analysis methods, the power input, aerosol carrier gas flow rate, and observation height are optimized to obtain high line-to-background ratios, low limits of detection, and minimum interferences[87,104,122,278] as discussed in Section I.C.6. Values for these quantities in the optimization of uranium determination are illustrated in Figure 19.[84] This example, among many others, indicates that for a given set of experimental conditions, the highest power that can be delivered to the discharge is not always selected for the optimum spectrochemical analysis.

Greenfield et al.[73] gave four advantages gained by operating with power of 5 kW or more dissipated in his argon-nitrogen ICP: greater sensitivity, frequent improvement in precision, elimination of band spectra, and elimination of chemical interferences. For ultimate sensitivity, high power is desirable, according to Greenfield,[73,169] because the sensitivity increases, maximizes, and decreases as the temperature of the discharge increases. He calculated temperatures, known as norm temperatures, at which signals maximize for Na, Mg I and II, B, and Ca II lines; measured signals for Na, Zn, and Al as a function of power up to 7 kW; and found that only Na had reached its norm temperature at 2.5 kW. This greater sensitivity with increased power can be employed to excite lines with high excitation energy or low transition probability or to increase the signal of a more easily excited line.[73] Boumans and de Boer[122] disagreed with Greenfield's calculated norm temperatures and derived lower values. They felt that norm temperatures provided a basis for qualitative understanding of the behavior of different spectral lines in the ICP discharge. Contrasting statements concerning optimum power in ICPs may be due to essential differences between excitation mechanisms occurring in ICP discharges operated with nitrogen-argon or only argon.[122] Although no experimental documentation is now available, a number of studies are underway or planned.

Intimately related to operating ICP discharges at moderate power levels is the problem of increased spectral continuum[169] compared to discharges with lower power input. This trend is indicated by the theoretical calculation of total radiation loss in Figure 17B. As the power is increased, a greater fraction is lost as continuum radiation in both argon and nitrogen discharges.[88,161] Greenfield[169] emphasized the importance of the formation of the ICP into an annulus and the injection of the sample into the central channel. In this way, analyte emission can be spatially segregated from the discharge continuum. Furthermore, Greenfield and coworkers substituted nitrogen for argon as the plasma (coolant) gas whenever moderate-power ICP discharges were operated to obtain a lower background emission than with argon. Hydrogen and oxygen were also effective.[54,73,158] Operating with power levels above 2 kW with nitrogen plasma (coolant) gas reduced the molecular emission often arising upon introduction of organic materials into an ICP. Figure 20 illustrates the spectra observed in an argon-nitrogen discharge at wavelengths between 400 and 800 nm when 2 ml/min methanol were nebulized; power levels ranged between 2 and 7 kW.[158] As the power level increases, the emission from CO and C_2 falls. Similar removal of these molecular emissions occurred at similar power levels with an argon ICP. Use of oxygen as the plasma (coolant) gas readily removes the molecular emission. With moderate power lev-

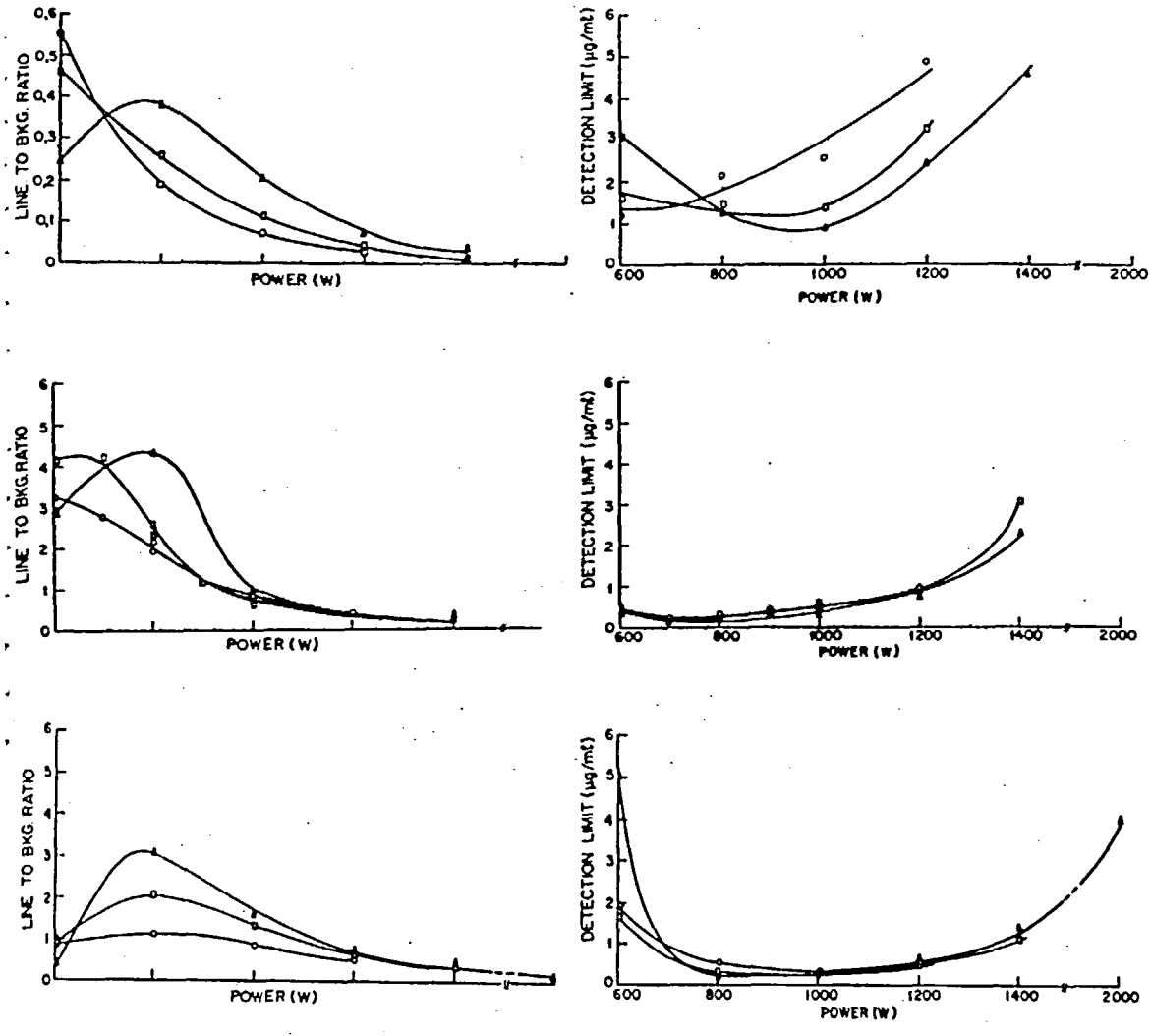

FIGURE 19. Line-to-background ratio (left) and detection limit (right) as a function of power and argon plasma (coolant) gas flow rate for uranium emission at 378.28 nm. A 10-µg/ml uranium solution was used for the line-to-background determination. O 10, l/min; □, 15 l/min; Δ, 20 l/mi. Top 10 mm above the induction coil; middle, 17.5 mm above the coil and bottom, 25 mm above the coil. (From Scott, R. H., Strasheim, A., and Kokot, M. L., *Anal. Chim. Acta*, 82, 67 (1976). With permission.)

els, Greenfield[169] found that nitrogen was the preferred plasma gas at 3 kW based upon analyte signal-to-noise ratios; however at 6 kW, nitrogen was preferred only for lines with high excitation energy. Argon provided better values for those with low excitation energy.

Finally, the energy required to desolvate sample aerosols introduced into the discharge limits the total mass of analyte accepted. With a 6-kW discharge, Greenfield et al.[170] noted that mineral acid concentrations as high as 60% (wt/wt) were introduced without difficulty in the discharge, whereas a low-power (0.8 kW) discharge was unstable, a similar result to when powders were injected. According to Watson et al.,[121] in an ICP similar to Greenfield's, the intolerance to high salt concentrations observed at nominal powers (less than 5 kW) disappeared above 9 kW with solid contents of greater than 15%. The analyte concentration was limited by nebulizer blockage rather than power input to the discharge. Watson et al. also observed that with increasing power the intensity of both atom and ion lines increased with a corresponding increase in background. The background could be lowered by high auxiliary (plasma) ar-

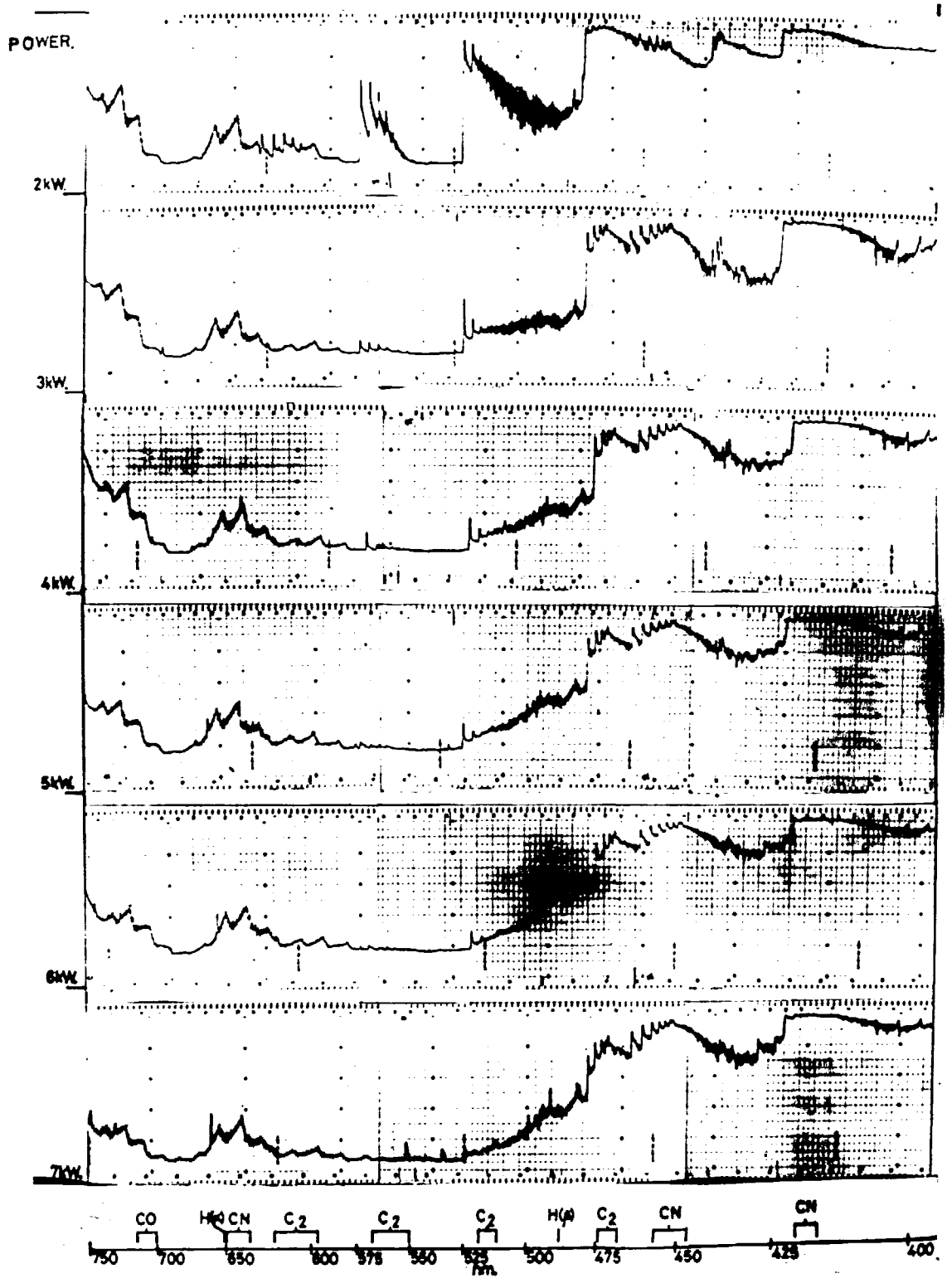

FIGURE 20. Spectra recorded photographically from ICP discharges into which 2 ml of methanol per minute is nebulized (operated with argon aerosol carrier and auxiliary gas flows and nitrogen plasma (coolant) flows) as a function of power from 2 to 7 kW. (From Greenfield, S., McGeachin, H. M., and Smith, P. B., *ICP Inf. Newsl.*, 2, 167 (1976). With permission.)

gon flow without significant loss in sensitivity. The optimum height for maximum sensitivity increased in the discharge as the power was increased.

The optimum operating power level in the ICP discharge is still a topic for discussion, since some investigators are making detailed comparison of the alternative power conditions.[167] Boumans and de Boer[122] questioned whether a mechanism proposed for excitation in argon leading to many of the advantages of the argon ICP would apply to the nitrogen-cooled ICP. The lack of experimental measurements for the argon-nitrogen ICP leaves unanswered the question of whether metastable argon species become partially or completely removed in the argon-nitrogen ICP.

The quest by manufacturers to produce low-power, inexpensive, compact generators and ICP arrangements will probably enlarge the gap between the advocates of low- and high-power levels in the ICP discharge. On the other hand, operating an ICP at a minimum power level without concern for analytical properties is of little value. Although Allemand[143,145] operated an ICP discharge with power as low as 200 W, the introduction of sample disturbed the discharge so that it could not be used analytically. Final power requirements depend upon the coil configuration and the geometry of the ICP discharge tubes.

f. Induction Coil Configuration

The shape and size of the induction coil surrounding the ICP may appear to be relatively simple, especially since vast experience exists in coil design for induction heating applications.[28-32] Coil configuration was not considered by either Greenfield et al.[3] or Butler et al.[4] in their tables of typical generating equipment, and Czernichowski and Jurewicz[37] mentioned coils only in passing. Babat[25,26] determined electric field lines in induction coils and designed several unique arrangements. Induction coil geometry used for spectrochemical analysis depends on the geometry of the quartz tube arrangements; the configurations described by Scott et al.[33] or Greenfield et al.[73] are typical. However, Abdallah et al.[72] employed a five-turn coil, whereas Boumans and de Boer[78] adopted a two-turn coil. Greenfield et al.[73] applied classical concepts to approximate relationships between the induction coil geometry, the discharge radius, and the generator frequency. Scott et al.[33] also attempted to calculate the optimum relationship between frequency and plasma radius. Unfortunately, these approaches are based upon assumptions about the discharge acting as a metallic cylinder and are limited in their application.[34]

The essential factor in coil design is the magnetic flux density the coil produces in the discharge. Allemand and Barnes[145] calculated the magnetic flux density required to operate ICP discharges of different diameters, assuming that the coil could be positioned to produce the necessary magnetic flux density. As indicated in Figure 21, greater flux is needed to operate ICP discharges as the diameter is reduced. To provide this higher flux density for the same coil current, more turns need be made in the same coil length. In practice, copper tubing is flattened and turns are placed closer together to achieve the higher flux. Discharges with an outer confinement tube diameter of 9 mm have been successfully operated. Barnes and Schleicher[161] calculated the effect of induction coil length on the temperature distribution in an ICP discharge and showed that a longer coil provided a larger volume of high temperature gas, but required, at a constant magnetic flux density, an increase in power dissipated in the discharge proportional to the effective length of the coil. Allemand[146] demonstrated that a large number of coil turns and a large voltage drop across the coil are desirable for discharge ignition.

g. Discharge Ignition

To transfer energy from the magnetic field induced by the induction coil, a closed conducting loop must exist within the discharge tube so that a current arises from the induced voltage. Techniques and experimental considerations in initiating induction discharges were reviewed by Eckert,[35] and Czernichowski and Jurewicz.[37] The ICP can be started by inserting a carbon rod until it becomes red hot, by reducing the discharge gas pressure, or by using an electrical starter like a Tesla coil. In practice, the electrical starter is the most common.

Allemand[143,146] studied the initiation of the ICP discharge to design an efficient RF power matching network for an unmanned ICP in-

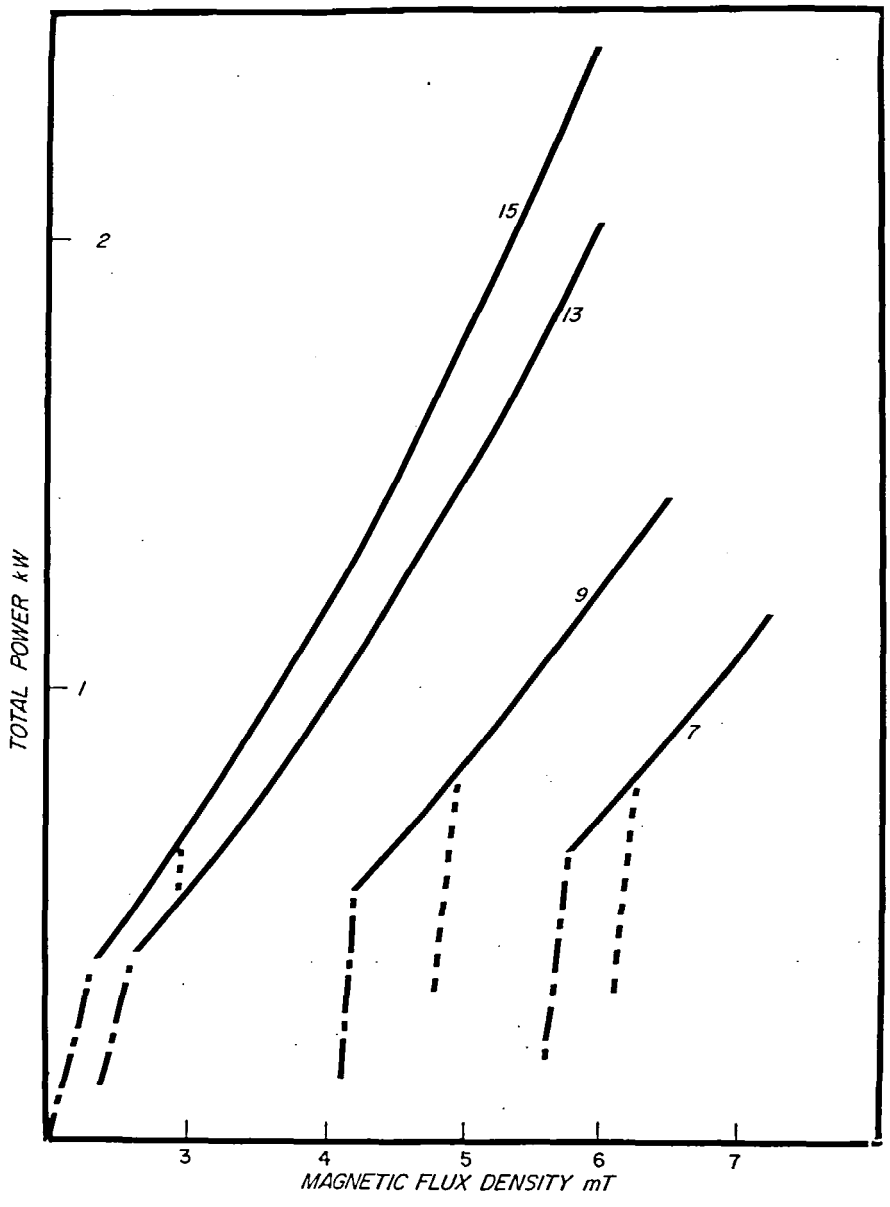

FIGURE 21. Computer predicted values of power in ICP discharges as a function of magnetic flux density at 27 MHz with outer confinement tube wall diameters of 15, 13, 9, and 7 mm. Dashed lines indicate end of stable range when average input velocity of the plasma (coolant) gas is identical for all arrangements, and dotted lines indicate flow common to torch with 13—mm diameter. (From Allemand, C. D. and Barnes, R. M., *Appl. Spectrosoc.*, 31, 434 (1977). With permission.)

strument. As he explains it, the phenomena involved in the ignition of the ICP take place between the moment ions are seeded in the cold gas flowing in the ICP tube assembly and the onset of stable operation of the discharge. The time elapsed during the total ignition process may be well below 0.1 sec or may be extended during any of the three successive ignition phases. Each phase can be maintained as a stable operation and corresponds to a different value of the electrical resistance of the discharge, starting with a high value for cold gas and ending with a minimum value for the fully ignited discharge.

The existence of three phases results essentially because, according to Allemand,[146] the

RF generator delivers a large portion of its output power to the fully ignited plasma (a desired condition that necessitates a good electrical matching between the RF generator output and the fully ignited discharge), consequently, not always allowing the ignition of a cold gas. Therefore, the matching network has to be modified during or immediately after the ignition process. The three successive phases are also specific to the arrangement geometry of the discharge tubes. These stages include:

> After ions have been seeded in the cold gas, filamentary ion paths are formed that follow the general direction of the gas flow.[173] Therefore, their shape depends on the particular gas dynamic condition of the considered torch and on the presence of a relatively high electric field.
>
> When the density of these ion filaments is high enough to form a closed loop of conducting gas, additional RF energy may be acquired by magnetic induction. This will initially occur in regions where ionization is easiest, for instance, when the flow is appropriately set in the low pressure of the plasma (cooling) flow between the intermediate and outer tubes (Figure 13). This mode could be observed and maintained in a boron nitride torch, which would withstand the heat generated by the nearby discharge. It can also take place in the region between the intermediate and the central tubes.
>
> With increasing power, obtained by a tuning of the matching network and/or by increasing the RF power output from the generator, the size of the visible plasma increases. When enough conductivity has been generated in the intermediate region between the outer plasma (coolant) flow and the central carrier flow, the discharge rapidly shifts from the plasma (coolant) flow into the intermediate region and fills it, or if it is already in the intermediate region, it simply grows.

Allemand suggested that the three stages result in three distinct electrical modes. In the first mode, the power is delivered by the electric field. Therefore, the matching network has to be tuned to produce a high electric field. In the second mode, the power is delivered by the magnetic field; however, the matching network is still tuned for the first phase of ignition, and only a small portion of the power from the generator is delivered to the discharge, the resistance of which, therefore, remains relatively high. The third mode is obtained after the matching network has been retuned to deliver a maximum RF power to the discharge, resulting in a lower plasma resistance.

Allemand and Barnes[146] investigated the impedance changes during the ignition process as well as after full ignition, when different samples are introduced into the discharge and increase its electrical resistance. A precise computer model was derived by Allemand for a particular matching network when unloaded and loaded with an argon discharge and an aqueous sample. Experimental and calculated results correspond closely.

2. Plasma Tube Arrangements

a. Configurations

The most critical component of the entire ICP instrument is the plasma tube arrangement (torch or burner) and its design and fabrication. Diverse configurations exist for engineering and spectrochemical applications,[3,4] but all share the common features of gas stabilization (Figure 1) first described by Reed.[39,40,42,43] The engineering arrangements offer a number of potential design directions for spectroanalytical configurations; however, most of them were designed with different power level and application objectives. Engineering ICP torches were illustrated in some detail in various reviews.[13,35,37,44]

Arrangements for spectrochemical analysis have similar critical features in providing two or three gas flows (Tables 1 and 8) but differ in exact dimensions and details with investigator and application. Plasma torches commercially available today do not significantly differ outwardly from the first designs of Greenfield et al.[50,52,53] shown in Figure 2. Versions of ICP torches for emission, absorption, and fluorescence have been fabricated from quartz, boron nitride, or brass.

Basically, the ICP discharge tube arrangement provides a container through which the discharge gas flows and in which the discharge is created and maintained. Analyte species are

transients in the tube, staying only long enough to undergo the precursory steps to absorption, emission, or fluorescence in the postdischarge region. The ignition of the discharge, the efficiency of gas utilization, the extent of energy transfer to the analyte, the stability of the background and analyte emission signals, the spatial distribution of analyte species, the extent of interferences, and the analysis properties of the ICP depend critically on the arrangement and fabrication of the ICP tubes.

The schematic diagram of the ICP arrangement in Figure 11 illustrates the basic constraints. Appropriate gas flow must be provided for two or three gas streams; the length of the tubes must be sufficient to prevent the discharge from jumping to the induction coil; accommodation must be made for viewing the desired radiation; and means and materials must be provided to prevent the confinement tube near the discharge from melting, reacting, or otherwise failing.

Greenfield et al.[3] tabulated flow patterns and type of plasma in their summary of ICP equipment; Butler et al.[4] reproduced diagrams of a number of the early torch arrangements; and in Table 10, Kornblum and De Galan,[189] give coil dimensions, gas velocities, and spectral observation data from many of the currently used ICP arrangements. The dimensions of popular arrangements are given by Scott et al.,[33,92] Fassel et al.,[6,95,119] Boumans and de Boer,[78,87,103,104] Greenfield et al.,[73] Ohls et al.,[81] and Genna and Barnes.[173] Allemand described tubes constructed with boron nitride,[143,145] and Mermet et al.[72,276] designed a torch with a brass central portion.

As indicated in Tables 1 and 8, the gas flow rates vary considerably, and even today with essentially identical tube configurations, gas flows tend to differ as the result of a variation in positioning the tube relative to the induction coil and in coupling effectiveness with the magnetic field. Many authors[33,78] have found that no auxiliary (plasma) flow is needed for routine work, and lower plasma (coolant) flow rates can be achieved by appropriately designing the outer and intermediate quartz tube[33,276] and/or modifying the plasma (coolant) gas swirl velocity.[173] The orifice diameter of the aerosol injection tube has been optimized empirically[33,170,276] so as to provide sufficient linear velocity from the injector to penetrate the base of the discharge but not to transport the aerosol through the discharge too rapidly. Under some operating conditions, aerosol droplets coalesce on the injection orifice after prolonged spraying of high concentration solutions, so that Scott and Kokot[92] affixed a capillary as the aerosol injection tube. Greenfield et al.[73,158,170] used borosilicate glass for the aerosol injection capillary; the tube arrangement described resulted from empirical evaluation of various tube dimensions. Careful design of the injector arrangement was stressed by Greenfield et al.[170] when organic solvents and acids were nebulized to keep the organic constituents contained within the central channel of the discharge. However, Peterson[277] found no numerical correlation between carrier flow rate or tube geometry and particle velocity in the discharge.

Both fixed and removable torch configurations have been described. For example, Dickinson and Fassel,[62] Boumans and de Boer,[71] Alder and Mermet,[131] Mermet et al.,[72,276] Ohls and Krefta,[177] and Lichte and Koirtyohann[178] employed holders into which the plasma tubing could be inserted or removed at will, whereas Greenfield et al.,[73] Scott et al.,[33,92] and others worked with single or two-piece prealigned torches.

A number of new arrangements have been developed recently. For example, Apel et al.[179] fabricated a boron nitride torch with tangential plasma (coolant) gas flow directed by a ring with offset slots along the perimeter. Genna et al.[173] developed a novel tube arrangement similar to that described by Scott et al., except the circular velocity of the plasma (coolant) gas was increased by an order of magnitude by injection through a nozzle. This reduced the amount of plasma gas needed to initiate and sustain the discharge and improved the ease of ignition by reducing the pressures in the center of the torch.

Mermet et al.[72,129,276] devised configurations for emission and absorption; in the emission configuration, everything except the outermost tube was constructed with brass, and no plasma (coolant) gas was used. Instead, auxiliary (plasma) flow through an optimally dimensioned annular injector was employed. In the AAS configuration, a lens was fitted into the base of the tube holder, and the sample is in-

jected on-axis through a 2-mm alumina tube. The absorption path extended axially through the central channel of the discharge. Lichte and Koirtyohann[175] viewed the ICP axially with a conventional tube arrangement in emission, and plasma tube configurations for atomic fluorescence (AF) spectroscopy were evaluated and applied by Montaser and Fassel,[176] who extended the length and constricted the diameter of the outer quartz tube of the usual torch design[6,95,119] and found optimum AF signals at distances of 45 to 65 mm above the load coil. Other arrangements for AAS were described in References.[57,59,61,64 through 71] These workers generally measured the absorption radially in the region beyond the induction coil.

Probably the most unusual development in ICP discharge configurations was the work of Allemand[143] in the design of an unmanned ICP-AES instrument and in the improvement of routine spectrochemical analysis.[145] Plasma torch design and shapes were studied experimentally and by computer simulation to facilitate ignition, concentrate the sample into a narrow central channel, raise the sample to excitation temperature with optimal efficiency, and to avoid clogging by organic samples such as residual oil. In preliminary tests,[143] 36 different torch arrangements were tested for ease of ignition, minimum gas flow for stable operation, and confinement of the sample. These studies indicated that ignition was facilitated by recirculatory flow of plasma gases, argon consumption could be drastically reduced by careful design, and laminar flow would confine the sample better than other flows. Operating conditions of torches with diameters from 7 to 18 mm were calculated using a computer model (Figure 21). Small torches required high magnetic flux density. The ratio of intermediate tube-to-outer tube diameters was also computer simulated, and a geometry with a large ratio of intermediate-to-outer diameter (e.g.,> 0.9) was easier to maintain.[145] Particle decomposition predictions were also made (Figure 22) for 7,9- and 15-mm diameter torches, which indicated that particle residence time before decomposition was longer in larger diameter torches. An experimental arrangement was fabricated with boron nitride to test the predictions, and spectroanalytical results indicated improved limits of detection compared to a conventional torch arrangement,[33] smaller spatial spread of emission from diverse elements, easier discharge ignition, low power consumption, reduction of argon flow, and increased tolerance to high solution sample injection rates.

b. Gas Composition

The ICP can be operated with any gas if sufficient power and correct geometry are used. Czernichowski and Jurewicz[37] compiled a list of working gases in electrodeless discharges, and Dresvin[36] considered the parameters of induction plasma generated in molecular gases. Kleinmann and Polej[7] included a table of gas atmospheres for HF discharges. Unlike microwave discharges[5] or induction discharges operated at reduced pressures or high power levels,[25,26,44-47] the ICP employed in spectrochemical analysis is restricted by the size of the RF generator, cost, and the convenience of argon or argon-nitrogen mixtures (Table 1). Argon is the preferred operating gas for ICP-AES because of its ease of operation, purity, relatively low cost, and inertness. Greenfield et al.[3] have argued for argon discharges cooled with nitrogen. If an appropriate generator is available, the results appear to be suitable. Direct performance characteristics under common conditions for argon and argon-nitrogen ICP discharges are not available, although Abercrombie and Silvester[139] observed limits of detection with a nitrogen plasma (coolant) gas at 2.8 kW approaching those obtained with argon plasma flow at 1.6 kW. Boumans and de Boer[122] compared the signal-to-background ratios of some ion lines observed in their argon ICP under compromise conditions for simultaneous multielement analysis (1.1 kW) with values reported by Greenfield for a 6-kW argon-nitrogen ICP discharge and noted differences of one to over two orders of magnitude in favor of the argon ICP.

Barnes and Nikdel[88,180] considered pure argon and pure nitrogen ICP discharges in a computer simulation study. They verified the requirement of high power and magnetic flux density to maintain the nitrogen discharge and predicted lower maximum temperature, shallower thermal gradients, higher axial velocities, and shorter residence times for the nitrogen discharge compared with the argon discharge. However, they also found more complete sam-

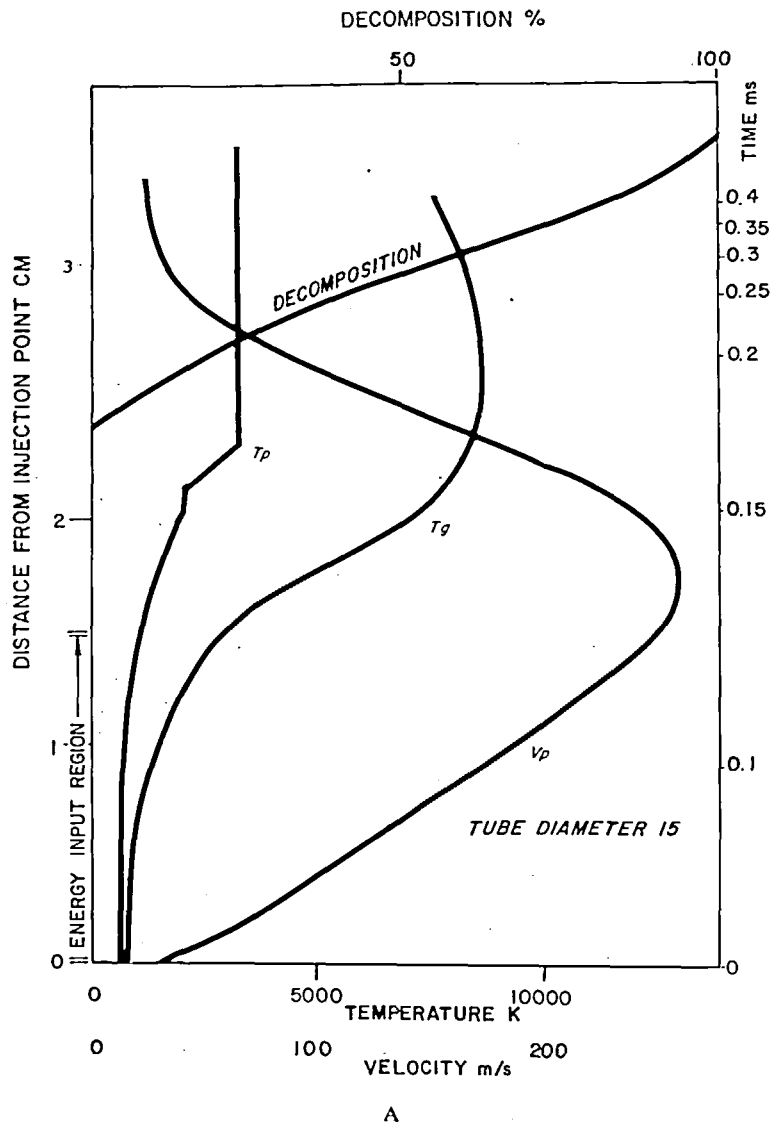

FIGURE 22. Computed decomposition of a 5-μm diameter aluminum oxide particle traveling along the central axis of the ICP discharge for confinement tube diameters of 15 mm (A) and 7 mm (B). Vp, particle velocity; Tp, particle temperature; Tg, gas temperature; and decomposition expressed as percentage (top). The scale to the right indicates the time the particle spent traveling from the point of injection below the induction coil (represented by the energy input region) to that particular height. (From Allemand, C. D. and Barnes, R. M., *Appl. Spectrosc.*, 31, 434 (1977). With permission.)

ple decomposition and vaporization in nitrogen than in argon because of the higher thermal conductivity of nitrogen at the temperature of injected solid particles. Energy balance, temperature distributions, and radial power input distributions were also calculated. These predictions have not been experimentally verified, although they will be studied in the near future.

Since the computer simulation is general, any molecular gas can be treated.[180] As a preliminary step toward the computer simulation of mixed argon-nitrogen discharges, Barnes and Nikdel[181] measured the concentrations of nitrogen and argon in and around a conventional ICP discharge by gas chromatography and observed substantially different mixing patterns

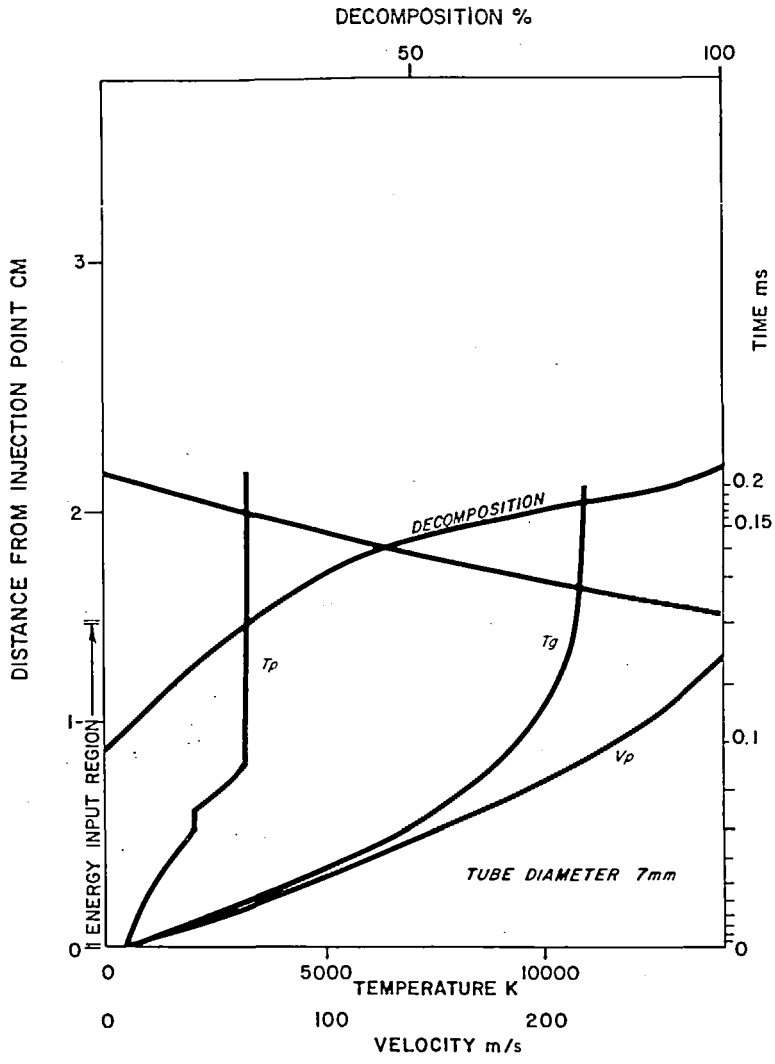

FIGURE 22B

for gas flow with and without the discharge and aerosol carrier gas flow.

A number of studies have been conducted with argon-doped gas mixtures in the ICP discharge for diagnostics and analysis. Abdallah and Mermet[134] investigated the behavior of nitrogen, oxygen, and air as the aerosol carrier gas in an argon ICP discharge and found comparable rotational temperatures derived from the molecular ion spectrum and excitation temperature from injected elements. The relative advantages of nitrogen as aerosol and plasma (coolant) gases were judged by the spectra produced. Alder et al.[110] introduced nitrogen produced by the reduction of ammonium ion, into the ICP for the determination of trace levels of ammonium in aqueous solutions. Alder and Mermet[131] studied gas mixtures of argon and methane, sulfur dioxide, hydrogen sulfide, sulfur hexafluoride, phosphorus trichloride, hydrochloric acid, and bromine. They observed atom and single-ion lines for P, Br, Cl, and S and atom emission for F, as gases, but no emission from sulfur or halogens in solution. Temperature profiles, electron number density, and effect of additives were measured in the argon-methane plasma. Jarosz and Mermet[126] continued the spectroscopic investigation of argon-hydrogen sulfide discharges to find new S I and S II lines and to establish the electron density and ionization temperature that indicates a lack of LTE in the discharge. The appearance of cer-

tain lines, especially S II, could only be explained by a mechanism involving excitation from metastable levels of ionized argon. Alder et al.[136] investigated the spectrum of atomic sulfur introduced as sulfur dioxide (0.1 l/min) in the ICP, and Abdallah and Mermet[134] characterized the behavior of nitrogen excited in an argon ICP. Addition of small amounts of hydrogen for plasma diagnostics is common,[130,155] and Truitt and Robinson[163] made spectroscopic studies of various gases and hydrocarbons introduced into an argon ICP discharge.

c. Gas Flow

Gas flow is one of the three critical parameters used in adjusting the ICP for optimum operation. Typically, plasma (coolant) and auxiliary gas flow rates are set, and the aerosol carrier flow rate is varied; analyte and background radiation and noise are then monitored as functions of power and observation zone.[78,104,122] These relationships are illustrated in Figure 20. As indicated in Figure 8, a change in the central flow rates can move the position of maximum emission along the central axis of the discharge;[113,182] this is demonstrated in Figures 9 and 10. The radial temperature and electron number density in the discharge vary substantially with a change in the aerosol carrier flow rates. Although Edmonds and Horlick[113] observed the upward shift in the emission spatial pattern for Ca I (Figure 8) as a result of an increase in plasma (coolant) flow, they observed a strong change in the intensity of the emission for Ca II rather than a change in position. Because of these effects, diagnostic studies and investigations of interelement effects depend upon gas flow rate as a major variable.[128,165,182,189] Among the possible variables for minimizing interferences from alkalis in single-element determinations, the carrier gas rate was selected by Boumans and de Boer[122,278] as the most convenient and efficient parameter for this purpose. Figure 11 illustrates the dependence of the interference effect of KCl on the carrier gas flow rate at constant power and observation height for their argon ICP arrangement. Since Boumans and de Boer found both net line signals and interference effects to depend critically on the carrier gas flow rate, they used a precision pressure gauge for controlling and a mass flowmeter for monitoring the carrier gas flow rate with a cross-flow pneumati nebulizer. This configuration enabled them t control the flow rate to within 0.75% at an up stream pressure of 2×10^5 Pa (30 psig). For ex ample, Kirkbright and Ward[96] demonstrate how a dilution of the atomic concentration i the discharge modified the analytical curve when the auxiliary (plasma) gas flow rate wa altered. A reduction of analyte particle densit occurred when auxiliary gas flow was used, s that Kirkbright and Ward observed an increas in the linear range for Ca and Zn.

Discharge ignition is strongly dependen upon gas flow.[143,145,173] Although coaxial lami nar[51] flow arrangements have been explored,[18] the tangential introduction of the plasma (cool ant) gas (Figure 13) has proven popular and ef fective for analysis and for its operating prop erties including ignition.

Reed's entire basis for obtaining a stabilized induction plasma was the particular arrangement of gas flow.[39,43] His patent specified that recirculatory flow produced by the turbulence of the vortex or tangentially introduced gas provided continual reignition and stability of the discharge. Huska and Clump[183] not only reviewed the approaches for gas stabilizing induction discharges, but introduced a new approach (jet suction) which appeared to be superior to both coaxial laminar and tangential flows. The gross recirculatory flow pattern in all three systems was the same: a recirculatory flow along the longitudinal axis of the tube opposite in direction to the bulk flow. The flow pattern prevented passage of reactants directly through the central region of the discharge if not corrected by an appropriately designed and located carrier flow injection.

Axial gas flow characteristics in induction-heated plasmas were measured experimentally by Chase,[184,185] Dundas,[186] and Klubnikin et al.[187,188] These measurements indicated complex recirculatory patterns in the discharge. Until recently, measurement of the gas flow patterns in spectroanalytical ICP discharges had not been attempted, and the extent to which these results could be extrapolated was not known. Boulos[192] computed recirculatory flow patterns of the ICP (Figure 23).

Barnes et al.[173,190,191] measured velocity distributions in a spectroanalytically useful ICP discharge by means of photographic and pressure

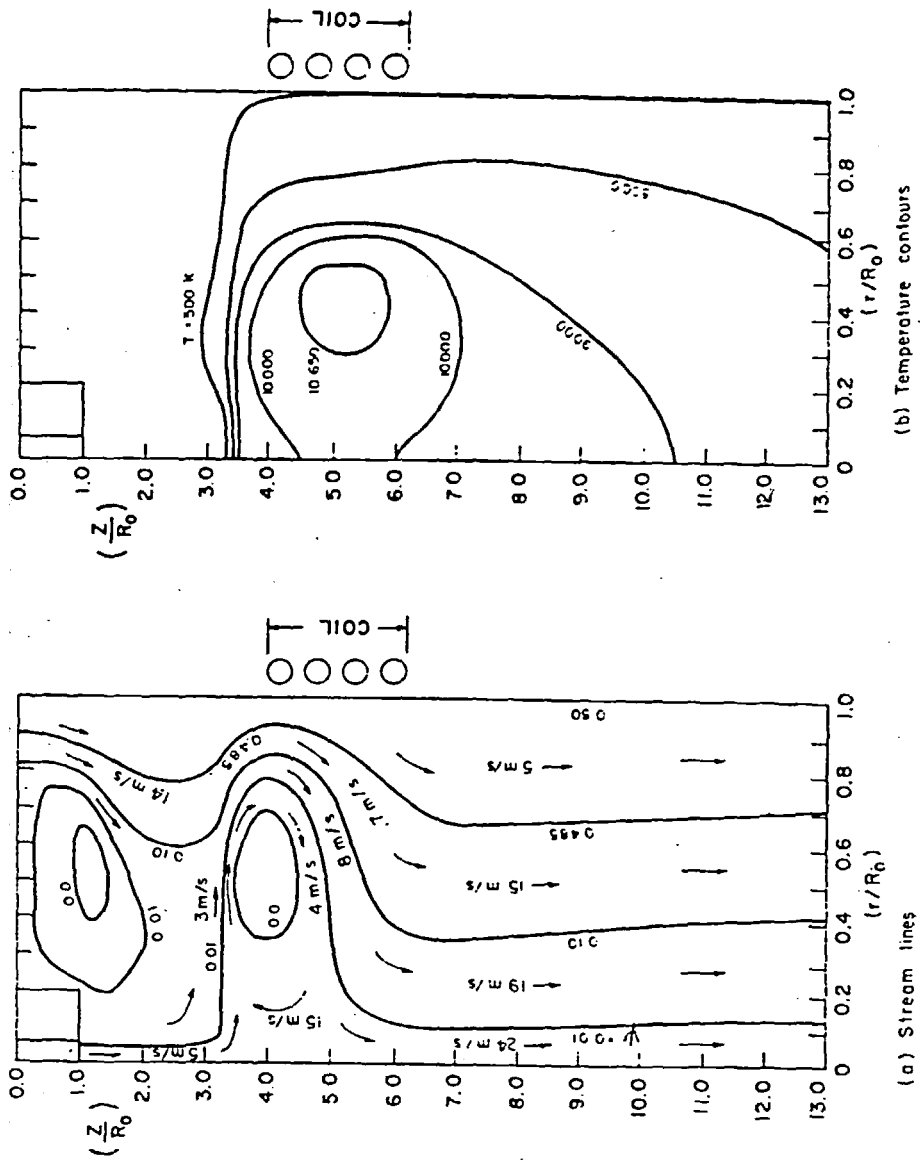

FIGURE 23. Streamlines (a) and temperature contours (b) calculated for an induction discharge operated at 3 MHz and 4 kW with aerosol carrier flow of 0.4 l/min, auxiliary flow of 0.2 l/min, and plasma flow of 16 l/min. Typical velocities are also given in (A). (From Boulos, M. I., 3eme Symposium International de Chemie des Plasmas, Communication, Paper No. S. 3.2, Limoges, France, 1977. With permission.)

probe techniques. High pressures and velocities are found along the central axis of the discharge due to the aerosol carrier gas and along the confinement tube walls due to the plasma (coolant) flow. In general, the aerosol carrier stream expanded from the injection nozzle then remained constant in width inside the induction coil; however, at the end of the coil, the flow began to expand again. The velocities and pressures varied with dimensions and positions of the injection nozzle and discharge operating conditions. The introduction of plasma (coolant) flow with a large circular (swirl) velocity component substantially lowered pressures throughout the discharge. Pressure and velocity also changed with power input and auxiliary flow. Gas flow patterns teamed with effective temperatures provide a basis for studying the heating of analyte in the discharge.

Since the discharge initiation depends upon the gas flow,[143,145,146,173] a number of studies have led to easily ignited discharge conditions. Recirculatory flow and lower local gas pressures increase ionization probability and reduce ignition time; during discharge initiation, ionization paths should be made to conform to ring-shaped patterns, producing closed loops of conducting gas. Both reduced pressure and ring-shaped ionization paths have been produced by means of controlled tangential velocity when the plasma (coolant) gas was injected at a velocity ten times higher than normal.[173] Allemand[143] enhanced recirculatory flow by using a flared auxiliary tube which created a strong turbulence or by a Venturi effect obtained with a small hole in the side of the auxiliary tube which pulled the gas in a reverse direction in the auxiliary tube region. The Venturi configuration allowed operation at very low power with easy ignition.

Since spatial spectral characteristics are studied for gas flow rates and power levels by conventional optical arrangements which limit the observation zone to a single location, Edmonds and Horlick[113] and Franklin et al.[182] obtained detailed spatial spectral distributions directly and conveniently using photodiode arrays. Profiles were measured for atom and ion lines of several elements as a function of plasma power, aerosol flow, and plasma (coolant) flow rates (Figure 8). The ICP discharge displays complex but characteristic emission spatial patterns which depend upon both flow and power.

3. Sample Introduction

a. General

Sample introduction with the ICP is in many ways similar to that found with other spectrochemical plasma sources, so that very similar problems, limitations, and advantages exist. Many of the sample introduction techniques developed for AAS, AFS, and microwave and DC plasma AES can be applied with suitable modification for the ICP. However, some of the characteristics of the ICP uniquely define the type, form, and rate of sample introduction, so that conversion of a sample technique from another spectrochemical source to the ICP requires some care.

Considering the extensive work of Kranz[204,205] on aerosol introduction in plasmas, Boumans and de Boer[116,124,149] reported the difficulty with the spectrochemical applications of high-temperature plasmas is the introduction of the sample effectively and reproducibly into the discharge. This problem has been elegantly solved for the ICP by forming the discharge into a toroidal shape with the sample traveling into the discharge along the centerline, surrounded by an inviting, warm environment, ideal for sample decomposition.[50,52,53,73] The formation of the toroidal discharge depends upon the aerosol carrier gas flow, the geometry and location of the injection orifice, and in a minor way the frequency.[116] All of these parameters are readily controlled. Thus, the ICP discharge offers the analyst an environment for sample treatment unique among electrical excitation sources.

During the Noordwijk ICP Conference,[196] Mermet systematically reviewed the sample introduction techniques used with the ICP. This scheme is reproduced in Figure 24 for liquids, solids, and gases. Liquids can be treated in categories according to their viscosity, their chemical reactions, or their volume. Solid handling depends upon the form of the sample-powder, solid, or molten solid. Gases are often considered separately, because of the relative ease with which they are handled.

A need exists for substantial research directed toward sample introduction methodology for the ICP discharge. For example, fundamental and practical investigations should be done to characterize pneumatic and ultrasonic nebulizer droplet generation, to define the limitation and properties of the desolvation stages,

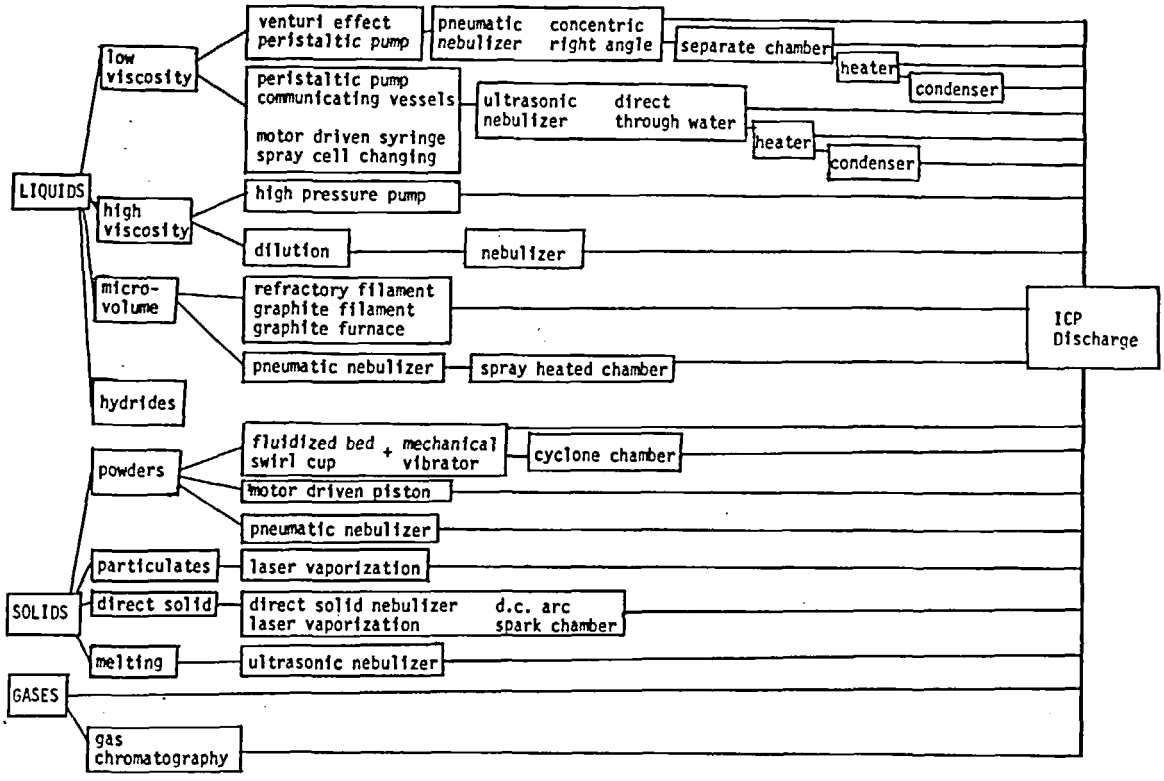

FIGURE 24. Schematic diagram for sample introduction of liquids, solids, and gases into the ICP discharge. (After Mermet, J. M., *ICP Inf. Newsl.*, 2, 70 (1976).)

and to control the distribution of aerosol or individual droplets for optimum spectroanalysis. Microvolume solution techniques also require development, either independently or in conjunction with nebulizers, and the generation of gases or vapors needs considerable study. For the analysis of solids, a reliable and inexpensive device is essential, and the extent to which it introduces solid state interferences must be documented. Powder sampling demands a considerable research effort. In this field much might be learned from both the experience gained with powder insufflation methods in AC and DC plasma spectrometry[206,207] and the results of investigations concerned with solid state interferences in DC carbon arcs and the borate fusion technique for overcoming these interferences.[208,209] Powder sampling in general and more particularly for ICP-AES still demands a considerable research effort. Since sample introduction currently appears to represent the most serious practical limitation in the application of ICP-AES and since it provides many opportunities for innovative development in analytical laboratories equipped with ICP instruments, significant progress can be expected in the near future.

Syty[193] critically reviewed methods of sample injection and atomization in atomic spectroscopy and emphasized electrothermal atomizers and chemical vaporization techniques. Fassel[147] narrowed the topic to liquid samples of limited volumes in a comparison of ICP-AES with electrothermal atomizers. Greenfield et al.,[3] Butler et al.,[4] and Dahlquist[213] surveyed ICP-AES methods for analyzing solutions and solids as powders. Analysis by ICP-AES is most commonly performed using solution samples, although solid and gas samples can be analyzed with special techniques.

b. Liquids

Depending upon the physical and chemical properties of the liquid, aerosols may be produced in a number of ways (Figure 24). Liquids of moderate and low viscosity can be nebulized pneumatically or ultrasonically either by transporting the liquid by the Venturi effect or by

pump to the nebulizer. Viscous liquids require pumping or dilution. Microvolume sample sizes necessitate special handling, and various electrothermal devices desolvate and vaporize without nebulization. Spray chambers and other arrangements are used to improve sample aerosol production efficiency and stability,[33,165] and desolvation facilities may be required with high-efficiency nebulizers; however, they may introduce desolvation interferences.[87,147]

The two most commonly employed, traditional pneumatic nebulizers, the concentric[198] and the right-angle,[197] are used with some modification for ICP-AES for aqueous and nonaqueous liquids.[170] Pneumatic nebulizers have been applied with the ICP for aqueous[33,59,81,120,122,137,170,177,179] as well as nonaqueous solutions.[73,143,170,194,195] Conventional concentric nebulizers, generally metallic, have been adapted from flame spectrometry; however, they are often limited because the high flow of gas operating the nebulizer is too high for optimum performance of the ICP, and a portion of the aerosol and gas flow must be vented. Kniseley et al.[95,120] fabricated a right-angle nebulizer which operates with an argon flow of approximately one liter per minute and draws solution at approximately 3 ml/min. Although care must be taken in fabrication and positioning its capillaries,[92,120] and precautions must be taken to prevent clogging,[199] Abercrombie and Silvester[139] and Wohlers[200] found that in comparisons of metal concentric, glass concentric, and right-angle nebulizers the right-angle nebulizer performed better than the two others with solutions containing high salt concentrations. Some of the dissolved salts precipitated at the tip of the concentric glass nebulizer; otherwise, the stability, sensitivity, detection limits, and memory effect of the three nebulizers were essentially identical.

Fassel et al.[194,277] used a pneumatic nebulizer in the analysis of oils after dilution; however, Pforr[195] pumped oil directly into a pneumatic nebulizer, and Allemand[143] incorporated a domestic oil burner nozzle in a pressure sprayer for the analysis of residual oils heated to reduce their viscosity. Elimination of solvent dilution in this latter arrangement increased the absolute sensitivity.

In a study of the nebulization effect with acid solutions, Greenfield et al.[170] correlated the influence of the physical properties of five mineral acids, three organic acids, and methanol with spectral intensities of five elements emitted in a high-power (6 kW) ICP discharge. Nebulization and emission signals of analyte in concentrated mineral acids depended on reduction in sample uptake due to increased sample viscosity, and variations were reduced by pumping at a constant rate and correcting for volume flow rate. With the 6-kW discharge, no significant interferences or other discharge difficulties were encountered. Organic acids and solvents enhanced emission signals because of changes in the nebulization rate which was semiempirically related to the viscosity, surface tension, and density. Injection of high concentrations of mineral acids into flames was impossible, and Greenfield et al. cautioned against extrapolating the absence of plasma interferences at 6 kW to lower power levels. Dahlquist and Knoll[94] obtained essentially identical results with a moderate (1.6 kW) operating power in an argon ICP discharge, and they demonstrated that the use of an internal reference element or normalization for a measured uptake rate of mineral acids could compensate for changes in the nebulization and transport subsystems.

Kirkbright and Ward[96] demonstrated the effect of sample uptake rate on the linear range of analytical curves for Ca II and compared the effect to results obtained with AAS. When Ohls[137,297] replaced a metallic, concentric AAS nebulizer with a concentric glass nebulizer, he found improved efficiency of gas flow and sample uptake, relative intensities increased by 1 to 2 decades, optimum emission for all elements studied in a single location, and the ability to replace sequential recording on single elements with simultaneous multichannel observations. Apel et al.[179] studied several different pneumatic nebulizer designs and observed that a fritted-disk nebulizer provided an overall efficiency of over 60% compared with the 5% efficiency of a right-angle nebulizer. Chambers into which pneumatic nebulizers spray their aerosol were designed by Scott et al.[3] to reduce fluctuations in the aerosol by separating forward and reverse aerosol flows, by Larson et al.[115] to reduce cleanout time, by Greenfield and Smith[201] to desolvate microvolume samples, and by Kniseley et al.[119] for clinical solution analysis.

The production of aerosols by means of ultrasonic breakdown of liquids has been applied extensively throughout the development of ICP discharges.[51,58,62,71,73,77,78,82,87,102-4,149] Nonetheless, ultrasonic nebulizers are not commonly available with commercial ICP-AES instruments. Ultrasonic nebulizers produce a finer aerosol mist and provide superior limits of detection than do pneumatic nebulizers.[73,78,87,102,103,122] Apparatus for the desolvation of aerosols was described for ICP instruments by Veillon and Margoshes,[304] Boumans and de Boer,[78,87,103,104,149] Butler et al.,[95] Dickinson and Fassel,[62] Kornblum and de Galan,[82] and Souilliart and Robin.[77] Desolvation may be necessary to remove molecular solvents from the aerosol stream prior to entering the discharge; consequently, when the discharge is operated at low power, it does not become unstable.

Characteristics of ultrasonic nebulizers were reviewed by Olson et al.[102] Greenfield et al.[3] cited the difficulty in sample handling as the single marked disadvantage of ultrasonic nebulizers. In the past, this precluded automatic operation. Desolvation apparatus must also be used if the discharge is extinguished upon introduction of large quantities of solvent. Recently, Olson et al.[102] described a chemically resistant, reliable, easy-to-build, ultrasonic nebulizer which provided rapid and convenient sample changing capability, acceptably short cleanout time, and long-term stability. When combined with a conventional desolvation apparatus, they achieved an improvement of an order of magnitude or more in simultaneous multielement detection limits for a representative set of 14 elements when compared to the right-angle nebulizer with or without desolvation. Many of these values are listed in Table 7. Previous inequalities in limits of detection were traced to a dissimilarity in the rate of sample delivery to the ICP arising from diverse nebulizing systems. The direct measurement of the overall efficiency of nebulization indicated that an approximate tenfold (11 vs. 1.1%) greater rate of sample delivery was responsible for the superior powers of detection achieved with the ultrasonic nebulizer compared with the pneumatic nebulizer. However, the ultrasonic nebulizer required desolvation, and when applied without it, either the discharge became unstable or the sample introduction rate was reduced and detection limits were degraded. Desolvation with pneumatic nebulization only marginally improved detection limits. Cost estimates of a commercial version of this type of nebulizer set its price at about $2000 compared with about $200 for a concentric glass pneumatic nebulizer.

In comparing ultrasonic with pneumatic nebulization, Boumans and de Boer[122] found detection limits five times poorer with the right-angle nebulizer. In practical analysis, however, the right-angle nebulizer provided an equal or improved detection power, because the salt content of solutions with the right angle-nebulizer could reach 1% safely without exceeding a ±10% interference level. On the other hand, the ultrasonic nebulizer had to be limited to about 0.1% solids to reach the same low level of interferences. Boumans and de Boer[87] also found that the maximum permissible salt content with ultrasonic nebulization had to be kept below 0.4% to prevent memory effects resulting from salt deposits on the plasma tubes. Boumans and de Boer[104] investigated the factors which affect efficiency and injection rate of wet aerosol with their ultrasonic nebulizer assembly; these factors included solution uptake rate, carrier gas flow, dimensions of the inlet and aerosol chamber, and the desolvation apparatus. The performance of their ultrasonic nebulizer was dependent on the carrier gas flow, and effects were observed during desolvation related to the concentration of concomitant.[87] Adapting two ultrasonic nebulizers with independent desolvation units, Boumans and de Boer[87] separated interferences that resulted from processes in the plasma and in the nebulizer-desolvation apparatus. The magnitude of the desolvation effect varied between ±10% at an optimum desolvation temperature of 140°C and was related to the difference in volatility between matrix and analyte.

Greenfield et al.[73] found that pneumatic nebulizers without desolvation generally gave poorer limits of detection than did ultrasonic nebulization with desolvation. Desolvation improved sensitivity but not precision, and occasionally it led to memory effects.

Turning to microvolume samples, Greenfield and Smith[201] injected 1- to 25-μl volumes of solution from a micropipette or syringe into a

pneumatic nebulizer in the analysis of oil, organic compounds, and blood samples with a relative SD of about 5%. Both heated and conventional spray chambers were connected directly to the aerosol injection tube of the ICP assembly. The heated chamber provided an order of magnitude improvement in sensitivity. Later, Kniseley et al.[119] also introduced 25-μl volume samples of diluted whole blood and plasma from a micropipette directly into a pneumatic nebulizer, desolvation apparatus, and ICP discharge. Reproducibility of 5% was improved to 3% when 100-μl volume samples were nebulized. Greenfield and Smith integrated the signals photographically, and Kniseley et al. measured the transient signal photoelectrically.

Dahlquist patented[202] and developed[203] a novel device called the graphite yarn atomizer for electrothermally vaporizing microvolume samples into the ICP discharge. A sample was deposited on a continuous graphite yarn, desolvated electrothermally, and vaporized electrically into the discharge. Although this procedure (using a prototype device) compares favorably with pneumatic nebulization (comparable relative and superior absolute limits of detection), no commercial product has become available.

Nixon et al.[210,211] described and applied a filament vaporization arrangement employing tantalum filaments or pyrolytic graphite substrates[147] for 200-μl volume samples. A low current through the filament vaporized the solvent and ashed the deposit, and a high current applied to the filament caused the sample to vaporize into an aerosol carrier gas stream. Relative SD was approximately 4%. Relative and absolute limits of detection generally exceeded those obtained with pneumatic nebulizers[203,210] and equaled those for other electrothermal atomizers in AAS. However, interelement effects arising from physical changes or refractory compound formation and spectral interferences presented formidable problems which were not resolved. In contrast, Kirkbright et al.[305,306] used a commercial graphite-rod electrothermal atomizer for trace analysis of uranium metal and other materials.

c. Solids

Unlike nebulization of liquids into the ICP, presentation of solids as powders, particulates, vapors, or metal aerosols has received neither the same attention nor enthusiasm from spectrochemists. In their survey of solids introduction techniques, Greenfield et al.[3] described almost exclusively powder techniques; even the technology developed for the engineering applications of induction discharges for processing solids[36,37] has contributed essentially nothing to recent developments.

Dahlquist[213] considered various possibilities for direct analysis of solids, including a number of novel devices and approaches for relatively specific applications. For example, a device for the direct atomization of solids was patented and developed commercially by Dahlquist et al.[203,212] Originally marketed as a sampling device for other spectrochemical sources,[214,215] the direct solids nebulizer (DSN) employed an electric arc struck between an annular counter electrode connected as the anode and the solid material to be sampled as the cathode. The arc current caused ejection of very small droplets of material which solidified and were removed as a fine metal aerosol by the argon carrier gas. In one version,[212] the DSN was ingeniously engineered as a hand-held device which could be attached to the ICP-AES instrument by an umbilical cord as long as 20 m for remote sampling. Precision values obtained for standard materials compared well with established methods, and linear analytical curves were published. Approximately equivalent amounts of steel were injected into the ICP for both the DSN and a conventional nebulizer using a 0.5 wt% steel solution. Because of the lower noise produced by liquid nebulizers, the power of detection of liquid nebulizers was marginally better than the DSN for most elements. Background equivalent concentrations were comparable for both devices, with the DSN showing slightly better analytical performance. The commercially available arrangement has experienced only limited sales, presumably as a result of its cost relative to alternative sampling excitation sources such as spark discharges.

Taking an alternative tack to the DSN for solid sampling, Human et al.[216] adapted a conventional high-voltage spark, operating at 50 Hz, for nebulizing materials from conducting samples. Adequate amounts of material were sparked from the solid for analysis by ICP-AES, although substantial changes in intensi-

ies occurred during the first few minutes of sparking, and relatively long times were required for analysis. Alternative spark sources and conditions were suggested to increase the sensitivity and decrease the analysis time.

A laser sampling device was described by Abercrombie et al.[217] in an application for air particulate analysis used in airborne geochemical exploration. A pulsed carbon dioxide laser was focused on single small spots of air particulate matter impact collected on sticky tape during aircraft flights. The laser pulse evaporated the material which was then carried into the ICP by the argon aerosol carrier flow. Because samples were collected on a continuous roll of tape, a fully automated instrument allowed the analysis of a new sample for 25 elements every 10 sec, and as many as 3400 samples have been analyzed in a single day.

Powder injection devices were described and applied by Greenfield et al.,[50,52,53] Hoare and Mostyn,[58] Dickinson,[218] Dagnall et al.,[171] Pforr and Aribot,[219] and Scott[220] for analysis using the ICP for vaporization and excitation. Furthermore, a variety of powder feeding devices for induction plasmas have been developed and used in engineering and spectroscopic studies.[37,42,43,183-185,221-229] The major problem with powder introduction into the ICP has been one of obtaining a representative cloud of particles — the segregation of particles according to size and density, the relatively large particle diameters available as powders compared to dried aerosols produced from solution nebulizers, and the dependence of the success of a particular sampling device on the unique properties of individual samples add to the complexity of powder analysis.[3,4]

In the powder feeding device recently described by Scott,[220] the action of a repetitive, energetic spark discharge (between two graphite electrodes located in a sample vial above the powder sample) removed fine particles from the sample which then were transported into the ICP discharge by a low-flow (0.2 l/min) argon stream after mixing with the aerosol carrier flow stream. Presumably, the acoustic energy of the spark sustained the process and may also have caused particle breakup, producing small particles or vapors of the material. Since the spark action was independent of the gas flow, a high ratio of particles-to-aerosol carrier gas volume was possible. Because of the initial decrease in intensity, common to powder feeders, signals were measured at a fixed time, and they varied by 15 to 30%. Successful and universal powder introduction to ICP discharges awaits a major technological development, although powder introduction may be accomplished today for tailored sample types.

d. Gases

The introduction of gases in mixture with argon presents minimal problems in ICP-AES, although there has been relatively little practical development of gas analysis using the ICP discharge. Mermet et al.,[126,130,131,135] Alder et al.,[136] and Truitt and Robinson[163] introduced various gases and vapors into the ICP mainly for spectroscopic studies. However, Alder et al.[110] recently generated nitrogen from ammonium ions, recorded the NH emission intensity in the ICP at 336.0 nm, and obtained a practical detection limit of 0.1 μg of nitrogen per ml for 5-ml aqueous solution samples of exchangeable ammonium in soil.

Dahlquist et al.[203] described the ICP-AES preliminary analysis of urine for Hg and As; it was based upon the generation of hydrides by reaction with sodium borohydride and the subsequent transport of the hydrides and hydrogen produced into the ICP with the aerosol carrier gas. Air must be scrupulously excluded, and even with an argon-5% hydrogen aerosol carrier gas mixture, Nixon[210] found the rapid evolution of hydrogen extinguished the discharge. With a faster aerosol gas flow, the hydrogen reduced analyte residence time to a degree that the hydride method was not pursued. Ward[230] discussed the need for instrumental background corrections in the analysis of free mercury and some metal hydrides (generated chemically and transported as vapors into the ICP discharge). None of these techniques was totally successful until recently when Kirkbright[305] and Kirkbright et al.[306] devised a simple arrangement for the determination of As, Sb, Bi, Se, and Te in geochemical materials using hydride generations with sodium borohydride.

Probably the most controllable and widely exercised gas analyzer — the gas-liquid chromatograph (GLC) — has been adapted to the ICP only once. Denton and Windsor[231] investigated the ICP discharge as a GLC detector for

carbon, hydrogen, sulfur, nitrogen, oxygen, phosphorus, chlorine, and bromine. This promising combination can be expected to find numerous applications, although less expensive devices such as microwave-induced plasmas operated at atmospheric pressure in He as described by Beenakker[307,308] might turn out to be more economical.

4. Spectroscopic Measurement Systems

a. Introduction

Conduction, dispersion, detection, and analysis of radiation from the ICP discharge represent a well-established technological field in emission spectroscopy, yet developments in each step unique to ICP-AES continue to be reported. At the Noordwijk ICP Conference, Bernhard[232] discussed optics and data handling, Kirkbright[233] considered information content, and Scott[234] outlined analytical performance.

b. Optics and Image Transfer

The definition of the spatial volume of radiation observed by the optical transfer system is important in plasma diagnostics and routine analysis[189] because of the unique spatial distribution of radiation found in the ICP (e.g., Figures 8 and 9) discharge with the sample introduced and transported along the central axis. Table 8 includes a listing of observation heights heights and windows used in a significant number of recent ICP studies. Simple lens systems with unity magnification focused on the vertical entrance slit of a monochromator or spectrometer are common.[33,86] The zone of observation is determined by the entrance slit height and the relative location of the discharge to the optical path. Boumans and de Boer[78,87,122] projected an image of the discharge with twofold magnification on a rectangular diaphragm, and the intermediate image was focused on the grating by crossed cylindrical lenses. A rotating beam splitter was used for a dual-beam, dual-channel system. According to Boumans[78] this arrangement was adopted because interferences exhibited dependence on the concentricity of the entire torch and because the slightest disturbance in the arrangement while the source image was projected on the entrance slit made the interference effect change significantly. The latest version of the optical arrangement of Boumans and de Boer[122] includes a spherical field lens in the vicinity of the intermediate image to prevent radiation losses due to vignetting. Franklin et al.[182] also used crossed cylindrical lenses with a monochromator and linear photodiode array.

The optical arrangement used by Kornblum and de Galan[82] provided for flexible and simple Abel transformations of lateral intensity distributions into true radial distributions. It permitted measurements in emission as well as in absorption, and the region of observation in the discharge did not depend on the slit width of the monochromator, so that the window could be varied for each spectral line. In emission, radiation was sampled over the entire depth of the discharge (with the cross section determined by threefold magnification on a limiting diaphragm), focused on the grating, and evenly distributed over the photocathode. Kalnicky et al.[235] discussed the criteria for the optical system used to obtain reliable Abel inversions. Montaser and Fassel[176] designed an optical arrangement for atomic emission and fluorescence with the ICP discharge.

Allemand and Benzie[236] described an ICP stand adapted to a standard 3.4-m Ebert spectrograph optical bar. Imaging optics relayed the emission from the ICP to a regular arc stand and reproduced an image on the entrance slit of the spectrograph. Cassegrain-like arrangements were designed as collecting and reimaging lenses.

c. Spectroscopic Instruments

A variety of monochromators, spectrometers, and spectrographs have sorted emission radiation from the ICP discharge, and many are described in Section II.A.1 as components of the overall ICP-AES instrument. A number of fundamentally different approaches have been taken or suggested for ICP-AES, especially in attempting to meet the flexibility that the ICP provides for multielement analysis. Commercial systems almost exclusively adapt fixed-array multichannel spectrometers (with their particular requirements for unwanted radiation, background correction, and line selection) to the ICP discharge. The stable output of the ICP with unlimited sample volume encouraged development of alternative sequential approaches.

i. Multichannel Spectrometers

The performance characteristics of the multichannel spectrometers used with the ICP dis-

iarge were reported by Larson et al.,[165] Davi-
ın et al.,[74] Winge et al.,[93,97] Dalager et al.,[99,243]
id Allemand.[240] The problem creating the
ost concern during the past few years was the
scovery of substantial unwanted radiation re-
ilting from the concentration of certain sam-
e components.[92,119] Background and matrix
)rrections as well as line selection represent
·eas of immediate concern in utilization of
ultichannel spectrometers.[243]

Larson et al.[165] observed and investigated
ibtle changes in background that occurred
ıring ICP analysis of samples with composi-
ons that varied as a result of spectral interfer-
ıces, indirect changes of spectral background,
id stray light. Since the bias resulting from
ray light could be mistaken for an interelee-
ent matrix effect instead of a limitation or de-
ct in the spectrometer, Larson et al.[165] consid-
ed the extent that stray light arises from
·ating imperfections — the primary source of
ray light — and from spectrometer design de-
cts. They proposed and tested diverse tech-
ques for reducing, eliminating, or correcting
nwanted radiation, which have been adopted
ı part by commercial instrument manufactur-
·s.[74,99,240] Spectrometer-scattered light, con-
sting of light leaks, reflection from spectrom-
:er hardware, fixtures, and other internal
arts, can be reduced by masks, baffles, black-
ıing of nonoptical surfaces, traps, light tun-
-els, and appropriate entrance optics. Grating-
:attered light (comprising ghosts, far scatter,
nd near scatter) was reduced by substitution
f holographically prepared gratings for ruled
ratings and the use of solar blind photomulti-
lier tubes and optical filters, especially narrow
andpass UV-interference filters[136,241] located
nmediately in front of the detectors.

A two-step approach was taken toward the
olution of matrix-related background
hifts.[93,97,243,245] The first step was to minimize
he sources of stray light; the second was to de-
elop techniques for correcting the remaining
tray light. Calcium and magnesium in the sam-
les were identified as major sources of stray
ght, because of the very intense ion lines emit-
ed in the discharge. Once the sources were
lentified, specific correction techniques were
pplied. In addition to those general techniques
ıentioned previously, selective pre- and post-
ilters were employed to keep the radiation
rom reaching the spectrometer.[97,232]

Empirical corrections for matrix-related background shifts and spectral line interferences were made by relating the intensity of another spectral line of the interferent, using standard computer programs supplied with commercial ICP-AES instruments.[97,139,243,244] However, this method failed when applied by Winge et al.[97] to the ICP background shifts resulting from calcium and magnesium, because mimic lines did not satisfactorily match the combinations of stray light and other sources of background shift associated with these elements. Calcium ion lines (Figure 5) at 393 and 397 nm almost completely accounted for the stray light from calcium, but these lines exhibited different degrees of self-absorption. Neither line could be employed to correct stray light produced by the combination of the two, and monitoring the linear response of the Ca II, 315.89-nm line also failed. Winge et al.[97] recommended using the total integrated peak area rather than peak intensity for correction.

Background corrections with multichannel spectrometers present a classical problem which has been dealt with for ICP-AES instruments through the use of spectral scanning devices.[93,97,139,143,144,242,245] Winge et al.[97] affixed a stepping motor to reposition the entrance slit of a concave grating spectrometer, and Allemand[143,144,245] used a digital scanning device. Both approaches are now used commercially. In Allemand's device, the computer-controlled deflection of entering radiation was produced by moving a calcium fluoride or quartz plate in steps. This provided wavelength profiles or multiple offset readings at each exit slit with sufficient wavelength coverage to make background and interference corrections. These background correction techniques do not account for background shifts arising in the secondary optics of the spectrometer. Winge et al.[97] also emphasized that empirical corrections introduce additional uncertainties into the analytical results. Abercrombie and Silvester[139] found that the narrow bandpass interference filter gave the best overall spectral interference correction when compared with both computed and spectral scan techniques.

Line selection for a multichannel spectrometer with an ICP discharge source poses problems not normally encountered with DC arc or spark sources for which the line selection has been well established through experience.[243] For

the excitation temperature assumed in the ICP discharge, the relative spectral intensities do not correspond to those expected for a discharge in LTE. For many elements, the most intense spectral emission arises from ions rather than from atoms.[77,104,114,118,122] This unexpected result has become more understandable in light of recent hypotheses concerning the excitation processes in the discharge that are discussed in Section III.B.5. Boumans[239] indicated six factors useful in determining the minimum number of spectral windows (lines) needed for a universal analysis:

1. Number of analysis elements of interest
2. Concentration ranges covered
3. Types of matrices to be studied
4. Useful dynamic range of detector
5. Dynamic range of source emission
6. Spectral resolution of spectrometer

Boumans[238,239] cited spectral interferences as the most severe problem associated with analysis of multiple matrices and pronounced that a compromise must be reached between spectral resolution and the number of spectral windows adopted. These compromises strike a balance between flexibility to cover many matrices and the total number of exit slits possible. A roving slit-detector assembly such as that incorporated in the M.B.L.E.-Philips ICP-spectrometer[123] (Table 9) or monochromator added as a separate channel to a spectrometer, as is found in the Jarrell-Ash ICP-spectrometer[294] (Table 9), substantially enhances the flexibility of fixed-slit spectrometers, as discussed by Ward.[294]

ii. Spectrographs and Multichannel Echelle Spectrometers

Considering universal analysis in the sense of survey analysis covering a large variety of both analytes and matrices, Boumans et al.[237-239,279] mentioned as possible alternative spectroscopic instruments: (1) classical spectrographs with photographic detection combined with an automatic computerized plate reader, (2) computerized multichannel spectrometers using electronic imaging devices (TV-type spectrometers), and (3) computerized multichannel spectrometers using image dissectors. All of these instruments offer flexible and universal approaches to spectrochemical data taking and handling. However, both hardware and software development are expensive, and, according to Boumans,[279] an investment in equipment and software for universal analysis can be justified only to the extent that a universal analysis is an economic possibility in the appropriate laboratory.

Boumans et al.[293] are developing systems for quantitative survey analysis using an ICP, a 3.4-m Ebert spectrograph, and a computerized microphotometer.[310] They are first developing a system (ICP K-system) for major and minor constituents that will have to supplement and replace the DC carbon arc K-system method of Addink,[311] achieving better precision and accuracy. To reduce photographic measuring errors, they limit the transmittance measurements of lines and background to the range of 0.05 to 0.80 T. To extend the dynamic range of the detector, they employ a step filter at the entrance slit (1:1/3:1/10), take stepped exposure times (t and t/10), and use stepped dilution (1:1 and 1:10) of the samples. In this approach, they exploit the unique features of the ICP discharge: steady-state sample introduction and high temporal stability (permitting stepped exposures) and high detection power, large linear range, and low matrix effects (allowing stepped dilution). The disadvantage of needing to take 6 samples and having to measure from 8 to 12 spectra of each sample does not weigh heavily, because spectra taking and sample changing can be easily automated with an ICP source, while the measurements are committed to an automatic controller that measures and processes rapidly (1 cm/sec of a photographically recorded spectrum) with reliability that has been tested during many years of experience with the DC arc method. Boumans et al.[293] are compiling a library of spectral interferences based upon actual measurements in the spectral windows of the analysis lines using aqueous solutions of possible interferents. In selecting analysis lines, they apply their previous experience with an ICP-monochromator system, general data on ICP spectra available in the literature, and the NBS Tables of Spectral-Line Intensities derived from the NBS copper arc.[312] Their experience with their argon ICP reveals that the intensities tabulated in the Tables are (as to their order of magnitude) representative for computing relative detection limits in the ICP within either the ionic or the atomic spec-

tra. However, the ionic lines yield detection limits one to two orders of magnitude better (compared to the atomic lines) than would follow from the NBS tables. They are evaluating to what extent these findings can be generalized and quantified.[293,303,316]

In an alternative approach, Danielsson et al.[138,141] reported the combined application of an ICP with an echelle spectrometer equipped with an image dissector system. This arrangement is currently being evaluated by Applied Research Laboratories as a commercial system.

Betty and Horlick[105] developed a cross-correlator as a readout system for a photodiode array spectrometer with ICP source. With this system, a reference spectrum is stored in a transient recorder and used as an electronic correlation mask for the detection and measurement of the same spectral signal. This procedure represents a unique approach for the measurement of atomic emission signals, since the only spectral information that can contribute to the correlator output is that which is identical to the stored reference spectrum.

iii. Programmable Monochromators

Boumans et al.[237-239] argued that high flexibility in choice of analysis lines, the ability to check for spectral interferences and correct for background, and the capability to cover the concentration ranges required for ICP-AES could be met by a computerized programmable monochromator.[237,313-315] In the computerized version,[237,316] the computer is used to control the program during an analysis and, more essentially, to check and control the wavelength positioning. This approach would not only permit a simpler and cheaper mechanical design, but would also provide for automation of the programming for new analytes and/or matrices. The sequential mode of measurement limits the applications to analyses in which a fairly small number of analytes are to be determined and for which enough sample is available. Boumans et al.[278] considered flexible single-element analysis of nonroutine samples as an important area of application of computerized programmable monochromators. They demonstrated that rather simple "cookbook" rules could be followed in ICP-AES single-element analysis of nonroutine samples, of which some essential information is already available. They envisaged that 90% of the operator's task might be committed to a programmable monochromator coupled to a mini- or microcomputer. A crucial point was that, according to their experience, the compromise conditions for simultaneous multielement ICP analysis were entirely satisfactory for single-element analysis; thus, the operator need not be concerned with irksome source optimizations.

Winefordner et al.[91] also felt that a programmable monochromator represented a viable alternative to fixed multichannel spectrometers. As studies progress with the ICP and computerized monochromators or spectrometers, the dominant position of the multichannel spectrometer in commercial ICP-AES instruments may be challenged in nonroutine applications where a limited number of element determinations are to be made.[91] One instrument manufacturer, Instruments SA, Inc. (Metuchen, N.J.), recently introduced a sequential spectroanalyzer consisting of a 1-m Czerny-Turner monochromator with holographic grating, stepping motor wavelength scanning controls, and a minicomputer.[317]

d. Detectors and Readout Systems

The ICP source challenges the optical dynamic range of emission spectrometers.[243] The discharge's high signal-to-background intensity ratios, low detection limit, and long linear analytical range[96] demand detection capabilities that only photomultiplier tubes can provide. For example, solar blind photomultiplier tubes furnish both dynamic range and rejection of stray light when used in multichannel spectrometers.[245] However, these characteristics generate substantial demands on the readout system, especially in a multichannel spectrometer. Winefordner et al.[91] evaluated multielement detection systems for AES.

Boumans[239] suggested that, as photodiode systems with improved electronics approach the signal-to-noise ratio of photomultiplier tubes,[309] multiple photodiodes could be arranged in lieu of exit slits for simultaneous analyte and background readings. Franklin et al.,[182] Betty and Horlick,[105] and Edmonds and Horlick[113] have applied self-scanning linear silicon photodiode arrays as spatial and wavelength spectral detectors to ICP-AES, and Gold[166] utilized 16- and 32-element photodiode

arrays to measure velocities in the ICP discharge. Franklin et al.[182] aligned a 512-element array parallel to the exit slit of a stigmatic monochromator to obtain a spatial profile of emission from the axis of an ICP discharge. Operating under computer control, the photodiode array recorded vertical profiles from Ca emission which were automatically corrected for background over a range of 10 to 35 mm above the induction coil. The profiles indicated major changes in intensity distribution due to aerosol carrier flow rate and additions of potassium. Horizontal profiles of Ca in the presence and absence of K were also recorded automatically at different axial locations in the discharge. With a 256-element linear photodiode array, Edmonds and Horlick[113] recorded profiles of analyte emission as functions of aerosol carrier and plasma (coolant) flow rates, input power, and the presence of concomitant. A typical set of results for Ca I is given in Figure 8. The spatial position of peak neutral atom line emission depended upon the analyte excitation and/or ionization charcteristics; however, the spatial peak position of ion line emission appeared to be independent of the species for the elements (Ca, Ba, Sr, Ti, Co, and Ag) studied. In Figure 8, for example, as the power was increased, the intensity of the Ca I emission increased and the peak in the emission spatial profile shifted to a lower position in the discharge. The application of photodidode arrays to obtain spatial information from the ICP provides a convenient, rapid, and completely automated means to record analyte emission and background to correct emission for background. Betty and Horlick[105] applied a 1024-element array with cross-correlation readout system for ICP-AES.

Danielsson et al.[138,141] combined the ICP discharge with an image dissector-echelle spectrometer system,[246] which provided the dynamic range capabilities of the electron multiplier with the flexibility in choice of an unlimited number of spectral positions. The system also provided single-photon counting and dynamic background measurement capability. Engineering developments are currently underway on this type of system which should lead to a marketable product.

Myers and Huchital[247] applied a copper-selective pulsed modulator to detect resonance emission at 324.7 nm excited in an ICP discharge. A fivefold improvement in the detection limit appeared to be unaffected when the bandpass of the monochromator following the modulator was increased by ten.

Studies of noise characteristics of the ICP and detector system are rare, although the relative standard deviation of background signal was found to be approximately constant for diverse operating conditions.[87,100,122,150] Metcalf et al.[248] reported recently that the signal-to-noise ratio was directly proportional to the emission signal or analyte concentration at and near the detection limit, and the limiting noise was background emission noise and not amplifier or quantization noise. The background emission noise was primarily nonfundamental flicker noise rather than fundamental shot noise. At higher analyte concentrations or emission signals, the signal-to-noise ratio leveled off at 30 to 40 with 1-sec integration time and at about 80 to 120 with 13-sec integration time for all elements studied. Measurements were analyte emission flicker noise limited. The noise was proportional to the signal and might have resulted from fluctuations in the atomic population of the analyte in the observed volume element of the discharge. Fundamental shot noise was negligible. Boumans[238] derived a formula for the relative SD in the net line signal for such a system, which was denoted as a system limited by signal-carried and background-carried fluctuation noise, corresponding to the classification made by Wineforder et al.[91] The type of limiting noise will probably depend on the radiation flux conducted to the detector and therefore on the spectral radiance of the ICP zone selected for observation, the efficiency of the entrance optics between the ICP source and spectrometer, and the slit widths of the spectroscopic instrument.

Data acquisition systems differ for each experimental arrangement, and commercial ICP-AES systems include dedicated computers and computer programs for routine analysis. Winge et al.[97,249] described a data acquisition system in which signals from a multichannel spectrometer were processed by a digital time-sliced averaging technique in which the signal was digitized 60 to 600 times per second depending upon the number of detectors monitored for the preset measurement period. An autorange mode provided computer adjustment of the amplifier

gain for each channel prior to measurement period. Automatic background correction procedures have been developed and integrated into commercial instruments.[144,230,245]

III. DISCHARGE CHARACTERISTICS

A. Plasma Diagnostics

1. Introduction

The measurement of physical properties of the ICP (pressure, spectral line and continuum emission, scattering, and magnetic and electrical fields) by spectroscopic and physical means provides the basis for the computation of electron number densities, plasma and analyte velocities, temperatures, and number densities and for their correlation with experimental parameters. In turn, the experimental facts establish the foundation for descriptions of the fundamental processes occurring in the discharge and interaction of plasma with analyte. Only preliminary measurements of these parameters with ICP discharges designed for spectroanalysis have been reported so far, although this activity will intensify considerably. Paralleling experimental plasma diagnostics investigations, theoretical models of the same plasma processes are in embryonic stages. However, those models which have been applied are providing useful working hypotheses upon which further experimental activities can be based.

Plasma measurement results fall into two distinct time periods divided by the acceptance of the ICP in spectrochemical analysis. Until very recently, flow, temperature, and density analyses were made on a variety of induction discharges operating under dissimilar conditions. In contrast, detailed and complete measurements are now being reported on a relatively few, but compatible, configurations of ICP discharges with the common objective of defining processes related to spectrochemical analysis.

Comprehensive reviews of these early measurements were made by Eckert,[35] Dresvin,[36] Raizer,[13] Czernichowski and Jurewicz,[37] Greenfield et al.,[3] Barnett et al.,[71] and Mermet.[250] Current papers by Kalnicky et al.,[114,235] Kornblum and de Galan, and[82,83,189] Mermet[132] update these surveys with emphasis on recent ICP measurements. Few laboratories have made spectroscopic diagnostic measurements on spectrochemical ICP discharges. Foremost among these efforts are the reports by Mermet et al.,[126-128,130-132,134,250] Kalnicky et al.,[114,235] and Kornblum and de Galan.[82,83,189] Major spectroscopic investigations of interferences were performed by Fassel et al.,[115,151,235] Kornblum and de Galan,[189] Mermet et al.,[127,128] and Boumans and de Boer.[87,104,122,150]

The importance of spatial distributions in these spectroscopic measurements is paramount, and the methods for Abel inversion transformations were described by Kornblum and de Galan,[82,83,189] Kalnicky et al.,[114,235] and Mermet and Robin.[252] Recently, Jarosz et al.[318] reported results of a new study of smoothing experimental curves for Abel transformation. These along with other basic investigations have led to an appraisal of the existence of LTE in the ICP operated in argon[83,114,126,127,134,160,235] and the postulation of excitation mechanisms.[122,126,128,135] Barnes et al.[173,181,190,191,336] measured pressure and compositional distributions in the ICP, and Human and Scott[85] determined line widths.

2. Discharge Properties

a. Temperature and Electron Number Density

The excitation parameters (temperature and electron number density) in an ICP argon discharge at atmospheric pressure depend upon the plasma geometry and the measuring procedure.[83] Representative examples of excitation temperature and electron number density as functions of aerosol carrier flow and location of observation zone are illustrated in Figures 9 and 10.

After surveying the literature on ICP temperature measurements and reviewing techniques for determining excitation, electron, and kinetic temperatures, Kornblum and de Galan[83] concluded that the largest uncertainty in finding excitation temperatures arises from the inaccuracy of oscillator strengths, a contention well demonstrated by Kalnicky et al.,[235] Jarosz et al.,[318] and Alder and Mermet.[131] They devised a dual emission and absorption procedure to determine excitation temperatures in an argon ICP without using the transition probabilities; the results were more reliable than with previous methods. They also emphasized that although temperatures may differ in an ICP discharge one electron density exists (i.e., on

the order of 10^{16} cm^{-3}) in the argon ICP and that significantly deviating values were found in the literature only when the electron number density was derived from the Saha-Eggert equation.

Kornblum and de Galan[83] reported radial distribution values for excitation temperatures derived from Ar I, Ca I and II, Mg I and II, and Fe I lines, gas kinetic temperatures for OH, electron number density from Ar continuum intensities, and atom number densities for Ar, Fe I, and Ca I at four or five axial locations for a 0.53-W discharge with a 16-l/min plasma (coolant) flow and two (1.36 and 4.5 l/min) aerosol carrier flow rates. They argued that the various temperatures measured provided ample evidence that the ICP was not in LTE for either flow condition. Unfortunately, these excellent measurements were made at impracticably high aerosol central flow rates (e.g., compared to Figure 8), so that the two conditions investigated represent the upper limit of spectroanalytical applications. Furthermore, in future measurements, greater axial resolution in discharges at power levels between 0.8 and 2.0 kW would be valuable.

Kalnicky et al.[114] enumerated the inconsistencies among values for excitation temperature and electron number density leading up to their work, including the preliminary results published by Kornblum and de Galan.[82] They reported refined spatially resolved radial excitation temperatures experienced by a typical analyte, Fe I, and the support gas, Ar I, in the presence and absence of an easily ionizable element (Figures 9 and 10). Comparisons were made between electron number density distributions calculated from ionization equilibrium considerations and Stark broadening. When the temperatures in Figure 9 at 1.3 l/min are compared to those given by Kornblum and de Galan[83] for Fe I (Figure 8 in Reference 83) the major discrepancies cited for preliminary data[235] were substantially reduced. Although the excitation temperatures from Kalnicky et al.[114] who operated the discharge at 1 kW with 12 l/min plasma (coolant) flow appear slightly higher than the data obtained by Kornblum and de Galan at 0.5 kW and 50 MHz, the radial and axial trends are comparable. Results comparable to the electron number density distributions calculated from the Saha equilibrium equation in Figure 10 were not published by Kornblum and de Galan. However, the effective electron densities derived from Stark broadening by Kalnicky et al. at the same location above their induction coil appear to be rather close to the axial values derived from absolute continuum measurements by Kornblum and de Galan. The inequality between Saha- and Stark-calculated electron number densities led Kalnicky et al. to support the hypothesis that LTE did not exist for the discharge operating condition they employed. Finally, the presence of easily ionized sodium appeared to change the excitation temperature and electron density by negligible amounts compared to what would be expected in an equilibrium discharge.

Using a 1 kW, 27 MHz ICP discharge, Human and Scott[85] measured the profiles of spectral lines of calcium, strontium, and argon by means of a Fabry-Perot interferometer at 10, 15, 20, and 25 mm above the induction coil. Gas kinetic temperatures derived from the Doppler-line broadening were considerably lower than those in Figure 9 for Ca I and Sr I and II but similar or higher for Ar I. The shapes of these lines conform to a model of the discharge at observation heights of 20 and 25 mm above the coil, consisting of an emitting core surrounded by an absorbing layer. In contrast, at 10 and 15 mm above the induction coil, the model corresponds to a core containing only absorbing atoms surrounded by a region of emitting atoms. These models rationalize the absence of self-reversal occurring at these locations even though considerable broadening due to self-absorption was indicated.

Mermet, Robin and co-workers completed a number of diagnostic measurements in two ICP discharges. Alder and Mermet[131] found similar temperature values from molecular rotational line intensities and multiple Ar line intensities in an argon-methane (10%) ICP discharge. Jarosz et al.[130] measured the electron number density distribution in an argon hydrogen-doped ICP discharge from Stark broadening of Ar and H lines. They derived a generalized form of the Saha-Eggert equation which was used to calculate ionization temperatures. Subsequently, Jarosz and Mermet[126] determined electron densities and excitation temperature distributions in argon hydrogen-sulfide-doped ICP discharges, and they found a similar incongruity between excitation and ionization temperatures.

Mermet[132] also measured excitation temperature distributions with Ar, Fe I, and Ti II lines at heights of 0, 5, and 10 mm above the induction coil and flow rates from 0 to 2 l/min in a 5-MHz argon discharge. Electron density values derived from Ar I Stark broadening showed the greatest change along the central axis at flow rates of 1.5 l/min or less. Based on these results, calculated ionization temperatures were more than 2000 K higher than the measured values, which suggested that LTE did not prevail in the discharge. Extending these measurements with a new 40-MHz generator operating at substantially lower power (1.8 kW) in the discharge,[72] Robin and Trassy[129] observed negative absorption in an AAS measurement of Al I and Ti II lines. Furthermore, in studies of the influence of sodium on the enhancement of P I emission, Mermet and Robin[127] could not rationalize the enhancement on the basis of Saha equilibrium calculations or the absence of a change in the radial intensity of Ar I in the presence of sodium. Abdallah et al.[128] later found this enhancement to be related to the desolvation temperature and considered it an atomization interference. Mermet and Trassy[133] again found inequalities in ionization and excitation temperatures in the 40-MHz argon discharge; however, Abdallah and Mermet[134] obtained good agreement between the gas kinetic temperatue derived from the rotational spectrum of nitrogen molecular ion and the excitation temperatures from elements injected into a nitrogen-doped argon discharge.

Based on the accumulated evidence from these experiments, Mermet et al.[126,132,135] postulated specific excitation reactions with metastable levels of the argon atom and ion by Penning ionization to account for the high intensities of Ca II, Nb II, Mn II, Ti III, S II, Br II, and Cl II lines compared to atom lines. Accordingly, Mermet and Trassy[133] measured the metastable concentration of argon atoms using AAS. Values of 6×10^{11} to 3×10^{12} cm^{-3} in the center of the 2.1-kW discharge fall to below 10^{11} cm^{-3} at 15 mm above the induction coil. Under equilibrium conditions, the density would have been 6×10^{6} cm^{-3}.

Apparently, other diagnostic techniques dependent upon light scattering[253,254] have not yet been applied to the ICP discharge as they have in arc discharges[255] to help establish electron temperature and number densities independently.

b. Pressure and Flow

In addition to the spectroscopic investigations discussed above, pressure and flow studies are among a few other areas in which physical diagnostic techniques have been applied to the ICP discharge. The importance of flow analysis in the ICP is seen when attempting to interpret the interference effects resulting from transport and vaporization phenomena and from the spatial emission distributions (Figure 8), temperature (Figure 9), electron number density (Figure 10), and analyte or argon distributions[189] as functions of gas flow conditions.

Barnes et al.[173,181,190,191] determined spatial pressure and concentration distributions by means of direct Pitot tube measurements and particle velocities using photographic techniques. An example of the spatial pressure distribution at two aerosol carrier flow rates is given in Figure 11. Gas velocities at the top of the induction coil increase from about 18 m/sec with little or no aerosol carrier gas flow (i.e., insufficient to puncture the base of the discharge) to about 30 m/sec with 0.9 l/min and 90 m/sec with 1.35 l/min aerosol flow [10 l/min plasma (coolant) flow at 0.75 kW]. The introduction of auxiliary flow decreased pressures and velocities as the discharge was displaced downstream from the induction coil, whereas increased plasma (coolant) flow decreased back pressures in the discharge. Comparing experimental with computer predicted velocities and temperature distributions resulted in refined models of the discharge, which were subsequently applied in the development of new ICP torches.[145,173] An effort is underway to improve spatial resolution of these measurements, especially close to the outer confinement tube, measure three-dimensional flow velocities, and develop two-dimensional computer models of the discharge.

Gold[166] measured particle velocities in an ICP using photodiode arrays by determining the emission from NaCl introduced axially into the induction discharge. He found values between 5 and 30 m/sec as well as velocity modulation caused by generator power supply ripple. Peterson[277] used a high-framing-speed camera, similar to the one applied previously by Barnes

and Schliecher to measure particle velocities and total light modulations in a number of ICP systems. Velocities obtained with three aerosol flow rate injector tubes and flow rates did not correspond to the calculated cold velocity at the nozzle tip.

Earlier, Chase[184,185] and Klubnikin et al.[187,188] obtained velocity values and flow distributions for discharges, and recently, Gouesbet[251] found the velocity of injected particles to be about half the velocity of argon in the central zone of a nominally 5-kW, 5-MHz induction discharge using laser Doppler anemometry. The applications of laser Doppler anemometry to ICP discharges under spectrochemical operating conditions have demonstrated feasibility only for measuring velocity and particle density within the ICP discharge.

3. Sample Processes — Interelement Interferences

a. Introduction

Each step in the total sample process — nebulization, desolvation, transport, vaporization, atomization, excitation, emission, and recording — is subjected to close scrutiny in the ICP discharge to establish the competitive position of the ICP relative to other excitation sources and to explain and understand interference effects which may be associated with each of these steps. Greenfield et al.,[170] Boumans,[256] and Boumans and de Boer[104] classified and categorized interference effects found in spectrochemical discharge sources. Kornblum and de Galan,[189] Larson et al.,[115,151] and Boumans and de Boer[87] surveyed the literature on interferences in ICP discharges. In particular, the review by Kornblum and de Galan[189] is complete and current.

Operating parameters can be selected so that interferences typically found in flames and electrical discharges can be reduced to triviality in ICP-AES or at least minimized in compromise with other analytical features. As Kornblum and de Galan[189] emphasized in their critical review, the observed interference effects vary with almost all known variables in the ICP. Despite this behavior, no studies to investigate the effect of the observation volume have been reported, leading Kornblum and de Galan to suspect that measurements with spatially integrated intensities could cloud the interpretation of the observations. Kornblum and de Galan collected and tabulated values of parameters employed during interference studies as well as values for known interelement combinations investigated for possible interference effects. These compilations are reproduced as Tables 8 and 10. Until recently, the influence of possible deviations from LTE had not been considered in interpreting these results.

b. Nebulization, Desolvation, and Transport

Interferences resulting from changes in the rate at which the sample is transported and delivered to the discharge include physical interferences related to liquid nebulization,[170] segregation and sizing in powder feeding,[3,4] and selective vaporization in sampling solid and molten metals[218] or dried residues on heated filaments,[147] as well as secondary interferences such as those found in the desolvation of solution aerosols.[87,128]

Greenfield et al.[170] considered in some detail the physical interferences in nebulizing viscous mineral acids, organic acids, and solvents into an ICP discharge. Although physical interferences related to liquid nebulization are presumably well characterized from study in flame spectrochemical analysis, the analytical dynamics and tolerances of ICP-AES challenge the analyst to present the discharge with samples in forms and concentrations beyond any experienced in flame spectrochemistry. Particular caution should be maintained to insure that a new sample will not encourage changes in the rate of sample delivery to the discharge.

Desolvation interferences[87,128] are substantially less well characterized, since desolvation is practiced almost exclusively with ultrasonic nebulization.[102] The effort of Boumans and de Boer[87] to localize and identify desolvation interferences stemmed from an experimental arrangement consisting of two identical ultrasonic nebulizers and desolvation assemblies and an experiment designed specifically to segregate interferences due to processes in the discharge and the nebulizer-desolvation apparatus. The desolvation effect, which varied in magnitude between ±10%, was related to the difference in volatility between the matrix KCl and analyte Zn.

The transport of aerosol or analyte into the

TABLE 10

Interelement Combinations Investigated in the ICP Discharge in Various References

Element	Wavelength (nm)	Concomitant														
		Ag	Al	Ba	Ca	Cd*	Co	Cr	Cu	Fe	Hf	Mg	NH_4	Ni	PO_4	Zn
Ag	328.1	—	—	—	61	—	—	—	61	—	—	—	—	—	—	—
Al I	396.2	—	—	—	—	87,150	—	—	—	87	—	87	87	—	150	—
B I	249.7	—	—	—	171	—	58	58	—	58	—	—	—	58	—	—
Ba I	553.6	—	—	87	—	87,150	—	—	—	87	—	87	87	—	127,150	—
Be I	234.9	—	—	—	171	—	—	—	—	—	—	—	—	—	—	—
Ca I	422.7	—	—	—	—	87	—	—	—	87	—	87	87	—	—	—
Cd I	228.8	—	87	—	—	—	—	—	—	87	—	87	87	—	87	—
Cu I	327.4	61	87,216	—	—	87	—	—	—	87	—	87	87	—	—	216
Fe I	372.0	—	87	—	—	87,150	—	—	—	—	—	87	87	—	150	—
Ga I	417.2	—	—	—	—	150	—	—	—	—	—	—	—	—	150	—
Li I	610.4	—	87	—	—	150	—	—	—	—	—	—	—	—	150	—
	670.7	—	87	—	—	87	—	—	—	87	—	87	87	—	—	—
Mg I	285.2	—	87	—	—	87	—	—	—	87	—	—	87	—	150	—
Mn II	257.6	—	87	—	—	87	—	—	—	87	—	87	—	—	—	—
Mo I	390.3	—	115,151	—	—	—	—	—	115,151	—	—	—	—	—	—	115,151
Mo II	281.6	—	115,151	—	—	—	—	—	115,151	—	—	—	—	—	—	115,151
Ni I	352.4	—	—	—	—	150	—	—	—	—	—	—	150	—	—	—
	362.4	—	—	—	—	150	—	—	—	—	—	—	150	—	—	—
P	213.62	—	—	—	—	—	—	109	—	109	—	109	—	109	—	109
S	182.04	—	109	—	—	—	—	—	109	—	—	109	—	—	—	109
Ti I	498.2	—	—	—	—	150	—	—	—	—	—	—	—	—	150	—
Ti II	334.9	—	—	—	—	150	—	—	—	—	—	—	—	—	150	—
U I	378.28	—	86	—	86	—	—	—	—	86	—	—	—	—	—	—
V I	437.9	—	—	—	—	150	—	—	—	—	—	—	—	—	150	—
V II	309.3	—	87	—	—	87	—	—	—	87	—	87	87	—	87	—
Zn I	213.8	—	87	—	—	87	—	—	—	87	—	87	87	—	87	—
Zr II	343.82	—	—	—	—	150	—	—	—	—	—	—	—	150	—	—
	349.64	—	—	—	—	—	58	58	—	58	58	—	—	—	—	—

* Reference 150 used $CdSO_4$; Reference 87 used $CdCl_2$.

From Kornblum, G. R. and de Galan, L., *Spectrochim. Acta*, B32, 455 (1977). With permission.

discharge depends on the configuration of the spray chamber and the injection orifice of the discharge tube assembly. Greenfield et al.[170] compared injection geometries for organic aerosols; Scott et al.[92] modified their injector geometry to reduce coalescence of aerosol droplets; and Peterson[277] measured particle velocities for a few injection geometries. Studies of the geometry of the spray chamber have concentrated on memory effects and cleanout time; volatilization phenomena within the spray chamber[108] have not been reported for ICP-AES.

Boumans and de Boer[104] compared the extent of interference effects obtained by pneumatic and ultrasonic nebulizers and found that the rate at which the aerosol was injected into the discharge was about ten times greater for the ultrasonic nebulizer than for the pneumatic nebulizer. Since the interference levels for the ultrasonic and the pneumatic nebulizer were about equal when the matrix concentration in the test solution with the ultrasonic nebulizer was about one tenth of that used with the pneumatic nebulizer, Boumans and de Boer concluded that the interference level depended primarily on the rate at which the matrix was injected into the discharge and not on the particle size and its distribution or the concentration ratio of matrix to analyte.

c. Vaporization

Vaporization effects, especially solute vaporization interferences, were recently investigated phenomenologically[113,115,127,128,151,182,189,257] generally either as a benchmark against which to judge the relative performance of the ICP and other spectroscopic sources or as a basis upon which to understand the phenomena. As an example, Figure 15B illustrates the emission intensity changes for Ca I as a function of addition of Al in both ICP and microwave discharges.

Kornblum and de Galan critically reviewed literature reports on the interaction of phosphate and aluminum with calcium, and they measured the influence of phosphate and cesium on calcium emission and absorption in an 0.53-kW ICP at two aerosol flow rates. Compound formation or reduced volatility was determined from ground state populations derived from absorption measurements. From radial distributions of particle density for Ca atoms and ions calculated from Abel-inverted absorbances at high (4.5 l/min) aerosol carrier flow rates, Kornblum and de Galan detected an apparent volatilization interference for both phosphate and cesium additions. In the low-flow (1.35 l/min) condition, the addition of 100 mg Cs per liter to Mg appeared to change Mg I intensities predominately as a volatilization effect. With an excess of matrix (Cs or phosphate) in the dry aerosol particles, Kornblum and de Galan concluded that the analyte atoms were released more slowly and were displaced toward the region of higher kinetic temperatures. Phosphate showed a stronger volatilization interference than cesium. At low aerosol carrier flow for the 0.5-kW discharge, the interferences were reduced significantly, but were not completely removed at any observation height.

In studies by Larson et al.[115,151] and Scott,[251] the interference effect on ion and atom intensities appeared to be 5 and 15% for molar ratios of phosphate-to-calcium up to 1000. Boumans and de Boer[87] found less than a 1% effect at a molar ratio of 2000. After observing an initial enhancement in signal, Mermet and Robin[127] observed no change in intensity for barium added to calcium up to a molar ratio of 1000. Larson et al.[115] found an observation height and the operating parameters for which the influence of Al on Ca was minor with Al-to-Ca ratios of 100 and negligible for additions of Na to Ca. The substantial differences in the magnitude of effects are illustrated in Figure 15 for the ICP and microwave discharge sources. These data led Larson et al.,[115] Abdallah et al.,[128] and Boumans and de Boer[87] to conclude that solute vaporization interferences can be eliminated or reduced to negligible proportions in the ICP discharge.

d. Atomization and Ionization

The influence of concomitant elements, especially those easily ionized, on the emission and absorption signals in the ICP has been investigated to establish the extent of various contributions to the observed interferences, particularly ionization interferences. The results from these efforts emphasize that the action of alkali elements is not explained simply as ionization suppression in an equilibrium condition.

Kornblum and de Galan[189] measured the changes in Ca and Mg atom and ion emission and absorption in the presence of Cs; Kalnicky et al.[114] determined excitation temperatures and electron number densities in the presence of Na (e.g., Figures 9 and 10); Larson et al.[115,151] recorded the effects of sodium on various atom and ion emission signals (e.g., Figure 14) ; and Mermet et al.[127,128] also determined the influence of sodium under various experimental conditions. Boumans and de Boer[87,104,122] made detailed studies with KCl and supplementary observations with other matrices in separating plasma from nebulizer-desolvation effects and establishing compromise operating conditions for simultaneous multielement analysis. Franklin et al.[182] reported exploratory results with K addition.

As illustrated by Figures 9 and 10, Kalnicky et al.[114] found, as Mermet and Robin[127] had previously found for Ar I radial intensities, that the addition of Na only slightly altered the electron number density and excitation temperatures at different heights and aerosol flow rates. These observations cannot be consistently explained by ionization suppression, which is often found in systems in LTE when alkali elements are added. For example, in a DC arc, ionization suppression upon alkali addition results because the temperature is decreased and, if much alkali is introduced, also because the electron number density is raised.[319] In flame, on the other hand, the temperature is unaffected, but the electron number is raised.[320] Although the reasons for ionization suppression in the LTE systems are different,[189] the extent of the effects in both systems sharply contrasts that which is observed in the ICP discharge under properly chosen conditions. Kalnicky et al. did observe some analyte ionization suppression, apparent in Figure 10 as lateral shifts and Fe I intensity changes. Larson et al.[151] found changes of relative intensities of Ca, Cr, and Cd in the presence of Na (for a fixed power and flow) at three locations in the discharge. These results could not be explained by ionization suppression either, and Larson et al. suggested that other factors should be considered. In an analogous experiment, Scott[257] measured Ba, Ca, Mg, and Zn in the presence of Li in different regions of a similar discharge without reaching a satisfactory conclusion about the role played by the lithium.

Mermet and Robin[127] found that the enhancement of P and Cr by additions of Na could not be explained by a change in particle equilibrium in the discharge, and Abdallah et al.[128] recorded the influence of sodium on Ca, Cd, P, and Cr at various heights and for various flow conditions in a second discharge. The Na interference on Ca intensities decreased with increased power (2 kW), and the P effect was traced to a desolvation interference in the desolvation apparatus.

Boumans and de Boer[104] measured the influence of KCl on the intensities of Li I, Mn I, and Ba II over a range of operating conditions and found changes in intensity to vary over a broad range (Figure 7). Under appropriate conditions for spectrochemical analysis, the intensity changes could be kept to within ±10%. In a subsequent detailed study,[87] they distinguished true plasma effects from nebulization-desolvation effects, and plasma interference effects were small.

The results obtained by Kornblum and de Galan[189] for the influence of cesium and phosphate on the ground state number densities of the calcium atom and ion indicated a clear departure from thermal equilibrium. The influence of Cs on the emission intensity of Ca I resulted from a reduction in the ground state population due to a combination of volatilization interference, a shift in the ionization equilibrium, and an increase in the excitation temperature of the first excited level of Ca. Similarly, reduced volatilization, suppressed ionization, and enhanced excitation processes were suggested for Mg I observations. The effect of Cs was much less pronounced at low aerosol carrier flow than at high flow. Under these conditions (which more closely resemble typical analytical operating values), interferences were greatly reduced; the volatilization effect was predominant with a small shift in ionization and enhancement of the excitation temperature. Hopefully, duplicate experiments of this type will be performed at power levels commonly encountered in spectrochemical analysis. With high aerosol carrier flow, the discharge was not in thermodynamic equilibrium. Reduction of the flow greatly enhanced ionization temperature and ion-line intensities; however, the excitation conditions in the discharge were no more thermal than in the high-flow discharge.

e. Excitation

The inability of Mermet[132] to correlate electron number densities with excitation temperatures required the proposal that nonthermal ionization processes were dominant in the ICP discharge under appropriate experimental conditions. Jarosz et al.[318] arrived at a consistent picture by substituting ionization temperatures of 6700 to 7300 K instead of the measured excitation temperature of 4800 K into the Saha equation. On the other hand, Mermet[135] proposed a Penning ionization reaction with metastable argon atoms as an ionization-excitation mechanism. He further suggested that the appearance of spectral emission from S II and other lines might result from a similar charge-transfer reaction with metastable states of the argon ion. After a complete study of the sulfur spectrum produced in an ICP discharge, Jarosz and Mermet[126] reemphasized this excitation pathway to rationalize the excitation of S lines up to 30 eV and the absence of Ar II lines from 35 eV. Mermet and Trassy[133,160] measured argon atom metastable level densities in the ICP and discovered the densities to be more than 10^5 times higher than would have been predicted for a discharge in LTE. The direct verification of argon ion metastable populations by absorption has not yet been possible.

Boumans and de Boer[122] established experimentally that ion-to-atom line intensity ratios exceeded calculated ratios based on LTE by 10- to 1000-fold for ICP operating conditions used for spectrochemical analysis. They also found overpopulations of high-energy levels of Mg II with respect to the resonance level of Mg II when an LTE temperature of 5850 K derived from Zn I line intensities was taken as a starting point. The overpopulations of the high-energy levels of Mg II corresponded to excitation temperatures in the range between 7600 and 9100 K with respect to the resonance level of Mg II.

f. Spectral Interferences

Spectral interferences must also be considered as interference effects for the ICP discharge,[3,165,211,238] because spectral interferences result in analytical errors unless an accurate correction is made for their contribution to the total line intensity or background. Three sources of spectral interferences are atomic spectral line emission and molecular vibrational-rotational emission produced by concomitants or decomposition products and stray light resulting from intense radiation from concomitants at wavelengths of the analyte.

Boumans[238] presented some possibilities and examples of correcting for spectral interferences. Generally, spectral interferences are avoided by selecting interference-free lines. However, Boumans argued that with modern instrumentation corrections for spectral interferences offer a realistic alternative approach to the laborious task of insuring that the analyte lines are interference-free. He developed a correction formula for which a catalog of appropriate factors could be compiled for routine operating conditions. He evaluated two examples, and after an analysis of errors, he determined that the limitation of the method was in the inability to make unambiguous background readings.

Nixon[211] found that for the practical analysis of biological fluids, such as urine and blood, the amount of organic and inorganic materials varied on a daily basis and gave rise to changes in the spectral background through stray light effects. Unless corrections were made, the stray light could be mistaken for other types of interelement interferences.[165]

Using a double monochromator to minimize instrumental stray light, Larson and Fassel[321] identified line broadening and radiative recombination background sources in the ICP discharge. Stark-broadened wings of very strong emission lines can produce significant continuum as far removed from the central wavelength as 10 nm or more. Several definitive examples of the interference caused by spectra continua arising from radiative recombination processes involving concomitants (e.g., Al, Ca, Mg) were also reported for the first time.

B. Models

1. Introduction

Quantitative descriptions of phenomena related to the generation, sample processes, and excitation in any discharge necessitate the development and application of mathematical relationships based upon either fundamental principles or models. The ICP has been subject to modeling since the publications of Thomson[11,12] and Babat,[25,26] and today, this source holds the potential for becoming one of the best

experimentally and theoretically characterized discharges in spectrochemical analysis.

Presently, models are being developed for coupling of the RF generator to the induction plasma and for describing two-dimensional temperature and velocity fields in the discharge, the pathways travelled by particles introduced into the discharge, the transport of heat and mass between the particles and plasma, and the excitation of analyte emission in the discharge. Some of these models naturally depend upon semiempirical relationships or simplifying assumptions for practical reasons; however, in test situations, experimental and theoretical values correspond to within 5 to 10%. The efforts are not restricted to applied spectroscopy, but are also underway in plasma engineering as well.

In their review on temperature and other physical properties in the ICP source, Greenfield et al.[3] surveyed much of the early, fundamental work on modeling induction plasmas, measured and calculated plasma temperatures, and other numerical treatments. Czernichowski and Jurewicz[37] also included most of the early publications giving experimental and theoretical treatment of the induction coil, ignition of the discharge, pressure, frequency, power, heating efficiency, plasma diameter, and temperature. Raizer's review[13] detailed a number of models and calculations describing discharge generation. Dresvin[36] described the temperature determinations, gas dynamics, deviations from thermal equilibrium, electrical parameters, energy consumption, and calculation of particle motion in induction discharges. Eckert,[35] who has made a number of substantial experimental and fundamental contributions in the field of induction plasmas, also reported the status of both experimental and theoretical descriptions of the induction plasma. His detailed section on theoretical analysis includes discussion of heat balance, comparison with experiments and nonequilibrium effects, two-dimensional convection effects, and magnetic pumping.

2. Discharge Ignition and Coupling

Allemand[143,146] has developed an exact model of the matching network between the RF generator and the ICP discharge. The model is based upon a determination of the impedance changes during the ignition process, and after full ignition when samples are introduced into the discharge, and of the electrical equivalent circuit incorporating these impedance changes. A precise computer model simulates a particular matching network, both unloaded and loaded, with an argon ICP discharge, with an aqueous sample injected. The plasma resistance was measured experimentally by inserting various dummy loads in the induction coil until matching conditions for the dummy load were identical to that for the plasma. Schleicher and Barnes[117] used a less well-developed model to determine the parameters needed in the design of a conjugate network tuning circuit.

3. Fluid Dynamics and Energy Distributions

The first significant attempt to analyze the energy distribution in an induction plasma was made by Miller and Ayen,[258] who obtained the two-dimensional temperature field in an induction plasma with flowing argon by solving a two-dimensional energy equation together with one-dimensional electrical and magnetic field equations. However, they made no attempt to calculate flow field in the discharge; actually, they assumed a two-step flat flow with the velocity in the central region being much lower than along the periphery of the tube. A number of one-dimensional temperature field calculations that provided information on the energy input and one-dimensional temperature, magnetic field, and electric field distributions were performed prior to the work of Miller and Ayen.[35]

Barnes et al.[161,180,181] modified Miller's program to accommodate the geometry of popular spectrochemical ICP discharges by introducing three concentric flows and assigning a velocity field distribution to the aerosol carrier flow. Using a number of assumed velocity distributions, they calculated the two-dimensional temperature distributions, velocity profiles, energy loss balances, and power, electrical, and magnetic field distributions in argon and nitrogen discharges for a variety of conditions of interest in spectrochemical analysis. Figures 17 and 21 illustrate the relationships obtained between the power input to the ICP as a function of magnetic flux density for various frequencies and discharge diameters. Experimental determination of velocity profiles[190,191] permitted refinements of the flow profiles employed with the

model for torch design.[145,173] Delettrez[259] extended Miller's model and was able to calculate two-dimensional flow as well as temperature fields. Delettrez clearly showed recirculatory flow patterns for the simple geometry used by Miller and Ayen.

Recently, Boulos[260] developed a two-dimensional model of the induction discharge in which the solution of the corresponding momentum, energy, and continuity equations, expressed in a vorticity-stream function form, was obtained numerically and simultaneously with the one-dimensional magnetic and electric field equations. The existence of a magnetic pumping effect produced two recirculatory eddies in a geometry with plasma (coolant) flow similar to that used by Miller. As the plasma (coolant) flow rate was increased, the downstream eddy was swept away, leaving only one recirculatory eddy on the upstream side of the discharge, which produced a backflow of about 20 m/sec. Barnes and Chandra[261] added a swirl component to Boulos' treatment and demonstrated that the swirl velocity of the plasma gas was damped out by the discharge. Boulos[262] recently introduced carrier flow into the model for aerosol flows of 0 to 0.6 l/min with 0.2 l/min auxiliary and 16 l/min plasma flows. Figure 23A shows the streamlines and velocities calculated for a central flow of 0.4 l/min, and Figure 23B shows the corresponding temperature distribution. Higher central flow rates have not yet been computed.

Numerical techniques have been developed which have the capability of providing three-dimensional models of the induction plasma discharge; however, considerably more development and experimental verification of the two-dimensional models need to be done. Nonetheless, the results obtained to date have been enlightening and a useful step in understanding the flow and energy in the ICP discharge. Eckert[263] recently investigated the feasibility of detecting trace metals in induction-heated discharges sealed in cylindrical or spherical quartz bulbs, and he developed a two-dimensional analysis of the temperature field of a static thermal induction discharge enclosed in a cylindrical container containing Ar at atmospheric pressure.[264]

4. Particle Trajectory, Heating, and Emission

Prerequisite to a theoretical description of emission of analyte in an ICP discharge is a description of the trajectory and heating that wet or dried analyte aerosol experiences from the time it leaves the injection nozzle and flows to the discharge region until it is totally vaporized and the atoms are distributed spatially and energetically throughout the discharge. Limited theoretical developments combined with experimental measurements have already provided a revealing picture of particle interaction in spectroanalytical ICP discharges.

Dresvin[36] reviewed the dynamics and heating of high-temperature melting particles in plasma jets, and experimental studies of particle transport and reactions in induction discharge were performed and reviewed.[174,184,185,223-229,267] Chase[184,185] made experimental and theoretical investigations of gas flows and magnetic forces in an induction plasma and demonstrated the rejection of particles introduced upstream to the discharge. His work served as the basis for a number of subsequent investigations.

Borgianni et al.,[221] Capitelli et al.,[222] and Johnston,[266] through experimental and theoretical considerations, investigated the behavior of metal oxide particles injected into an argon induction plasma, and Boulos and Gauvin[268] modeled the behavior of single particles injected into the tailflame of a DC or RF plasma jet. Bonet et al.[269] theoretically studied the heat and mass transfer during evaporation of a spherical superrefractory particle inside a thermal plasma.

Barnes and Schleicher[161] adapted the treatment of Borgianni et al.[221] to their predictions of two-dimensional fields, and they assigned velocity profiles and used the combined model to predict the extent and location of decomposition of alumina in the ICP under various operating conditions.[145,161,181] Results of typical calculations for a 10-μm diameter alumina particle traveling along the discharge centerline for two ICP discharge diameters are given in Figure 22. The particle temperature and velocity were computed as well as the gas temperature, so that the extent of decomposition as a function of location and residence time could be determined. With particle densities and temperature distributions available, Barnes and Schleicher[161] assumed a thermal discharge and computed the spatial distributions of continuum and analyte spectral emission (i.e., Al I and II). However, without previous knowledge

of the flow pattern and particle trajectory, this model provided a means to predict trends. Its quantitative applications required experimental verification.[190,191]

Since the model developed by Boulos[260] includes the calculation of two-dimensional flow, Boulos[262] recently extended it to the calculation of the trajectories and temperature histories of particles injected into the induction discharge. Figure 25 presents the trajectories of alumina particles ranging in diameter from 10 to 250 μm injected at two radial positions from the aerosol injector tube for a carrier flow rate of 0.4 l/min for the discharge (represented by the temperatures and streamlines in Figure 23). The size of the circles designates the position of the particles and also indicates their approximate diameters; a solid is represented by an open circle and a liquid by a closed circle. The 10-μm diameter particle (Figure 25A) tended to follow the streamlines of flow and was entrained by the plasma (coolant) gas until midway through the induction coil where the particle was drawn into the discharge by the electromagnetic pumping and vaporized. The 30-μm particle was too large to be drawn into the discharge (Figure 25B), and larger diameter particles have penetrated because they have increased initial momentum, so that they were no longer repelled by the backflow from the discharge (Figure 25C). The trajectory was substantially different if the same particle began slightly displaced from the central axis (Figures 25D, E, and F) where the initial gas velocity was lower. Efforts to extend these calculations to discharges treated previously by Barnes et al. and to experimentally verify the predictions are currently underway.

In the models developed to date that apply to the spectrochemical ICP discharge, numerous assumptions were applied out of necessity; however, the results have been encouraging and experimental verification and refinements are underway. As research on the ICP discharge continues during the next few years, an accounting should be made of solution aerosol droplets in place of dry solid particles, the entrainment of molecular gases from the atmosphere and the decomposition of analyte aerosols in the discharge, and nonthermal spectroscopic excitation mechanisms. Experimental results for the desolvation, evaporation, and atomization of aerosol droplets in the ICP that contain concomitants will provide challenging objectives for theoretical modeling in future years.

5. Ionization — Excitation

Recently, Boumans and de Boer[122] proposed a mechanism for the role played by argon metastable states in the ICP to explain qualitatively the nonthermal excitation effects observed in argon ICP discharges at low power levels. The mechanism is based upon metastable argon acting as both an ionizer of analyte species through Penning ionization and as an ionizant (an easily ionzable constituent) to account for the nonthermal overpopulations of ionic levels and elimination of ionization interferences under properly chosen operating conditions. They extended the proposal made by Mermet et al.[126,132,133,135] for argon metastable excitation through Penning ionization, although the primary mechanism by which a metastable argon atom population density is created and the influence of experimental conditions on the primary mechanism is not specified. Boumans and de Boer found the basis of their proposals in part in the work of Cabannes et al.,[322-326] who investigated a so-called secondary DC plasma-jet. This secondary jet results from the mixing of hot and cold argon and shows both in this respect and in physical properties a close resemblance to a toroidal ICP. "Possibly," Boumans[327] stated recently, "the principal feature of this resemblance is a fairly sharp boundary with steep gradients between the hot and cold argon in the vicinity of the energy addition region. This might lead to a strongly enhanced ambipolar diffusion of electrons and argon ions from the hot to the cold region, as suggested by Eckert.[328,329] The subsequent recombination of argon ions and electrons to metastable argon atoms could then result in an overpopulation of metastables." Eckert[328] also suggested that "freezing" of excited states of particles diffusing into the cold gas as a result of a quick decrease in collision frequency might be a feasible mechanism for the creation of an overpopulation of metastables, as has been observed by Limbaugh[330] in DC plasma-jets expanding into vacuum.

Boumans and de Boer[122] set up a simple mathematical model in which an LTE system

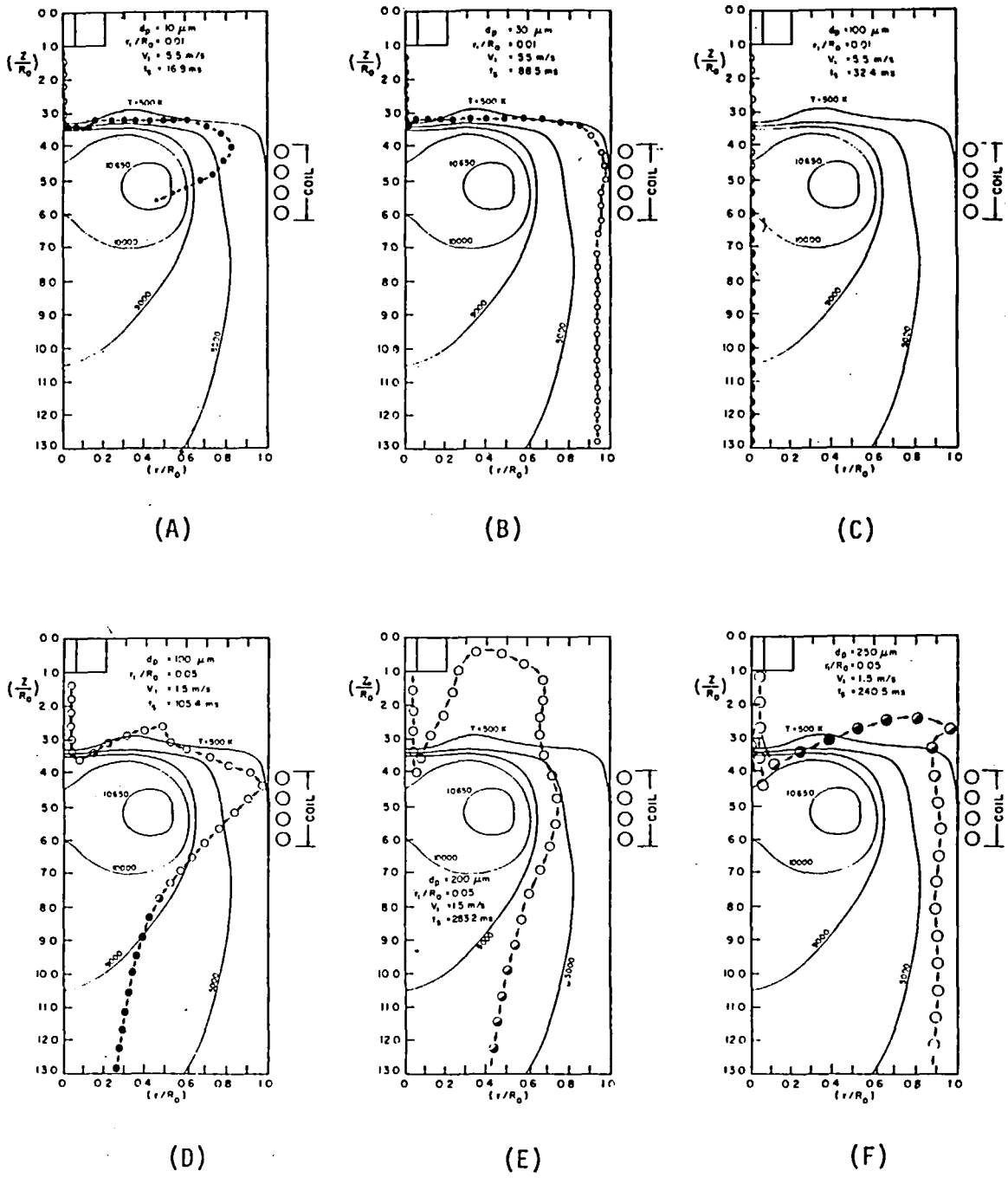

FIGURE 25. Particle trajectory and decomposition in the same discharge as Figure 23. (A), 10 μm; (B), 30 μm; (C), 100 μm; (D), 100 μm; (E), 200 μm; and (F), 250 μm displaced from center line. (From Boulos, M. I., 3eme Symposium International de Chimie des Plasmas, Communications, Paper No. S. 3.2, Limoges, France, 1977. With permission.)

was perturbed by an inflow of metastable argon atoms. The magnitude of the rate constants of the perturbing processes served as the principal parameters for determining the degree of departure from LTE. The metastable argon levels were considered to be easily ionizable with an ionization potential of only 4.21 V; thus, a high population of metastables provided a high electron number density through ionization equilibrium with the metastable levels. In a pure argon

discharge, a suprathermal electron density value could be accounted for if the ratio of the rate constants that dictate the metastable argon inflow into the plasma volume and the loss through recombination is large compared to the Saha ionization constant of the metastables. The suprathermal electron number density would then be independent of the LTE temperature and Saha ionization constant. If the inflow of argon metastables were to decrease to zero, the LTE value of the electron number density would be established and thermal ionization would become dominant.

Boumans and de Boer also argued that if Penning ionization by metastable argon atoms were to govern ionization of analyte atoms, this would not only explain the observed high sensitivity of ion lines, but also make this high sensitivity compatible with the observed high electron number density and low ionization interferences. The LTE conditions preclude this compatibility. However, Boumans and de Boer also emphasized that the rate constant for Penning ionization must exceed the rate constant for ionization by electron impact by a factor of 10^3 to 10^5, should Penning ionization assume the role they believe it plays here.

Finally, Boumans and de Boer explained the low ionization interferences by pointing to the suprathermal electron number density, which would not be disturbed by the addition of an easily ionizable matrix element, because the number density of the atoms and ions of the latter will be small compared to that of the electrons. In fact, the system would not be disturbed at all, because the matrix atoms would be ionized predominately by Penning ionization and the liberated electrons would recombine with argon ions to form metastable argon atoms. The net effect would be that matrix ions replaced argon ions, whereas the number densities of electrons and metastables remained unaffected. Therefore, the metastables would act not only as an ionizant that furnishes an excess of electrons in a pure argon plasma, but would also act as a very effective buffer when an easily ionizable matrix is introduced. The ionization potential of the buffer species would be as low as 4.21 V.

In different regions of the discharge, the mechanism of argon metastable ionization-excitation, according to Boumans and de Boer, can be gradually converted from nonthermal to thermal as the overpopulation of argon metastables decreases. Thus, externally controllable factors governing the influx of metastable argon atoms into the spectroanalytical region dictate the extent to which the discharge deviates from thermal equilibrium.

Boumans and de Boer[122,327] emphasized that the model must be considered primarily as a working hypothesis. It permits a qualitative understanding of various analytical favorable properties of argon ICPs, such as the high sensitivities of ion lines and the low ionization interferences. The model must be substantiated by a measurement of the number density of the metastable argon atoms, which should be on the order of 10^{14} cm^{-3}, before the model can be considered valid. Similarly, the effect of adding molecular species such as nitrogen, which might change the mechanism from non-LTE to LTE, and the changes of metastable populations with experimental conditions remain to be investigated. Mermet and Trassy[133] recently found 6×10^{11} to 3×10^{12} cm^{-3} metastable argon atom concentrations in the center of their 2.1-kW discharge.

In other models related to excitation, Mermet[275] derived a semiempirical relationship between detection limits obtained in a 40-MHz discharge and the spectral properties of ten injected elements. With this relationship, he suggested the evaluation of detection limits of the same or other elements although using other lines. Human and Scott[85] employed a model with two spatial distributions of absorbing atoms to explain experimentally observed spectral line profiles.

IV. APPLICATIONS

A. Introduction

Applications of the ICP discharge for spectrochemical analysis are growing with the increasing sale of commercial instruments. Greenfield et al.[3] tabulated references to analytical applications of the ICP to metals and alloys, minerals, blood, oil, refractory oxides, organophosphorus compounds, soil, deposits, effluents, mineral acids, rare earths, and proteins. An expanded list of samples tested by Greenfield et al.[73] also includes various chemicals, organic polymers, and commercial prod-

ucts. Other methods for specific analyses are finding their way into conference proceedings, newsletters,[89] and journals.

As Boumans[256] has phrased it, "...the analytical capabilities of ICPs have been definitely documented; a more widespread application in routine analysis can be expected once it has become clear to potential users that the initial investment for complete analysis equipment (ICP plus spectrometer) will be repaid by an improved analytical output and/or reduced personnel costs." Boumans[239,256,293] also considers the ICP a likely candidate for universal analysis to replace the DC arc and revitalize spectrographic analysis, especially when automated microphotometers or electronic readouts relieve much of the burden of line searches and identification.

In the following section, some of the recently reported applications of ICP-AES are discussed. Much of the applications development work is currently underway, so that specific results are not yet available for comparison and evaluation. However, a major growth in publications on the methods and applications of ICP-AES will certainly occur during the next decade, providing ample opportunity for more critical reviews. A typical example is the recent compilation of invited ICP-AES conference lectures edited by Barnes[27] comprising a review of applications, description of sampling approaches, discussion of factors influencing precision and accuracy, and application examples for food, geochemistry, airborne particulates, plant tissue digests, and metals.

B. Recent Applications

In a number of industries, the value of ICP-AES was recognized immediately; already, detailed methods and routine analyses have been documented. In other fields, the tempo has been slow, but the interest apparent. Perhaps by virtue of the sample form, water analysis has already proven to be a popular application area for the ICP. Winge et al.[93,97] applied ICP-AES in the simultaneous determination of more than 20 trace elements in soft, hard, and saline waters. The ICP-AES allows quantitative determination, without preconcentration, of most elements at concentrations below the Environmental Protection Agency (EPA) recommended criteria levels for public water supplies and for continuous-use irrigation water. The reproducibility is given for a reference sample analysis in Table 4. Few problems were found with soft waters, and hard waters required care because of stray light arising from calcium and magnesium. For saline waters, unlike other spectrochemical sources, the high NaCl content did not seriously affect the detection limit. However, detection capabilities were sufficient only for the direct determination of pollutants in saline waters. Elements found at normal levels in seawater required further pretreatment.

Ronan[270] determined 20 elements in fresh water samples, including drinking waters, surface waters, and domestic and industrial waste effluents, and compared results with EPA standard atomic absorption referee method. ICP-AES was applied successfully in the analyses of all municipal and nonmunicipal samples types collected for the National Pollution Discharge Elimination System.

Kerfoot and Crawford[271] applied a chelating-ion exchange matrix for preconcentration of 14 transition metals in seawater. Prefiltered 200-ml volumes of seawater were drawn through a laminated adsorptive disc holder at a rate of about 20 ml/min, and after a rinse, 5 ml of 1% ultrapure nitric acid was drawn through the disc to elute the concentrated metals. Half of the 14 elements were detected above the detection limit capabilities of the ICP-AES instrument, and acid recoveries varied from 13 to 88%. Reproducibility for replicate extraction for a 10-μg/l solution ranged from 4 to 11%.

Geology exploration and mining are fields in which ICP-AES has proven popular. Scott et al.[86] determined uranium in rock and ore samples with a detection limit of 0.1 μg/ml over the concentration range of 0.002 to 2% uranium oxide. Apart from sample dissolution, no pretreatment was necessary. No interference corrections were required in the range 0.02 to 2% uranium oxide, and pure aqueous uranium standards could be employed for standardization. A correction for Ca and Fe levels was needed at concentration levels below 0.02%. Since the analysis by AAS is particularly insensitive to uranium, the effectiveness of this single element analysis more than justified the cost of the equipment. Scott and Kokot[92] also determined Cu, Pb, Zn, Ni, and Co in geochemical soil samples; the results compared favorably

with AAS. Watson et al.[121,331] photographically determined minor and trace impurities in sulfide concentrates after fusion with sodium peroxide in a vitreous-graphite crucible. The precision varied between 2 and 6%, and the results agreed well with those of a number of other methods. Using a similar sample preparation procedure, Russell and Watson[331,332] determined major, minor, and trace elements in ferrochromium slags and chromite ores, with relative SD of 0.5 to 1.0%, Fe in zircon sands, and noble and base elements in matte-leach residues. Broekaert et al.[334] simultaneously determined all rare earth elements in standard minerals by applying an ICP-spectrographic procedure after complete sample decomposition in a borate fusion, and they measured sequentially some rare earth elements in monasite and bastnaesite with a monochromator. Alder et al.[110] determined nitrogen produced from ammonium reaction in soils by evolving nitrogen into the ICP after oxidation of ammonium by sodium hypobromite. The analysis of geological materials has proven very successful; at least one commercial analysis laboratory[139,217] operates a number of ICP-AES instruments on a fulltime routine basis.

Horticultural applications of ICP-AES can be expected to grow rapidly. Jones[27,272] described the determination of 16 elements in soil extracts and plant tissue ash solutions. ICP-AES showed a marked improvement over spark excitation analysis. Scott and Strasheim[84] determined six elements in plant materials and found ICP-AES to be sufficiently sensitive for the direct determination of Fe, Mn, Cu, Al, B, and Zn in solutions after a dry ashing procedure.

Aluminum,[27] steel,[81,95,333] ferromanganese,[234] ferrochromium,[331] and silicon[27] have been analyzed as solids[203,212,213] or as dissolved solutions using ICP-AES. Newland and Mostyn[101] spectrographically determined Co, Fe, Ta, Ti, and Zr in nickel alloys with a relative SD of 2 to 3% with no serious matrix effects. The nickel alloys were dissolved in HCl-HNO_3, and any insoluble residue was fused with $KHSO_4$. Results agreed well with certified values. Newland[333] also spectrographically determined traces of rare earth elements in plain carbon and low alloy steels using an Fe internal reference with a relative SD of 4 to 6%. Butler et al.[95] determined alloying and impurity elements in low- and high-alloy steels. The accuracy studies for five elements and a variety of NBS standard reference materials are summarized in Table 5, and data for the analytical curves obtained are given in Table 6. The accuracy obtained with synthetic reference solutions containing 0.5 wt% Fe showed that all concentrations determined fall within the range reported by NBS even though the iron content varied from more than 99 wt% to less than 1 wt%. The analysis of metals, especially for metals which give poor or marginal results by direct spark analysis, should continue to increase in popularity as more standard ICP-AES methods are developed.

The multielement determination of trace elements in foods and beverages is becoming a critical part of element monitoring for nutritional labeling of processed foods. Establishing toxic levels for elements in foodstuffs is of increasing importance. Gunn et al.[125] described a rapid, direct method for the determination of phosphorus in milk powder solutions with a detection limit of 0.1 μg/ml phosphorus and a precision of 2%. No significant interferences were caused by the calcium concentrations found in the sample. Boyer et al.[273] have reported the application of ICP-AES to multielement analysis of meat, canned foods, animal wastes and sewage sludge, and seaweed products. Warren[274] evaluated the ICP-AES for the analysis of heptan-2-one-diethyl-ammonium diethyldithiocarbamate (DDDC) metal chelate solutions resulting from chelation and solvent extraction of various trace metals in foodstuffs. Charalambous and Bruchner[335] reported the analysis of beer and brewing materials, and the analysis of coffee and wine also have been performed.

Another active field of methods development is in the analysis of energy and environmentally related materials. Although few publications have appeared, ICP-AES has been applied in the analysis of coal, oil shale, fly ash, naphtha, tar sands, petroleum, and environmental waters and air particulates associated with the mining or refining of these materials (e.g., References 93 and 97). Allemand[143] described an ICP-AES instrument intended for analysis of metals in residual fuel oils, and Fassel et al.[194,321] and Peterson[277] discussed the determination of 15 metals in lubricating oils. A solution of lubricating oil in 4-methyl-2-pentanone (MIBK) allowed

analysis of low- and high-viscosity oils. Peterson[277] developed methods for the simultaneous determination of trace elements in various oil matrices, including lubricating oils, fuel oil, centrifuged coal liquefaction products, crude soybean oil, and commercial edible oils. The particles in lubricating oil and coal liquefaction products did not appear to affect the analytical results, although incomplete recoveries were found for synthetic suspensions of large iron particles in oil.

The analysis of biological samples is one of the most lively areas of ICP-AES applications. Although Kniseley et al.[119] and Greenfield and Smith[201] first reported analysis of blood samples in the early 1970s, only recently have detailed investigations of analysis of biological materials been described. Irons et al.[152] and Dahlquist and Knoll[94] conducted particularly careful evaluations. Irons et al.[152] found that ICP-AES and XRF spectroscopy were highly reliable methods for biological matrices, and Dahlquist and Knoll[94] verified that ICP-AES is remarkably free from matrix and interelement effects for the determination of major and trace elements in biological materials and soil extracts. They concluded that the accuracy, precision, and sensitivity of ICP-AES (Figure 4) compared favorably with other instrumental techniques. Nixon[211] investigated diverse techniques for determination of rather difficult elements, and he devised a method for determination of As, Se, Sn, and Ge involving the digestion of biomedical samples followed by distillation of the volatile bromides. Concentrations of As, Se, Sn, and Ge were reported in samples of human urine, whole blood, plasma, and serum. The possibility for a routine ICP-AES clinical instrument to compete with AAS has more than once been seriously considered by manufacturers. As the thrust of instrument development continues toward lower cost and simple-to-operate ICP-AES instruments, the analysis of complex biological materials on a routine basis is no more than a few years away. In fact, one organization currently supports three ICP-AES systems solely for the analysis of hair, and methods for the determination of trace metals in food chemicals, drugs, and pharmaceuticals are also being developed.[27]

Recently Boumans et al.[293] sketched the basis for a new system of universal analysis, in the sense of a quantitative survey analysis, with an ICP combined with a spectrograph and computerized microphotometer for automatic evaluation of photographically recorded spectra.[310] This ICP system will supplement and, in part, replace the DC carbon arc methods of survey analysis presently used in their laboratory in order to achieve improved precision and accuracy.

Discussing flexible single-element analysis using an ICP-monochromator system, Boumans et al.[278] presented examples from daily practice of an analytical service group in the research group of a large electronics industry. Typically, nonroutine analysis problems were classified into three categories: (1) problems solved with both ICP-AES and another method, particularly chemical analysis including AAS techniques; (2) problems solved with ICP-AES which require a time-consuming separation or preconcentration when solved by another method, and (3) problems solved with ICP-AES that otherwise would have been impractical using other methods.

C. Conclusions

These few examples illustrate the range of sample materials and analytical problems which can be treated with ICP-AES. Each new sample type will require a major effort to be directed toward developing methods for sample preparation, establishing operating parameters for the analysis, and confirming accuracy and reliability relative to standard procedures. As Boumans[256,279] pointed out, the first problems to be solved will require accurate simultaneous multielement analysis of solutions and no objection to the purchase and maintenance of a multichannel spectrometer. Another solution will be provided for universal analysis, in which the ICP would replace the DC arc source and give qualitative and quantitative spectrographic results. This will be especially attractive if a reliable technique for introducing small quantities of powder into the discharge can be perfected. Also, the unique single-element determination which cannot otherwise be made with comparable analytical results (e.g., the determination of U) will readily justify purchase of an ICP and a relatively simple monochromator. As Boumans[256] indicated, the battle to show ICP-

\ES as a valuable spectrochemical approach as been won. Now, the hardest work of all is head.

ACKNOWLEDGMENTS

Preparation of this review was supported by he Department of Energy (Office of Basic Energy Sciences) through contract EE-77-S-02-4320.A000 and a grant from the Alcoa Foundation, Pittsburgh, Pennsylvania. The helpful discussions with enthusiastic ICP users and the cooperation of many researchers who supplied manuscripts, preprints, and commentaries is sincerely appreciated. The editorial review by Dorothy Barnes was of great assistance.

REFERENCES

1. Barnes, R. M., Ed., *Emission Spectroscopy,* Dowden, Hutchinson & Ross, Stroudsburg, Pa., 1976.
2. Barnes, R. M., *Anal. Chem.,* 48, 106R (1976); 50, 100R (1978).
3. Greenfield, S., McGeachin, H. McD., and Smith, P. B., *Talanta,* 22, 1 (1975); 22, 553 (1975); 23, 1 (1976).
4. Butler, L. R. P., Human, H. G. C., and Scott, R. H., Electric flames, in *CRC Handbook of Spectroscopy,* Vol. 1, Robinson, J. W., Ed., CRC Press, Cleveland, 1974, 816.
5. Sharp, B. L., *Sel. Anal. Rev. Anal. Sci.,* 4, 37 (1976).
6. Fassel, V. A. and Kniseley, R. N., *Anal. Chem.,* 46, 1110A (1974).
7. Kleinmann, I. and Polej, B., *Chem. Listy,* 65, 1 (1971), English translation available from R. Barnes, University of Massachusetts.
8. Boumans, P. W. J. M., Excitation of spectra, in *Analytical Emission Spectroscopy,* Part 2, Vol. 1, Grove, E. L., Ed., Marcel Dekker, New York, 1972, 1.
9. Fassel, V. A., Electrical flames, in *Colloquium Spectroscopicum Internationale XVI, Heidelberg, Oktober 1971. Plenary Lectures and Reports,* Adam Hilger, London, 1972, 63.
10. Hittorf, W., *Ann. Phys.,* (Leipzig), 21, 90 (1884).
11. Thomson, J. J., *Philos. Mag.,* 32(5), 321 (1891); 4(7), 1128 (1927).
12. Thomson, J. J. and Thomson, G. P., *Conduction of Electricity through Gases,* Vol. 2, 3rd ed., Cambridge University Press, Cambridge, England, 1933, 431.
13. Raizer, Yu. P., *Sov. Phys. Usp.,* 12, 777 (1970).
14. Townsend, J. S. and Donaldson, R. H., *Philos. Mag.,* 5(7), 178 (1928); 7, 600 (1929).
15. MacKinnon, K. A., *Philos. Mag.,* 8(7), 605 (1929).
16. Mavrodineanu, R. and Hughes, R. C., *Spectrochim. Acta,* 19, 1309 (1963).
17. Eckert, H. U., *ICP Inf. Newsl.,* 2(11), 327 (1977); *J. Appl. Phys.,* 48, 1467 (1977); Aerospace Report No. ATR-77(9472)-2, The Aerospace Corp., El Sungundo, Calif., February 28, 1977.
18. Barnett, W., Vollmer, J. W., and De Nuzzo, S. M., *At. Absorpt. Newsl.,* 15, 33 (1976).
19. Haarsma, J. P. S., de Jong, G. J., and Agterdenbos, J., *Spectrochim. Acta,* B29, 1 (1974).
20. Browner, R. F. and Keliher, P. N., Electrodeless discharge lamps, in *Analytical Uses of Plasmas,* Barnes, R. M., Ed., Interscience, New York, in preparation.
21. Barnes, R. M. and Winslow, R. J., *J. Phys. Chem.,* in press.
22. Hollahan, J. R. and Bell, A. T., Eds., *Techniques and Applications of Plasma Chemistry,* John Wiley & Sons, New York, 1974.
23. Winslow, R., Investigation of a RF Capacitively Coupled Low Pressure Discharge for Spectrochemical Analysis, Ph.D. dissertation, University of Massachusetts, Amherst, 1978.
24. Liang, C. S., Analytical Studies of Volatile Organomercurial Compounds, M.S. thesis, University of Massachusetts, Amherst, 1973.
25. Babat, G. I., *Vestn. Elektroprom.,* 2, 1 (1942); 3, (1942), English translation available from R. Barnes, University of Massachusetts, Amherst.
26. Babat, G. I., *J. Inst. Elect. Eng. Part 3,* 94, 27 (1947).
27. Barnes, R. M., Ed., *Applications of Inductively Coupled Plasma Atomic Emission Spectroscopy,* Franklin Institute Press, Philadelphia, 1978.
28. Brown, G. H., Hoyler, C. H., and Bierwirth, R. A., *Theory and Application of Radio-Frequency Heating,* D. Van Nostrand, New York, 1947.
29. Curtis, F. R., *High-Frequency Induction Heating,* 2nd ed., McGraw-Hill, New York, 1950.
30. Lozinskii, M. G., *Industrial Applications of Induction Heating,* Pergamon Press, New York, 1969.

31. May, E., *Industrial High Frequency Electric Power*, John Wiley & Sons, New York, 1950.
32. Stansel, N. R., *Induction Heating*, McGraw-Hill, New York, 1949.
33. Scott, R. H., Fassel, V. A., Kniseley, R. N., and Nixon, D. E., *Anal. Chem.*, 46, 75 (1974).
34. Barnes, R. M. and Schleicher, R. G., *Anal. Chem.*, 46, 1342 (1974).
35. Eckert, H. U., *High Temp. Sci.*, 6, 99 (1974).
36. Dresvin, S. V., Ed., *Physics and Technology of Low-Temperature Plasmas*, Atomizdat, Moscow, 1972; Eckert, H. U., Ed. (English translation), *Physics and Technology of Low-Temperature Plasmas*, Iowa State University Press, Ames, 1977.
36. Dresvin, S. V., Ed., *Physics and Technology of Low Temperature Plasmas*, Atomizdat, Moscow, 1972, translated by Eckert, H. U. and Pfender, E.
37. Czernichowski, A. and Jurewicz, J. *Pr. Nauk. Inst. Chem. Nieorg. Metal. Pierwiastakow Rzadkich Politech. Worcaw.*, 24, 3 (1975), English translation in *ICP Inf. Newsl.*, 2, special issue 1, 1 (1976).
38. Rykalin, N. N., *Pure Appl. Chem.*, 48, 179 (1976).
39. Reed, T. B., *J. Appl. Phys.*, 32, 821 (1961).
40. Reed, T. B., *J. Appl. Phys.*, 32, 2534 (1961).
41. Dymshits, B. M. and Koretskii, Y. P., *Sov. Phys. Tech. Phys.*, 9, 1294 (1965); *Zh. Tekh. Fiz.*, 34, 1677 (1964).
42. Reed, T. B., *Int. Sci. Technol.*, 6, 42 (1962).
43. Reed, T. B., U.S. Patent 3,324,334, June 6, 1967; *ICP Inf. Newsl.*, 3, 24 (1977).
44. Reed, T. B., Plasmas for high temperature chemistry, in *Advances in High Temperature Chemistry*, Vol. 1, Eyring, L., Ed., Academic Press, New York, 1967, 259.
45. Reed, T. B., Chemical uses of induction plasmas, in *The Application of Plasmas to Chemical Processing*, Baddour, R. F. and Timmins, R. S., Eds., M.I.T. Press, Cambridge, 1967, 26.
46. Beguin, C. P., Ezell, J. B., Salvemini, A., Thompson, J. C., Vickroy, D. G., and Margrove, J. L., Chemical syntheses in radio-frequency plasma torches, in *The Application of Plasmas to Chemical Processing*, Baddour, R. F. and Timmins, R. S., Eds., M.I.T. Press, Cambridge, 1967, 35.
47. Hamblyn, S. M. L. and Reuben, B. G., Use of radio-frequency plasma in chemical synthesis, in *Advances in Inorganic Chemistry and Radiochemistry*, Vol. 17, Emeleus, H. J. and Sharpe, A. G., Eds., Academic Press, New York, 1975, 89.
48. Greenfield, S., *ICP Inf. Newsl.*, 1, 3, (1975).
49. Fassel, V. A., *ICP Inf. Newsl.*, 1, 267 (1976).
50. Greenfield, S., Jones, I. L. W., and Berry, C. T., *Analyst*, (London), 89, 713 (1964).
51. Wendt, R. H. and Fassel, V. A., *Anal. Chem.*, 37, 920 (1965).
52. Greenfield, S., Jones, I. L. W., and Berry, C. T., U.S. Patent 3,467,471, September 16, 1969.
53. Greenfield, S., Jones, I. L. W., Berry, C. T., and Spash, D. I., British Patent 1,109,602, April 10, 1968.
54. Greenfield, S., Jones, I. L. W., Berry, C. T., and Bunch, L. G., *Proc. Soc. Anal. Chem.*, 2, 111, (1965).
55. Wendt, R. H. and Fassel, V. A., *Anal. Chem.*, 37, 920 (1965).
56. Greenfield, S., Berry, C. T., and Bunch L. G., Spectroscopy with a High Frequency Plasma Torch, Radyne International, Workingham, England, 1965.
57. Wendt, R. H. and Fassel, V. A., *Anal. Chem.*, 38, 337 (1966).
58. Hoare, H. C. and Mostyn, R. A., *Anal. Chem.*, 39, 1153 (1967).
59. Britske, M. E., Borisov, V. M., and Sukah, Yu. S., *Ind. Lab.*, 33, 301 (1967).
60. Pforr, G. and Kapica, V., *Collect. Czech. Chem. Commun.*, 31, 4710 (1966).
61. Veillon, C. and Margoshes, M., *Spectrochim. Acta*, B23, 503 (1968).
62. Dickinson, G. W. and Fassel, V. A., *Anal. Chem.*, 41, 1021 (1969).
63. Pforr, G., *XIV Colloquium Spectroscopicum Internationale, Debrecen, Hungary, August, 1967*, Vol. 2, Adam Hilger, London, 1967, 687.
64. Greenfield, S., Smith, P. B., Breeze, A. E., and Chilton, N. M. D., *Anal. Chim. Acta*, 41, 385 (1968).
65. Bordonali, C. and Biancifiori, M. A., *XIV Colloquium Spectroscopicum Internationale, Debrecen, Hungary, August 1967*, Vol. 2, Adam Hilger, London, 1967, 1153.
66. Biancifiori, M. A. and Bordonali, C., Com. Naz. Energia Nucl. (Rome) Rep., RT/CH(67)15, 1967.
67. Bordonali, C., Biancifiori, M. A., Donato, A., and Morello, B., Com. Naz. Energia Nucl. (Rome) Rep., TF/CHI(69)18, 1969.
68. Bordonali, C., Biancifiori, M. A., Donato, A., and Morello, B., *Metall. Ital.*, 61, 360 (1969).
69. Bordonali, C. and Biancifiori, M. A., U.S. Patent 3,684,884, August 15, 1972.
70. Barnett, W. B., Fassel, V. A., and Kniseley, R. N., *Spectrochim. Acta*, B23, 643 (1968).
71. Barnett, W. B., Fassel, V. A., and Kniseley, R. N., *Spectrochim. Acta*, B25, 139 (1970).
72. Abdallah, M. H., Diemiaszonek, R., Jarosz, J., Mermet, J. M., Robin, J., Trassy, C., *Anal. Chim. Acta*, 84, 271 (1976).
73. Greenfield, S., Jones, I. L. W., McGeachin, H. McD., and Smith, P. B., *Anal. Chim. Acta.*, 74, 225 (1975).
74. Davison, A. L., Bethune, J. R., and Ajhar, R. M., 24th Pittsburgh Conference on Analytical Chemistry and Applied Spectroscopy, Abstr., Paper No. 30, Cleveland, 1973.
75. Jones, J. L., Dahlquist, R. L., Knoll, J. W., and Hoyt, R. H., 24th Pittsburgh Conference on Analytical Chemistry and Applied Spectroscopy, Abstr. Paper No. 147, Cleveland, 1974.

76. Barnes, R., Ed., *ICP Inf. Newsl.*, 1, 25 (1975); 1, 159 (1975); 2, 275 (1977).
77. Souilliart, J. C. and Robin, J. P., *Analusis*, 1, 413 (1972).
78. Boumans, P. W. J. M. and de Boer, F. J., *Spectrochim. Acta*, B27, 391 (1972).
79. Mermet, J. M., *ICP Inf. Newsl.*, 1, 122 (1975).
80. Kirkbright, G. F., *Proc. Anal. Div. Chem. Soc.*, (London), 12, 8 (1975).
81. Ohls, K., Koch, K. H., and Grote, H., *Z. Anal. Chem.*, 284, 177 (1977).
82. Kornblum, G. R. and de Galan, L., *Spectrochim. Acta*, B29, 249 (1974).
83. Kornblum, G. R. and de Galan, L., *Spectrochim. Acta*, B32, 71 (1977).
84. Scott, R. H. and Strasheim, A., *Anal. Chim. Acta*, 76, 71 (1975).
85. Human, H. G. C. and Scott, R. H., *Spectrochim. Acta*, B31, 459 (1976).
86. Scott, R. H., Strasheim, A., and Kokot, M. L., *Anal. Chim. Acta*, 82, 67 (1976).
87. Boumans, P. W. J. M. and de Boer, F. J., *Spectrochim. Acta*, B31, 355 (1976).
88. Barnes, R. M. and Nikdel, S., *Appl. Spectrosc.*, 30, 310 (1976).
89. Barnes, R. M., Ed., *ICP Information Newsletter*, (Series), University of Massachusetts, Amherst.
90. Barnes, R. M., *ICP Inf. Newsl.*, 2, 62 (1976).
91. Winefordner, J. D., Fitzgerald, J. J., and Omenetto, N., *Appl. Spectrosc.*, 29, 369 (1975).
92. Scott, R. H. and Kokot, M. L., *Anal. Chim. Acta*, 75, 257 (1975).
93. Winge, R. K., Katzenberger, J. M., and Fassel, V. A., Development and Application of an Inductively Coupled Plasma Analytical System for the Simultaneous Multielement Determination of Trace Elemental Pollutants in Water, in Annual Progress Report for Interagency Agreement EPA-IAG-D6-0417, March 1, 1976 to February 28, 1977.
94. Dahlquist, R. L. and Knoll, J. W., *Appl. Spectrosc.*, 32, 1 (1978).
95. Butler, C. C., Kniseley, R. N., and Fassel, V. A., *Anal. Chem.*, 47, 825 (1975).
96. Kirkbright, G. F. and Ward, A. F., *Talanta*, 21, 1145 (1974).
97. Winge, R. K., Fassel, V. A., Kniseley, R. N., DeKalb, E., and Haas, W. J., Jr., *Spectrochim. Acta*, B32, 327 (1977).
98. Ajhar, R. M., Dalager, P. D., and Davison, A. L., *Am. Lab.*, 8(3), 71 (1976).
99. Dalager, P. D., Davison, A. L., and Harind, R. H., 28th Pittsburgh Conference on Analytical Chemistry and Applied Spectroscopy, Abst., Paper No. 402, Cleveland, 1977; *ICP Inf. Newsl.*, 2, 304 (1977).
100. Scott, R. H., *ICP Inf. Newsl.*, 2, 38, 117 (1976).
101. Newland, B. T. N. and Mostyn, R. A., *ICP Inf. Newsl., 2, 135 (1976); Materials Quality Assurance Directorate* (London) Report MQAD R 242, June 1976.
102. Olson, K. W., Haas, W. J., Jr., and Fassel, V. A., *Anal. Chem.*, 49, 632 (1977).
103. Boumans, P. W. J. M., de Boer, F. J., and de Ruiter, J. W., *Philips Techn. Rev.*, 33, 50 (1973).
104. Boumans, P. W. J. M. and de Boer, F. J., *Spectrochim. Acta*, B30, 309 (1975).
105. Betty, K. R. and Horlick, G., *Appl. Spectrosc.*, 32, 31 (1978).
106. Boumans, P. W. J. M., *ICP Inf. Newsl.*, 1, 222 (1976).
107. Barnes, R., Ed., *ICP Inf. Newsl.*, 1, 199 (1976); 3, 393 and 435 (1978).
108. Kirkbright, G. F., Ward, A. F., and West, T. S., *Anal. Chim. Acta*, 64, 353 (1973).
109. Kirkbright, G. F., Ward, A. F., and West, T. S., *Anal. Chim. Acta*, 62, 241 (1972).
110. Alder, J. F., Gunn, A. M., and Kirkbright, G. F., *Anal. Chim. Acta*, 92, 43 (1977).
111. Ward, A. F., Analytical Aspects of Atomic Spectroscopy at Wavelengths in the Far Ultraviolet, Ph.D. dissertation, University of London, 1973.
112. Allemand, C. D. and Barnes, R. M., *Appl. Spectrosc.*, 31, 434(1977).
113. Edmonds, T. E. and Horlick, G., *Appl. Spectrosc.*, 31, 536 (1977).
114. Kalnicky, D. J., Fassel, V. A., and Kniseley, R. N., *Appl. Spectrosc.*, 31, 137 (1977).
115. Larson, G. F., Fassel, V. A., Scott, R. H., and Kniseley, R. N., *Anal. Chem.*, 47, 238 (1975).
116. Boumans, P. W. J. M., *Z. Anal. Chem.*, 279, 1 (1976).
117. Schleicher, R. G. and Barnes, R. M., *Anal. Chem.*, 47, 724 (1975).
118. Fassel, V. A. and Dickinson, G. W., *Anal. Chem.*, 40, 247 (1918).
119. Kniseley, R. N., Fassel, V. A., and Butler, C. C., *Clin. Chem.* (N.Y.), 19, 807 (1973).
120. Kniseley, R. N., Amenson, H., Butler, C. C., and Fassel, V. A., *Appl. Spectrosc.*, 28, 285 (1974).
121. Watson, A. E., Russel, G. M., and Balaes, G., *ICP Inf. Newsl.*, 2, 205 (1976); National Institute for Metallurgy, Randburg, South Africa, Report No. 1815, April 15, 1976.
122. Boumans, P. W. J. M. and de Boer, F. J., *Spectrochim. Acta*, B32, 365 (1977).
123. Barnes, R., Ed., *ICP Inf. Newsl.*, 2, 280 (1977).
124. Boumans, P. W. J. M., *Philips Tech. Rev.*, 34, 305 (1974).
125. Gunn, A. M., Kirkbright, G. F., and Opheim, L. N., *Anal. Chem.*, 49, 1492 (1977).
126. Jarosz, J. and Mermet, J. M., *J. Quant. Spectrosc. Radiat. Transfer*, 17, 237 (1977).
127. Mermet, J. M. and Robin, J., *Anal. Chim. Acta*, 87, 329 (1976).
128. Abdallah, M. H., Mermet, J. M., and Trassy, C., *Anal. Chim. Acta*, 87, 329 (1976).
129. Robin, J. and Trassy, C., *C. R. Acad. Sci. Ser. B*, 281, 345 (1975).
130. Jarosz, J., Mermet, J. M., and Robin, J., *C. R. Acad. Sci. Ser. B*, 278, 885 (1974).
131. Alder, J. F. and Mermet, J. M., *Spectrochim. Acta*, B28, 421 (1973).

132. Mermet, J. M., *Spectrochim. Acta*, B30, 383 (1975).
133. Mermet, J. M. and Trassy, C., *Rev. Phys. Appl.*, 12, 1219 (1977).
134. Abdallah, M. H. and Mermet, J. M., *J. Quant. Spectrosc. Radiat. Transfer*, 19, 83 (1978).
135. Mermet, J. M., *C. R. Acad. Sci. Ser. B*, 281, 273 (1975).
136. Alder, J. F., Bombelka, R. M., and Kirkbright, G. F., *J. Phys. B*, 11, 235 (1978).
137. Ohls, K., *ICP Inf. Newsl.*, 2, 357 (1977).
138. Danielsson, A. and Soderman, E., *ICP Inf. Newsl.*, 2, 267 (1977).
139. Abercrombie, F. N. and Silvester, M., 28th Pittsburgh Conference on Analytical Chemistry and Applied Spectroscopy, Abstr., Paper No. 404; Cleveland, 1977; *ICP Inf. Newsl.*, 2, 306 (1977).
140. Fuller, C. W., Ed., *Annual Reports on Analytical Atomic Spectroscopy 1975*, Vol. 5, The Chemical Society, London, 1976, 29.
141. Danielsson, A.,27th Pittsburgh Conference on Analytical Chemistry and Applied Spectroscopy, Abstr., Paper No. 36, Cleveland, 1976.
142. Barnes, R., Ed., *ICP Inf. Newsl.*, 2, 67 (1976); 2, 101 (1976); 2, 150 (1976).
143. Allemand, C., *ICP Inf. Newsl.*, 2, 1 (1975).
144. Ward, A. F., Crawford, R. L., and Sobel, H. R., 3rd Annual Meeting FACSS, XIX CSI, and VI ICAS, Abstr., Paper No. 82, Philadelphia, 1976; *ICP Inf. Newsl.*, 2, 202 (1976).
145. Allemand, C. and Barnes, R. M., *Appl. Spectrosc.*, 31, 434 (1977).
146. Allemand, C. and Barnes, R. M., 27th Pittsburgh Conference on Analytical Chemistry and Applied Spectroscopy, Abstr., Paper No. 265, Cleveland, 1976; *Spectrochim. Acta*, B33, in press.
147. Fassel, V. A., Inductively coupled plasma-atomic emission spectroscopy: an alternative approach to flameless atomic absorption spectroscopy, in *Flameless Atomic Absorption Analysis: An Update, ASTM STP 618*, American Society for Testing and Materials, Philadelphia, 1977, 22.
148. Greenfield, S., *Metron*, (Rovigo) 3, 244 (1971).
149. Boumans, P. W. J. M. and de Boer, F. J. *Proc. Anal. Div. Chem. Soc.*, 12, 140 (1975).
150. Boumans, P. W. J. M., de Boer, F. J., Dahmen, F. J., Hoelzel, H., and Meier, A., *Spectrochim. Acta*, B30, 449 (1975).
151. Larson, G. F. and Fassel, V. A., *Anal. Chem.*, 48, 1161 (1976).
152. Irons, R. D., Schenk, E. A., Giauque, R. D., *Clin. Chem.*, 22, 2018 (1976).
153. Barnes, R., Ed., *ICP Inf. Newsl.*, 2, 161 (1976).
154. Boumans, P. W. J. M., *ICP Inf. Newsl.*, 1, 206 (1976).
155. Visser, K., Hamm, F. M., and Zeeman, P. B., *Appl. Spectrosc.*, 30, 34 (1976).
156. Deferrari, R., *ICP Inf. Newsl.*, 1, 6 (1975); 1, 75 (1975); 1, 280 (1976).
157. Linn, H., *ICP Inf. Newsl.*, 2, 51 (1976).
158. Greenfield, S., McGeachin, H. M. and Smith, P. B., *ICP Inf. Newsl.*, 2, 167 (1976).
159. Abdallah, M. H., Jarosz, J., Mermet, J. M., Trassy, C., and Robin, J., XVIII Colloquium Spectroscopicum Internationale, Paper No. 164, Grenoble, 1975; *ICP Inf. Newsl.*, 1, 758 (1975).
160. Kornblum, G. R., Wigman, J., and de Galan, L., Proceedings of the XXth Colloquium Spectroscopicum Internationale and 7th International Conference on Atomic Spectroscopy Praha 1977, Abstr., Paper No. 8, Statni Pedagogicke Nakladatelstvi, Prague, 1977; *ICP Inf. Newsl.*, 3, 187 (1977).
161. Barnes, R. M. and Schleicher, R. G., *Spectrochim. Acta*, B30, 109 (1975).
162. Eckert, H. U., *AIAA J.*, 9, 1452 (1971).
163. Truitt, D. and Robinson, J. W., *Anal. Chim. Acta*, 49, 410 (1970); 51, 61 (1970).
164. Reed, T. B. and Roddy, J. T., *Rev. Sci. Instrum.*, 36, 620 (1965).
165. Larson, G. F., Fassel, V. A., Winge, R. K., and Kniseley, R. N., *Appl. Spectrosc.*, 30, 384 (1976).
166. Gold, D., *J. Phys. E.*, 10, 395 (1977).
167. Ohls, K. private communication, March 1977.
168. Bogdain, B., Linn, H., and Gast, H., *ICP Inf. Newsl.*, 2, 269 (1977).
169. Greenfield S., *Proc. Anal. Div. Chem. Soc.*, (London), 19, 279 (1976).
170. Greenfield, S., McGeachin, H.M., and Smith, P. B., *Anal. Chim. Acta*, 84, 67 (1976).
171. Dagnall, R. M., Smith, D. J., West, T. S., and Greenfield, S., *Anal. Chim. Acta*, 54, 397 (1971).
172. Eckert, H. U., *J. Appl. Phys.*, 42, 3108 (1971).
173. Genna, J. L., Barnes, R. M., and Allemand, C. D., *Anal. Chem.*, 49, 1450 (1977).
174. Fauchais, P. and Bourdin, E., 3eme Symp. Int. de Chimie des Plasmas, Conferences Invitees, Paper No. G1 Limoges, France, 1977.
175. Lichte, F. E. and Koirtyohann, S. R., 3rd Annual Meeting FACSS, XIX CSI, and VI ICAS, Abstr., Paper No. 26 Philadelphia, 1976; *ICP Inf. Newsl.*, 2, 192 (1976); 2, 283 (1976).
176. Montaser, A. and Fassel, V. A., *Anal. Chem.*, 48, 1490 (1976).
177. Ohls, K. and Krefta, K., *ICP Inf. Newsl.*, 1, 168 (1976).
178. Lichte, F. E. and Koirtyohann, S. R., *ICP Inf. Newsl.*, 1, 200 (1976).
179. Apel, C. T., Bienewski, T. M., Cox, L. E., and Steinhaus, D. W., *ICP Inf. Newsl.*, 3, 1 (1977).
180. Barnes, R. M. and Nikdel, S., *J. Appl. Phys.*, 47, 3929 (1976).
181. Barnes, R. M. and Nikdel, S., *Appl. Spectrosc.*, 29, 477 (1975).

182. Franklin, M., Baber, C., and Koirtyohann, S. R., *Spectrochim. Acta*, B31, 589 (1976).
183. Huska, P. and Clump, C. W., *Ind. Eng. Chem. Process Des. Dev.*, 6, 238 (1967).
184. Chase, J. D., *J. Appl. Phys.*, 40, 318 (1969).
185. Chase, J. D., *J. Appl. Phys.*, 42, 4870 (1971).
186. Dundas, P. H.,NASA Contract Report, CR 1527, February 1970.
187. Voropaev, A. A., Dresvin, S. V., and Klubnikin, V. S., *High Temp.* (USSR), 7, 580 (1969).
188. Klubnikin, V. S. *High Temp.* (USSR), 13, 439 (1975).
189. Kornblum, G. R. and de Galan, L., *Spectrochim. Acta*, B32, 455 (1977).
190. Genna, J. and Barnes, R. M., 3rd Annual Metting FACSS, XIX CSI, and VI ICAS, Abstr., Paper No. 25, Philadelphia, 1976; *ICP Inf. Newsl.*, 2, 190 (1976); 2, 238 (1977).
191. Barnes, R. M. and Schleicher, R. G., XVIII Colloquium Spectroscopicum Internationale, Paper No. 16, Grenoble, 1975; *ICP Inf. Newsl.*, 1, 109 (1975).
192. Boulos, M. I., *IEEE Trans. Plasma Sci.*, 4, 28 (1976).
193. Syty, A. *CRC Crit. Rev. Anal. Chem.*, 4, 155 (1974).
194. Fassel, V. A., Peterson, C. A., Abercrombie, F. N., and Kniseley, R. N., *Anal. Chem.*, 48, 516 (1976).
195. Pforr, G., *Schmierstoffe und Schierrungstechnik* , VEB Deutscher Verlag fur Grundstoff Industrie, No. 25, Leipzig, 1968, 55.
196. Mermet, J. M., *ICP Inf. Newsl.*, 2, 70 (1976).
197. Mavrodineanu, R. and Boiteux, H., *Flame Spectroscopy*, John Wiley & Sons, New York, 1965, 85.
198. Meinhard, J. E., *ICP Inf. Newsl.*, 2, 163 (1976).
199. Scott, R. H. and Oakes, A. R., *ICP Inf. Newsl.*, 1, 223 (1976).
200. Wohlers, C. C., *ICP Inf. Newsl.*, 3, 37 (1977).
201. Greenfield, S. and Smith, P. B., *Anal. Chim. Acta*, 59, 341 (1972).
202. Dahlquist, R. L., U.S. Patent 3,832,600, August 27, 1974.
203. Dahlquist, R. L., Knoll, J. W., and Hoyt, R. E., 26th Pittsburgh Conference on Analytical Chemistry and Applied Spectroscopy, Abstr., Paper No. 341, Cleveland, 1975; Reprint 7002, Applied Research Laboratories, Goleta, Calif.
204. Kranz, E., *XVth Colloquium Spectroscopicum Internationale, Proceedings*, Vol. 4, Madrid 1969, Iberica, Madrid, 1969, 95.
205. Kranz, E., *Spectrochim. Acta*, B27, 327 (1972).
206. Zheenbaev, Zh., Karikh, F. G., Konavko, R. I., Urmanbetov, K., and Engel'sht, V. S., *Ind. Lab.*, 35, 1634 (1969); *Zavod. Lab.*, 35, 1343 (1969).
207. Yudelevich, I. G. and Cherevko, A. S., *Spectrochim. Acta*, B31, 93 (1976).
208. Boumans, P. W. J. M. and Maessen, F. J. M. J., *Spectrochim. Acta*, B24, 585 (1969); B24, 611 (1969).
209. Maessen, F. J. M. J., Elgersma, J. W., and Boumans, P. W. J. M., *Spectrochim. Acta*, B31, 179 (1976).
210. Nixon, D. E., Fassel, V. A., and Kniseley, R. N., *Anal. Chem.*, 46, 210 (1974).
211. Nixon, D. E.,The Determination of Ultratrace Quantities of the Toxic Metals in Biomedical and Environmental Samples, Ph.D. dissertation, Iowa State University, Ames, 1976.
212. Dahlquist, R. L., Jones, J. L., and Paschen, K. W., U.S. Patent 3,602,595, August 31, 1971.
213. Dahlquist, R. L., *ICP Inf. Newsl.*, 1, 148 (1975).
214. Jones, J. L., Dahlquist, R. L., and Hoyt, R. E., *Appl. Spectrosc.*, 25, 628 (1971).
215. Winge, R. K., Fassel, V. A., and Kniseley, R. N., *Appl. Spectrosc.*, 25, 636 (1971).
216. Human, H. G. C., Scott, R. H., Oakes, A. R., and West, C. D., *Analyst* (London), 101, 265 (1976).
217. Abercrombie, F. N., Silvester, M. D., and Stoute, G. S., 28th Pittsburgh Conference on Analytical Chemistry and Applied Spectroscopy, Abstr., Paper No. 406, Cleveland, 1977; *ICP Inf. Newsl.*, 2, 309 (1977).
218. Dickinson, G., Application of the Inductively Coupled Plasma to Analytical Spectroscopy, Ph.D. dissertation, Iowa State University, Ames, 1969.
219. Pforr, G. and Aribot, O., *Z. Chem.*, 10, 78 (1970).
220. Scott, R. H., *Spectrochim. Acta Part B*, 33, 123 (1978).
221. Borgianni, C., Capitelli, M., Cramarossa, F., Triolo, L., and Molinari, E., *Combust. Flame*, 13, 181 (1969).
222. Capitelli, M., Cramarossa, F., Triolo, L., and Molinari, E., *Combust. Flame*, 15, 23 (1970).
223. Rains, R. K. and Kadlec, R. H., *Metall. Trans.*, 1, 1501 (1970).
224. Waldie, B., *Chem. Eng.*, (N.Y.), 259, 92 (1972); 261, 188 (1972).
225. Waldie, B., *Trans. Inst. Chem. Eng.*, 49, 114 (1971).
226. Thursfield, G. and Davies, G. J., *Trans. Inst. Chem. Eng.*, 52, 237 (1974).
227. Charles, J. A., Davies, G. J., Jervis, R. M., and Thursfield, G., *Trans. Inst. Min. Metall.* (Sect. C), 79, C54-C59, C298-C299 (1970).
228. Triche, H., Saadate, A., Besombes-Vailhe, J., *Methodes Phys. Anal.*, 8, 26 (1972).
229. Triche, H., Saadate, A., Talayrach, B., and Besombes-Vailhe, J., *Analusis*, 1, 413 (1972).
230. Ward, A. F., 28th Pittsburgh Conference on Analytical Chemistry and Applied Spectroscopy, Abstr., Paper No. 310, Cleveland, 1977; *ICP Inf. Newsl.*, 2, 303 (1977).
231. Denton, M. B. and Windsor, D. L., 27th Pittsburgh Conference on Analytical Chemistry and Applied Spectroscopy, Paper No. 284, Cleveland, 1976; *ICP Inf. Newsl.*, 1, 263 (1976); *Anal. Chem.*, 50, in press.
232. Bernhard, A., *ICP Inf. Newsl.*, 2, 91 (1976).

233. Kirkbright, G., *ICP Inf. Newsl.*, 2, 108 (1976).
234. Scott, R., *ICP Inf. Newsl.*, 2, 117 (1976).
235. Kalnicky, D. J., Kniseley, R. N., and Fassel, V. A., *Spectrochim. Acta*, B30, 511 (1975).
236. Allemand, C. and Benzie, G., *ICP Inf. Newsl.*, 1, 273 (1976).
237. Boumans, P. W. J. M., van Gool, G. H., and Jansen, J. A., *Analyst* (London), 101, 585 (1976).
238. Boumans, P. W. J. M., *Spectrochim. Acta*, B31, 147 (1976).
239. Boumans, P. W. J. M., *Proc. Anal. Div. Chem. Soc.* (London), 14, 143 (1977).
240. Allemand, C., *ICP Inf. Newsl.*, 1, 238 (1976).
241. Stelmack, L. A., *ICP Inf. Newsl.*, 1, 253 (1976); 3, 388 (1978).
242. Hadosian, K., U.S. Patent 3,588,252, June 28, 1971.
243. Dalager, P. D., Davison, A. L., and Jones, J. L., 27th Pittsburgh Conference on Analytical Chemistry and Applied Spectroscopy, Abstr., Paper No. 186, Cleveland, 1976, *ICP Inf. Newsl.*, 1, 232 (1976).
244. Abercrombie, F. N. and Silvester, M. D., 27th Pittsburgh Conference on Analytical Chemistry and Applied Spectroscopy, Abstr. Paper No. 168, Cleveland, 1976; *ICP Inf. Newsl.*, 1, 229 (1976).
245. Wohler, C. C., 3rd Annual Meeting FACSS, XIX CSI, and VI ICAS, Abstr., Paper No. 78, Philadelphia, 1976; *ICP Inf. Newsl.*, 2, 196 (1976); 2 243 (1977).
246. Danielsson, A. and Lindblom, P., *Appl. Spectrosc.*, 30, 151 (1976).
247. Myers, S. A. and Huchital, D. A., 27th Pittsburgh Conference on Analytical Chemistry and Applied Spectroscopy, Abstr. Paper No. 72, Cleveland, 1976; *ICP Inf. Newsl.*, 1, 10 (1976).
248. Metcalf, S. G., Ingle, J. D., Jr., and Manabe, R. M.,32nd ACS Northwest Regional Meeting, Paper No. 52, Portland, Oregon, June 1977.
249. Kniseley, R. N., Rhinehart, W. A., Fassel, V. A., Winge, R. K., and Haas, W. J., Jr., 28th Pittsburgh Conference on Analytical Chemistry and Applied Spectroscopy, Abstr., Paper No. 408, Cleveland, 1977; *ICP Inf. Newsl.*, 2, 310 (1977).
250. Mermet, J. M., Etude Spectroscopique d'un Plasma Induit par Haute Frequence, Ph.D. dissertation, University Claude Bernard, Lyon, France, 1974.
251. Gouesbet, G., *C. R. Acad. Sci. Ser. B*, 280, 597 (1975).
252. Mermet, J. M. and Robin, J. P., *Rev. Int. Hautes. Temp. Refract.*, 10, 133 (1973).
253. Sheffield, J., *Plasma Scattering of Electromagnetic Radiation*, Academic Press, New York, 1975.
254. Lapp, M. and Penny, C. M., Eds., *Laser Raman Gas Diagnostics*, Plenum Press, New York, 1974.
255. Chan, P. W., Niimura, M., Churchill, R. J., and Schanberg, B. C., *IEEE Trans. Plasma Sci.*, 3, 174 (1975).
256. Boumans, P. W. J. M., Proceedings of the XXth Colloquium Spectroscopicum Internationale and 7th International Conference on Atomic Spectroscopy Praha 1977, Invited Lectures, Part I, Statni Pedagogicke Nakladatelstvi, Prague, 1977, 7; *ICP Inf. Newsl.*, 3, 71 (1977).
257. Scott, R. H., Report FIS 51, National Physical Laboratory, C.S.I.R., Pretoria, South Africa, 1974.
258. Miller, R. C. and Ayen, R. J., *J. Appl. Phys.*, 40, 5260 (1970).
259. Delettrez, J. A., A Numerical Calculation of the Flow and Electric Characteristics of an Argon Induction Discharge, Ph.D. dissertation, University of California, Davis, 1974.
260. Boulos, M. I., *IEEE Trans. Plasma Sci.*, 4, 28 (1976).
261. Chandra, S. and Barnes, R. M., 3rd Annual Meeting FACSS, XIX CSI, and VI ICAS, Abstr., Paper No. 24, Philadelphia, 1976; *ICP Inf. Newsl.*, 2, 189 (1976).
262. Boulos, M. I., 3eme Symposium International de Chimie des Plasmas, Communications, Paper No. S.3.2, Vol. 3, Limoges, France. 1977.
263. Eckert, H. U., *ICP Inf. Newsl.*, 2, 327 (1977); Aerospace Report No. ATR-77 (9472)-2, Aerospace Corp., El Sugundo, Calif., February 28, 1977; Aerospace Report No. ATR-78 (8209)-1, Aerospace Corp., El Sugundo, Calif., March 31, 1978.
264. Eckert, H. U., *J. Appl. Phys.*, 48, 1467 (1977).
265. Dresvin, S. V., Dynamics of motion and heating of high-melting particles in plasma jets, in *Physics and Technology of Low Temperature Plasmas*, Eckert, H. U., Ed. (English translation), Iowa State University Press, Ames, 1977, chap. 10.
266. Johnston, P. D., *Combust. Flame*, 18, 373 (1972).
267. Meubus, P., *Can. J. Chem. Eng.*, 51, 440 (1973); 52, 616 (1974).
268. Boulos, M. I. and Gauvin, W. H., *Can. J. Chem. Eng.*, 52, 355 (1974).
269. Bonet, C., Daguenet, M., and Dumargue, P., *Int. J. Heat Mass Transfer*, 17, 643 (1974); 17, 1559 (1974).
270. Ronan, R., Simultaneous Analysis of Liquid Samples for Metals by Inductively Coupled Argon Plasma Atomic-Emission Spectroscopy (ICAP-AES), U.S. Environmental Protection Agency, Chicago, Ill.; *ICP Inf. Newsl.*, 1, 164 (1976); 27th Pittsburgh Conference on Analytical Chemistry and Applied Spectroscopy, Abstr., Paper No. 361, Cleveland, 1976; *ICP Inf. Newsl.*, 1, 264 (1976).
271. Kerfoot, W. B. and Crawford, R. L., *ICP Inf. Newsl.*, 2, 289 (1977).
272. Jones, J. B., Jr., *Commun. Soil Sci. Plant Anal.*, 8, 349 (1977).
273. Boyer, K. W., Tanner, J. T., and Gajan, R. J., 28th Pittsburgh Conference on Analytical Chemistry and Applied Spectroscopy, Paper No. 168, Cleveland, 1977; *ICP Inf. Newsl.*, 2, 302 (1977).
274. Warren, J., *ICP Inf. Newsl.*, 2, 262 (1977).
275. Mermet, J. M., *C. R. Acad. Sci.*, 284, 319 (1977).

276. Mermet, J. M. and Trassy, C., *Appl. Spectrosc.*, 31, 237 (1977).
277. Peterson, C. A., Inductively Coupled Plasma-Atomic Emission Spectrometry: Trace Elements in Oils Matrices, Ph.D. dissertation, Iowa State University, Ames, 1977.
278. Boumans, P. W. J. M., Bastings, L. C., de Boer, F. J., and van Kollenburg, L. W. J., Proceedings of the XXth Colloquium Spectroscopicum Internationale and 7th International Conference on Atomic Spectroscopy Praha 1977, Abstr., Paper No. 15, Statni Pedagogicke Nakladatelstvi, Prague, 1977; *ICP Inf. Newsl.*, 3, 201 (1977); *Z. Anal. Chem.*, in press.
279. Boumans, P. W. J. M., *Mikrochim. Acta*, p. 339 (1978).
280. Boumans, P. W. J. M. and de Boer, F. J., Proceedings of the XXth Colloquium Spectroscopicum Internationale and 7th International Conference on Atomic Spectroscopy Praha 1977, Abstr., Paper No. 19, Statni Pedagogicke Nakladatelstvi, Prague, 1977; *ICP Inf. Newsl.*, 3, 228 (1977).
281. Fuller, C. W., Ed., *Annual Reports on Analytical Atomic Spectroscopy 1976*, Vol. 6, The Chemical Society, London, 1977.
282. Bochkova, O. P. and Shreyder, E. Ya., *Spectroscopic Analysis of Gas Mixtures*, Academic Press, New York, 1965.
283. Fassel, V. A., *Pure Appl. Chem.*, 49, 1533 (1977).
284. Fenner, F., *Spectrochim. Acta*, 1, 164 (1939).
285. Gatterer, A. and Frodl, V., *Ric. Spettrosc. Lab. Astrofis. Specola Vaticana*, 1, 201 (1946).
286. Gatterer, A., *Spectrochim. Acta*, 3, 214 (1948).
287. van Sandwijk, A., van Montfort, P. F. E., and Agterdenbos, J., *Talanta*, 20, 495 (1973).
288. van Sandwijk, A. and Agterdenbos, J., *Talanta*, 21, 360 (1974).
289. van Montford, P. F. E. and Agterdenbos, J., *Talanta*, 21, 660 (1974).
290. van Montfort, P. F. E., Agterdenbos, J., Denissen, R., Piet, M., and van Sandwijk, A., *Spectrochim. Acta*, B33, 49 (1978).
291. Agterdenbos, J. and van Montfort, P. F. E.,Proceedings of the XXth Colloquium Spectroscopicum Internationale and 7th International Conference on Atomic Spectroscopy Praha 1977, Abstr., Paper No. 21, Statni Pedagogicke Nakladatelstvi, Prague, 1977.
292. van Sandwijk, A., *Picogram Analysis by Spectral Emission from Sealed Cells*, Ph.D. dissertation, State University, Utrecht, The Netherlands, 1974.
293. Boumans, P. W. J. M., Witmer, A. W., de Boer, F. J., and Bosveld, M., Proceedings of the XXth Colloquium Spectroscopicum Internationale and 7th International Conference on Atomic Spectroscopy Praha 1977, Abstr., Paper No. 16, Statni Pedagogicke Nakladatelstvi, Prague, 1977; *ICP Inf. Newsl.*, 3, 213 (1977); *Spectrochim. Acta Part B*, in press.
294. Ward, A. F., *ICP Inf. Newsl.*, 3, 51 (1977).
295. Abdallah, M. H., Mermet, J. M., and Trassy, C., Proceedings of the XXth Colloquium Spectroscopicum Internationale and 7th International Conference on Atomic Spectroscopy Praha 1977, Abstr., Paper No. 11, Statni Pedagogicke Nakladatelstvi, Prague, 1977; *ICP Inf. Newsl.*, 3, 190 (1977).
296. Jarosz, J. and Robin, J., Proceedings of the XXth Colloquium Spectroscopicum Internationale and 7th International Conference on Atomic Spectroscopy Praha 1977, Abstr., Paper No. 4, Statni Pedagogicke Nakladatelstvi, Prague, 1977; *ICP Inf. Newsl.*, 3, 184 (1977).
297. Ohls, K., Koch, K. H., and Grote, H., *Z. Anal. Chem.*, 287, 10 (1977).
298. Plesch, R., *Z. Anal. Chem.*, 288, 63 (1977).
299. Boumans, P. W. J. M., *Z. Anal. Chem.*, 288, 64 (1977).
300. Jenkins, R,Proceedings of the XXth Colloquium Spectroscopicum Internationale and 7th International Conference on Atomic Spectroscopy Praha 1977, Invited Lectures, Part I, Statni Pedagogicke Nakladatelstvi, Prague, 1977, 219.
301. Fasssel, V. A., Layton, E. M., Peterson, C., and Kniseley, R. N., Proc. Workshop Anal. Needs Future Appl. Coal Liquefaction, (sponsored by National Science Foundation and Ashland Oil, Ashland, Kentucky); *Chem. Abstr.*, 87, 170275g.
302. Demers, D. R. and Priede, A. I., Proceedings of the XXth Colloquium Spectroscopicum Internationale and 7th International Conference on Atomic Spectroscopy Praha 1977, Abstr., Paper No. 18, Statni Pedagogicke Nakladatelstvi, Prague, 1977; *ICP Inf. Newsl.*, 3, 221 (1977).
303. Boumans, P. W. J. M.,personal communication, 1978.
304. Veillon, C. and Margoshes, M., *Spectrochim. Acta*, B23, 553 (1968).
305. Kirkbright, G. F., Proceedings of the XXth Colloquium Spectroscopicum Internationale and 7th International Conference on Atomic Spectroscopy Praha 1977, Abstr., Paper No. 17, Statni Pedagogicke Nakladatelstvi, Prague, 1977; *ICP Inf. Newsl.*, 3, 218 (1977).
306. Kirkbright, G. F., Gunn, A., and Millard, D., 29th Pittsburgh Conference on Analytical Chemistry and Applied Spectroscopy, Paper No. 396, March 1978, Cleveland; *ICP Inf. Newsl.*, 3, 379 (1978).
307. Beenakker, C. I. M., *Spectrochim. Acta*, B31, 483 (1976).
308. Beenakker, C. I. M., *Spectrochim. Acta*, B32, 173 (1977).
309. Bubert, H. and Hagenah, W.-D., Paper presented at 11th Spektrometertagung, Montreux, Switzerland, May 1976.
310. Witmer, A. W., Jansen, J. A. J., van Gool, G. H., and Brouwer, G., *Philips Tech. Rev.*, 34, 322 (1974).
311. Addink, N. W. H., *DC Arc Analysis*, Macmillan, London, 1971.

312. Meggers, W. F., Corliss, C. H., and Scribner, B. F., Tables of Spectral-Line Intensities, Parts I and II, *Nat. Bur. Stand. Monogr.*, 145, 213 (1975); 145, 387 (1975).
313. Malmstadt, H. V. and Cordos, E., *Am. Lab.*, 4(8), 35 (1972).
314. Cordos, E. and Malmstadt, H. V., *Anal. Chem.*, 45, 425 (1973).
315. Spillman, R. W. and Malmstadt, H. V., *Anal. Chem.*, 48, 303 (1976).
316. Boumans, P. W. J. M. and de Boer, F. J., to be published.
317. Barnes, R., Ed., *ICP Inf. Newsl.*, 3, 114 (1977); 3, 369 (1978).
318. Jarosz, J., Mermet, J. M., and Robin, J. P., *Spectrochim. Acta Part B*, 33, 55 (1978).
319. Boumans, P. W. J. M., *Theory of Spectrochemical Excitation*, Hilger and Watts, London; Plenum Press, New York, 1966.
320. Kornblum, G. R. and de Galan, L., *Spectrochim. Acta*, B28, 139 (1973).
321. Larson, G. F. and Fassel, V. A., Abstracts of the 1977 Federation of Analytical Chemistry and Spectroscopy Societies Meeting, Paper No. 23, Detroit, November 1977.
322. Cabannes, F., *Pure Appl. Chem.*, 39, 381 (1974).
323. Bourasseau, D., Cabannes, F., and Chapelle, J., *Astron. Astrophys.*, 9, 339 (1970).
324. Czernichowski, A., Chapelle, J., and Cabannes, F., *C.R. Acad. Sci. Ser. B*, 270, 54 (1970).
325. Ranson, P. and Chapelle, J., *J. Phys. (Paris) Colloq.*, 32, C5b-39/40 (1971).
326. Cabannes, F., Chapelle, J., Czernichowski, A., Decroisette, M., and Zamerlick, J., *Rev. Int. Hautes Temp. Refract.*, 7, 7 (1970).
327. Boumans, P. W. J. M. and de Boer, F. J., Proceedings of the XXth Colloquium Spectroscopicum Internationale and 7th International Conference on Atomic Spectroscopy Praha 1977, Abstr., Paper No. 3, Statni Pedagogicke Nakladatelstvi, Prague, 1977; *ICP Inf. Newsl.*, 3, 181 (1977).
328. Eckert, H. U., personal communication.
329. Eckert, H. U., *J. Appl. Phys.*, 43, 46 (1972).
330. Limbaugh, C. C., Determination of the Excited State Density Distribution Within a Nonequilibrium, Freely Expanding Argon Arcjet Plume, AEDC-Tr-77-23 Report, Arnold Engineering Development Center, Arnold Air Force Station, Tennessee, 1977.
331. Watson, A. E. and Russell, G. M., National Institute for Metallurgy, Randburg, South Africa, Report No. 1907, July 15, 1977; *ICP Inf. Newsl.*, 3, 273 (1977).
332. Russell, G. M. and Watson, A. E., National Institute for Metallurgy, Randburg, South Africa, Report No. 1934, November 30, 1977; *ICP Inf. Newsl.*, 3, 409 (1978).
333. Newland, B. T. N., Materials Quality Assurance Directorate, London, Report No. MQAD R 258, August 1977; *ICP Inf. Newsl.*, 3, 263 (1977).
334. Broekaert, J. A. C., Leis, F., and Laqua, K., *ICP Inf. Newsl.*, 3, 381 (1978).
335. Charalambous, G. and Bruckner, K. J., *Master Brew. Assoc. Am. Tech. Q.*, 14, 197 (1977); *ICP Inf. Newsl.*, 3, 239 (1977).
336. Genna, J. and Barnes, R. M., unpublished results.
337. Scott, R. H., Strasheim, A., and Wemyss, R. B., 24th Canadian Spectroscopy Symposium, Ottawa, October 1977; *Anal. Chem.*, 50, in press.